

PHYSICOCHEMICAL, BIOPHARMACEUTICAL AND ANTI-HEPATOCELLULAR CARCINOMA
PROPERTIES OF CURCUMIN DIETHYL DISUCCINATE

Mr. Chawanphat Muangnoi

A Dissertation Submitted in Partial Fulfillment of the Requirements
for the Degree of Doctor of Philosophy in Pharmaceutical Chemistry and Natural Products
Department of Food and Pharmaceutical Chemistry
Faculty of Pharmaceutical Sciences
Chulalongkorn University
Academic Year 2018
Copyright of Chulalongkorn University

บทคัดย่อและแฟ้มข้อมูลฉบับเต็มของวิทยานิพนธ์ตั้งแต่ปีการศึกษา 2554 ที่ให้บริการในคลังปัญญาจุฬาฯ (CUIR)
เป็นแฟ้มข้อมูลของนิสิตเจ้าของวิทยานิพนธ์ที่ส่งผ่านทางบัณฑิตวิทยาลัย

The abstract and full text of theses from the academic year 2011 in Chulalongkorn University Intellectual Repository (CUIR)
are the thesis authors' files submitted through the Graduate School.

คุณสมบัติทางเคมีกายภาพ ชีวเภสัชกรรม และการต้านมะเร็งระดับของเคอร์คิวมินไดเอทิลไดซัคซิเนต

นายชวัลพัชร เมืองน้อย

วิทยานิพนธ์นี้เป็นส่วนหนึ่งของการศึกษาตามหลักสูตรปริญญาวิทยาศาสตรดุษฎีบัณฑิต

สาขาวิชาเภสัชเคมีและผลิตภัณฑ์ธรรมชาติ ภาควิชาอาหารและเภสัชเคมี

คณะเภสัชศาสตร์ จุฬาลงกรณ์มหาวิทยาลัย

ปีการศึกษา 2561

ลิขสิทธิ์ของจุฬาลงกรณ์มหาวิทยาลัย

Thesis Title	PHYSICOCHEMICAL, BIOPHARMACEUTICAL AND ANTI- HEPATOCELLULAR CARCINOMA PROPERTIES OF CURCUMIN DIETHYL DISUCCINATE
By	Mr. Chawanphat Muangnoi
Field of Study	Pharmaceutical Chemistry and Natural Products
Thesis Advisor	Associate Professor Pornchai Rojsitthisak, Ph.D.
Thesis Co Advisor	Professor Suthiluk Patumraj, Ph.D.

Accepted by the Faculty of Pharmaceutical Sciences, Chulalongkorn University in
Partial Fulfillment of the Requirement for the Doctor of Philosophy

..... Dean of the Faculty of
Pharmaceutical Sciences
(Assistant Professor RUNGPETCH SAKULBUMRUNGSIL, Ph.D.)

DISSERTATION COMMITTEE

..... Chairman
(Professor Somboon Tanasupawat, Ph.D.)

..... Thesis Advisor
(Associate Professor Pornchai Rojsitthisak, Ph.D.)

..... Thesis Co-Advisor
(Professor Suthiluk Patumraj, Ph.D.)

..... Examiner
(Professor WANCHAI DE-EKNAMKUL, Ph.D.)

..... Examiner
(Assistant Professor Bodin Tuesuwan, Ph.D.)

..... Examiner
(Assistant Professor Flying Officer Pasarapa Towiwat, Ph.D.)

..... External Examiner
(Associate Professor Siriporn Tuntipopipat, Ph.D.)

ชวัลพัชร เมืองน้อย : คุณสมบัติทางเคมีกายภาพ ชีวเภสัชกรรม และการต้านมะเร็งระดับของ
เคอร์คิวมินไดเอทิลไดซัคซิเนต. (PHYSICOCHEMICAL, BIOPHARMACEUTICAL AND
ANTI-HEPATOCELLULAR CARCINOMA PROPERTIES OF CURCUMIN DIETHYL
DISUCCINATE) อ.ที่ปรึกษาหลัก : รศ. ภก. ดร.พรชัย โรจนสีทิสักดิ์, อ.ที่ปรึกษาร่วม : ศ. ดร.
สุทธิลักษณ์ ปทุมราช

เคอร์คิวมิน (Cur) เป็นสารที่มีฤทธิ์ในการต้านมะเร็งโดยการเหนี่ยวนำให้เซลล์มะเร็งเกิดการตายในแบบอะพอพโตซิส แต่อย่างไรก็ตาม Cur ยังมีข้อจำกัดในการนำไปพัฒนาเป็นยาที่มีคุณสมบัติในการต้านมะเร็งเนื่องจากความไม่คงตัวทั้งในน้ำและของเหลวภายในร่างกาย ส่งผลให้ค่าชีวปริมาณออกฤทธิ์ (bioavailability) ของ Cur ต่ำ เคอร์คิวมินไดเอทิลไดซัคซิเนต (CurDD) ซึ่งเป็นเอสเทอร์โปรดรักของ Cur ได้ถูกออกแบบและสังเคราะห์ขึ้นเพื่อเพิ่มความคงตัวให้กับ Cur ในการศึกษาที่ผู้วิจัยได้ทำการศึกษาคูสมบัติทางเคมีกายภาพ ชีวเภสัชกรรม และการต้านมะเร็งระดับทั้งในแบบหลอดทดลองและสัตว์ทดลองของ CurDD โดยเปรียบเทียบกับ Cur ผลการศึกษาพบว่า CurDD ช่วยเพิ่มความคงตัวในสารละลายบัฟเฟอร์ที่ pH 7.4 และในสภาวะการจำลองการย่อยให้กับ Cur ได้ การดูดซึมผ่านเซลล์ลำไส้พบว่า ปริมาณของ Cur ที่ถูกดูดซึมผ่านเซลล์ลำไส้ในกลุ่มที่ได้รับ CurDD มีค่าสูงกว่ากลุ่มที่ได้รับ Cur อย่างมีนัยสำคัญทางสถิติ ($p < 0.05$) และส่วนที่ผ่านการดูดซึมจากเซลล์ลำไส้ (bioavailable fraction) ที่ได้จาก CurDD มีความเป็นพิษต่อเซลล์มะเร็งตับ (HepG2) มากกว่าที่ได้จาก Cur อย่างมีนัยสำคัญทางสถิติ ($p < 0.05$) ส่วนที่ดูดซึมผ่านเซลล์ลำไส้ของ CurDD สามารถเหนี่ยวนำให้เซลล์มะเร็งตับเกิดการตายในแบบอะพอพโตซิสได้มากกว่าของ Cur อย่างมีนัยสำคัญทางสถิติ ($p < 0.05$) โดย CurDD สามารถเหนี่ยวนำให้มีการแสดงออกของโปรตีน Bax เพิ่มขึ้น และ Bcl-2 ลดลง ส่งผลให้เพิ่มการทำงานของเอนไซม์แคสเพส 3 และ 9 ทำให้เกิดการตายของเซลล์มะเร็งตับในแบบอะพอพโตซิสมากกว่ากลุ่มของ Cur อย่างมีนัยสำคัญทางสถิติ ($p < 0.05$) ผลในหนูเปลือย (nude mice) ที่ถูกเหนี่ยวนำให้เกิดเนื้องอกด้วยเซลล์มะเร็งตับ พบว่า CurDD สามารถลดการโตของเนื้องอกได้มากกว่า Cur อย่างมีนัยสำคัญทางสถิติ ($p < 0.05$) โดยสามารถลดการสร้างเส้นเลือดของเซลล์มะเร็งโดยการยับยั้งการผลิต VEGF และการแสดงออกของโปรตีน COX-2 จากผลการศึกษาที่แสดงให้เห็นว่า CurDD สามารถเพิ่มการดูดซึมผ่านเซลล์ลำไส้ให้กับ Cur ส่งผลให้ฤทธิ์ในการต้านเซลล์มะเร็งระดับของ Cur เพิ่มขึ้น ดังนั้น CurDD ซึ่งเป็นโปรดรักของ Cur น่าจะมีศักยภาพที่จะนำไปใช้ในการพัฒนาเป็นยาสำหรับรักษามะเร็งตับต่อไป

สาขาวิชา	เภสัชเคมีและผลิตภัณฑ์ธรรมชาติ	ลายมือชื่อ นิสิต
ปีการศึกษา	2561	ลายมือชื่อ อ.ที่ปรึกษาหลัก
		ลายมือชื่อ อ.ที่ปรึกษาร่วม

5676452533 : MAJOR PHARMACEUTICAL CHEMISTRY AND NATURAL PRODUCTS

KEYWORD: Curcumin diethyl disuccinate, Curcumin, Ester prodrug, Cellular transport,
Anti-hepatocellular carcinoma activity

Chawanphat Muangnoi : PHYSICOCHEMICAL, BIOPHARMACEUTICAL AND ANTI-
HEPATOCELLULAR CARCINOMA PROPERTIES OF CURCUMIN DIETHYL
DISUCCINATE. Advisor: Assoc. Prof. Pornchai Rojsitthisak, Ph.D. Co-advisor: Prof.
Suthiluk Patumraj, Ph.D.

Curcumin (Cur) has been reported for an anticancer activity by inducing apoptosis. However, the poor oral bioavailability of Cur due to chemical instability limits itself for further development as a chemotherapeutic agent. Previously, a succinate ester prodrug of Cur named as curcumin diethyl disuccinate (CurDD) has been designed and synthesized to enhance chemical stability of Cur. In this study, physicochemical and biopharmaceutical properties as well as *in vitro* and *in vivo* anti-hepatocellular carcinoma activities of CurDD were investigated and compared with those of Cur. CurDD could improve the stability of Cur in buffer pH 7.4 and simulated gastrointestinal fluids. The bioavailable fractions (BF) of CurDD had the significantly higher amount of transported Cur and exerted higher cytotoxicity against HepG2 cells comparing to those of Cur ($p < 0.05$). The BF of CurDD induced apoptosis by increasing and suppressing Bax and Bcl-2 expression, respectively, resulting in the activation of caspase-3 and -9 activities in the higher extent in comparison with Cur. CurDD also exhibited the better anti-hepatocellular carcinoma activity in HepG2-induced tumor mice after oral administration in comparison with Cur ($p < 0.05$). CurDD inhibited the angiogenesis by decreasing COX-2 expression and suppressing VEGF production. These results suggest that CurDD could improve the oral bioavailability as well as the anti-hepatocellular carcinoma activity of Cur. Therefore, CurDD, as a prodrug of Cur, has a potential to be further developed for the treatment of liver cancer.

Field of Study:	Pharmaceutical Chemistry and Natural Products	Student's Signature
Academic Year:	2018	Advisor's Signature
		Co-advisor's Signature

ACKNOWLEDGEMENTS

I would like to express my sincere gratitude to my thesis advisor, Associate Professor Pornchai Rojsitthisak, for his valuable guidance, constant encouragement and always being very understanding me. He has not only provided me the worth suggestions but also supported me when I encountered with good and bad period throughout my academic study.

My sincere gratitude is also conferred to Professor Suthiluk Patumraj, my co-advisor who always gives me the valuable comment, suggestion and helping my laboratory work especially the part of animal model. Without her kindness and hospitality, my academic life might not be as smooth and happy as it was.

My sincere gratitude has been contributing to Professor Somboon Tanasuptawat for being the thesis committee chairperson, and Professor Wanchai De-Eknamkul, Assistant Professor Bodin Tuesuwan and Assistant Professor Flying Officer Pasarapa Towiwat for being the examine members, and Associate Professor Siriporn Tuntipopipat for being the external examiner member and their kind suggestions to make my thesis complete.

I would like to thank the Pharmaceutical Research Instrument Center, Faculty of Pharmaceutical Sciences, Chulalongkorn University for supplying instruments. I also would like staffs and friends from Chulalongkorn University for their kind suggestions, help, support and always being my good friends and being beside me like my brother and sister.

This study is supported by the 90th Anniversary Chulalongkorn University Fund, Ratchadaphiseksomphot Endowment Fund, the Overseas Research Experience Scholarship from the Graduate School and Faculty of Pharmaceutical Sciences, Chulalongkorn University, the Annual Research Fund of The Asia Research Center (ARC), Chulalongkorn University and Chulalongkorn University; Government Budget.

Finally, I am very grateful to thank my family for their unconditional love and understanding and support in overcoming many obstacles which I have been facing through my research.

Chawanphat Muangnoi

TABLE OF CONTENTS

	Page
ABSTRACT (THAI)	iii
ABSTRACT (ENGLISH)	iv
ACKNOWLEDGEMENTS	v
TABLE OF CONTENTS	vi
LIST OF TABLES	xi
LIST OF FIGURES.....	xii
LIST OF ABBREVIATION.....	1
CHAPTER 1 INTRODUCTION	3
CHAPTER 2 LITERATURE REVIEW.....	7
2.1. Hepatocellular Carcinoma (HCC)	7
2.1.1. Incidence of HCC.....	7
2.1.2. Risk Factors of HCC	7
2.1.3. Pathophysiology and Biomarkers of Hepatocellular Carcinoma	8
2.1.4. Tumor Microenvironment	9
2.1.5. Inflammation	10
2.1.6. Oxidative Stress.....	12
2.1.7. The mechanism of cell response to oxidative stress and inflammation..	13
2.1.8. Histology of Hepatocellular Carcinoma	14
2.2. Apoptosis	15
2.2.1. Apoptosis pathway.....	16
2.2.1.1. Intrinsic pathway.....	16

2.2.1.2. Extrinsic pathway	17
2.2.2. Apoptosis and cancer.....	18
2.2.3. Pro-apoptotic regulation in tumour cells.....	19
2.2.4. Pro-survival regulation in tumour cells.....	20
2.2.5. Apoptosis and cancer treatment.....	21
2.3. Turmeric and bioactive compounds.....	22
2.3.1. Pharmacological activities and limitation of curcumin	23
2.3.2. Anti-cancer activities and mechanisms of curcumin	23
2.4. Limitation of curcumin for anti-cancer agent development.....	25
2.5. Prodrugs of curcumin.....	27
2.5.1. Curcumin- β -diglucosides.....	28
2.5.2. Acetoxy-curcumin	28
2.5.3. Curcumin-amino acids.....	28
2.5.4. Succinate ester prodrugs of Curcumin.....	28
2.6. Experimental mouse models for hepatocellular carcinoma.....	29
2.6.1. Chemical-induced liver cancer in animal models.....	29
2.6.1.1. Dimethylnitrosamine (DEN)	29
2.6.1.2. Carbon tetrachloride (CCl ₄).....	30
2.6.1.3. Thioacetamide.....	30
2.6.2. Xenograft models.....	31
CHAPTER 3 RESEARCH METHODOLOGY	32
3.1. Cell lines, Media, Chemicals and Equipments	32
3.2. Cur and CurDD	35
3.3. Investigation of physicochemical properties of Cur and CurDD.....	35

3.3.1. Investigation of water solubility of Cur and CurDD.....	35
3.3.2. Investigation of partition coefficient (log P) of Cur and CurDD	35
3.3.3. Investigation of stability of Cur and CurDD in buffer solution.....	36
3.3.4. Investigation of stability in simulated gastric and intestinal fluid of CurDD	36
3.4. HPLC condition for Cur and CurDD determination.....	37
3.4.1. HPLC instrumentation.....	37
3.4.2. Chromatographic condition.....	37
3.5. Determination of biopharmaceutical properties of Cur and CurDD.....	38
3.5.1. Cellular Uptake and Transport of Cur from Cur or CurDD	38
3.5.2. Cytotoxicity of Cur and CurDD	38
3.5.3. Cellular Uptake of Cur from Cur or CurDD.....	39
3.5.4. Transport of Cur from Cur or CurDD.....	39
3.6. Extraction of Cur	40
3.6.1. Extraction of Cur from cells	40
3.6.2. Extraction of Cur from solution of apical and basolateral compartments.....	41
3.7. Evaluation of <i>in vitro</i> anti-hepatocellular carcinoma activity and mechanism of bioavailable fraction of Cur or CurDD using HepG2 cells	41
3.7.1. Preparation of bioavailable fraction of Cur or CurDD.....	41
3.7.2. Evaluation of <i>in vitro</i> anti-hepatocellular carcinoma activity and mechanism of bioavailable fraction of Cur or CurDD.....	42
3.7.2.1. Cell viability test	43
3.7.2.2. Apoptosis test.....	43
3.7.2.3. Determination of caspase-3 and -9 activities.....	44

3.7.2.4. Western blot analysis	44
3.8. Evaluation of <i>in vivo</i> anti-hepatocellular carcinoma activity and mechanism of Cur or CurDD	45
3.8.1. AST, ALT and VEGF determination	48
3.8.2. Western blot analysis	48
3.9. Statistical analysis	49
CHAPTER 4 RESULTS	50
4.1. Investigation of physicochemical properties of Cur and CurDD.....	50
4.1.1. Investigation of water solubility of Cur and CurDD.....	50
4.1.2. Investigation of partition coefficient of Cur and CurDD	50
4.1.3. Investigation of stability of Cur and CurDD in buffer solution pH 7.4.....	50
4.1.4. Investigation of of stability of Cur and CurDD in simulated gastric and intestinal fluid	51
4.2. Determination of biopharmaceutical properties of Cur and CurDD.....	53
4.2.1. Cytotoxicity of Cur and CurDD in Caco-2 cells	53
4.2.2. Cellular Uptake of Cur from Cur or CurDD	54
4.2.3. Cellular Transport of Cur from Cur or CurDD.....	55
4.3. Evaluation of <i>in vitro</i> anti-hepatocellular carcinoma activity and mechanism of bioavailable fraction of Cur or CurDD using HepG2 cells	56
4.3.1. Effects of the BF of Cur and CurDD on caspase-3 and -9 activities.....	59
4.3.2. Effects of the BF of Cur and CurDD on Bax and Bcl-2 protein expression	60
4.4. Evaluation of <i>in vivo</i> anti-hepatocellular carcinoma activity and mechanism of Cur or CurDD	61
4.4.1. Effects of Cur and CurDD on tumour volume and tumour size.....	61
4.4.2. Effects of Cur and CurDD on body weight, AST and ALT activities.....	62

4.4.3. Effects of Cur and CurDD on Bax and Bcl-2 expression.....	64
4.4.4. Effects of Cur and CurDD on serum VEGF and COX-2 expression	64
CHAPTER 5 DISCUSSION AND CONCLUSION	67
REFERENCES.....	76
APPENDIX A Synthesis and Characterization of Cur and CurDD	89
APPENDIX B Chromatogram of Cur, DimethylCur and CurDD from HPLC.....	94
APPENDIX C Culture Media.....	95
APPENDIX D Cell Culture.....	97
APPENDIX E Characterization of Caco-2 and HepG2 cells	101
APPENDIX F Measuring Protein Concentration by BCA Assay	102
APPENDIX G Western Blot.....	103
APPENDIX H Chromatogram of Cur and CurDD from cellular uptake.....	106
APPENDIX I Chromatogram of Cur and CurDD from cellular transport	108
APPENDIX J Chulalongkorn University Animal Care and Use Protocol.....	110
VITA	111

LIST OF TABLES

	Page
Table 1 Water solubility and partition coefficient (log p) of curcumin (Cur) and curcumin diethyl disuccinate (CurDD).....	50

LIST OF FIGURES

	Page
Figure 1 Structure of curcumin.....	4
Figure 2 Structure of curcumin diethyl disuccinate (CurDD).....	5
Figure3 Several of risk factors and cofactors of hepatocellular carcinoma development	9
Figure 4 The mechanism of cell response to oxidative stress and inflammation	14
Figure 5 Histopathological progression of HCC	15
Figure 6 Intrinsic and Extrinsic Pathway of Apoptosis	18
Figure 7 Structure of bioactive compounds in turmeric 1: turmerone, 2: curcumin, 3: demethoxycurcumin and, 4: bisdemethoxycurcumin	23
Figure 8 Potential strategies targeting curcumin-induced apoptotic pathway to overcome chemoresistance in cancers	25
Figure 9 Degradation products of Cur from alkaline hydrolysis and autoxidation. The degradation pathway to hexanal (pathway with a question mark) has not been confirmed.....	26
Figure 10 Chemical structures of Cur and its major reductive metabolites	26
Figure 11 Methodology of study.....	34
Figure 12 Experimental design for the evaluation of anti-hepatocellular carcinoma activity and mechanism of Cur or CurDD in vivo	47
Figure 13 Chemical stability of Cur and CurDD in phosphate buffer solution pH 7.4 for 15, 30, 60, 120 and 240 min. Data presented is mean \pm SD values of triplicates, *p < 0.05 indicates significant differences from the Cur.....	51

Figure 14 Cur and CurDD stability in SGF for 5, 15, 30, 45 and 60 min. Data presented is mean \pm SD values of triplicates, * $p < 0.05$ indicates significant differences from the Cur.	52
Figure 15 Cur and CurDD stability in SIF for 15, 30, 60, 120 and 180 min. Data presented is mean \pm SD values of triplicates.	52
Figure 16 Cell viability of Caco-2 cells incubated with Cur or CurDD at various concentrations (0.1-50 μ M) for 4 h. Data presented is mean \pm SD values of four replicates * $p < 0.05$ indicates significant differences from the control group; # $p < 0.05$ indicates significant differences from the Cur group.....	53
Figure 17 Amounts of free Cur from uptake of Caco-2 cells derived from 5 μ M of Cur or CurDD at different time intervals. Data presented is mean \pm SD values of four replications. Columns with different superscript letters (a-g) are significantly different ($p < 0.05$, N=4).	55
Figure 18 Amounts of free Cur from transport across Caco-2 cells derived from 5 μ M of Cur or CurDD at different time intervals. Data presented is mean \pm SD values of four replications. Columns with different superscript letters (a-f) are significantly different ($p < 0.05$, N=4).	56
Figure 19 Cell viability of HepG2 cells incubated with the respective bioavailable fraction of Cur or CurDD for 24 h. Data presented is mean \pm SD values of four replications. Columns with different superscript letters (a-c) are significantly different ($p < 0.05$, N=4).	57
Figure 20 Flow cytometry results of HepG2 cells after treating with bioavailable fractions of Cur or CurDD. (A) Control group; (B) Treated with bioavailable fraction of Cur; (C) Treated with bioavailable fraction of CurDD. Q1 = Live cells, Q2 = Early apoptosis, Q3 = Late apoptosis and Q4 = Necrosis.	58
Figure 21 Effect of bioavailable fraction (BF) of Cur and CurDD on caspase-3 and -9 activities in HepG2 cells. Values represent means \pm SD of three independent experiments performed in triplicate. The different superscript letters (a, b and c) are significantly different ($p < 0.05$, N=4).	59

Figure 22 Effect of bioavailable fraction (BF) of Cur and CurDD on Bax and Bcl-2 expression in HepG2 cells. Values represent means \pm SD of three independent experiments performed in triplicate. The different superscript letters (a, b and c) are significantly different ($p < 0.05$, N=4).	60
Figure 23 Effects of Cur and CurDD on tumour volume of HepG2-transplanted tumours in nude mice and in treatment groups at 21 days after treatment. Values represent means \pm SD. The different superscript letters (a, b and c) are significantly different ($p < 0.05$).	61
Figure 24 Effects of Cur and CurDD on tumour size of HepG2-transplanted tumours in nude mice and in treatment groups at 21 days after treatment.	62
Figure 25 Effects of Cur and CurDD on body weight of HepG2- transplanted tumours in nude mice and treatment groups at 21 days after treatment. Values represent means \pm SD (N=8).	63
Figure 26 Effects of Cur and CurDD on AST and ALT activities of HepG2- transplanted tumours in nude mice and treatment groups at 21 days after treatment. Values represent means \pm SD (N=8).	63
Figure 27 Effects of Cur and CurDD on Bax and Bcl-2 expression from tumour tissue of HepG2-transplanted tumour in nude mice and in the treatment groups at 21 days after treatment. Values represent means \pm SD (N = 8). Columns with different superscript letters (a-c) are significantly different ($p < 0.05$).	65
Figure 28 Effects of Cur and CurDD on serum VEGF secretion of HepG2-transplanted tumour in nude mice and in the treatment groups at 21 days after treatment. Values represent means \pm SD (N = 8). Columns with different superscript letters (a-d) are significantly different ($p < 0.05$).	65
Figure 29 Effects of Cur and CurDD on (COX-2 expression from tumour tissue of HepG2-transplanted tumour in nude mice and in the treatment groups at 21 days after treatment. Values represent means \pm SD (N = 8). Columns with different superscript letters (a-d) are significantly different ($p < 0.05$).	66

Figure 30 The propose mechanism of BF of CurDD induced apoptotic cell death in hepatocellular carcinoma.....	71
Figure 31 The underlying mechanisms of CurDD for the anti-hepatocellular carcinoma activities in HepG2-induced nude mice	73
Figure 32 The underlying mechanisms of CurDD for the in vitro and in vivo anti-hepatocellular carcinoma activities	74
Figure 33 Mass spectrometry of Cur	91
Figure 34 Nuclear magnetic resonance (NMR) spectroscopy of Cur	91
Figure 35 Mass spectrometry of CurDD.....	92
Figure 36 Nuclear magnetic resonance (NMR) spectroscopy of CurDD.....	92
Figure 37 The chromatogram of curcumin, dimethyl curcumin and curcumin diethyl disuccinate from HPLC	94
Figure 38 Caco-2 cells at 21 days after confluence.....	101
Figure 39 HepG2 cells about 50% confluence.....	101
Figure 40 Chromatogram of Cur from cellular uptke of Cur at 4 h	106
Figure 41 Chromatogram of Cur and CurDD from cellular uptke of CurDD at 4 h....	107
Figure 42 Chromatogram of Cur from cellular transport (bioavailable fraction) of Cur	108
Figure 43 Chromatogram of Cur and CurDD from cellular transport.....	109

LIST OF ABBREVIATION

ALT	Alanine aminotransferase
AST	Aspartate aminotransferase
ATCC	American Type Culture Collection
BF	Bioavailable fraction
BW	Body weight
COX-2	Cyclooxygenase-2
Cur	Curcumin
CurDD	Curcumin diethyl disuccinate
DMEM	Dulbecco's modified Eagle's medium
DMSO	Dimethyl sulfoxide
°C	Degree Celcius
DMAP	4-(<i>N,N</i> -dimethylamino)pyridine
DMC	Dimethylcurcumin
EDTA	Ethylenediamine tetraacetic acid
g	Gram
GI	Gastrointestinal
h	Hour
IC ₅₀	Half maximal inhibitory concentration
HPLC	High-performance liquid chromatography
HCC	Hepatocellular carcinoma
kg	Kilogram
m/z	Mass-to-charge ratio
MW	Molecular weight
µg	Microgram
µL	Microliter
µM	Micromolar
mg	Milligram
mL	Milliliter

mm	Millimeter
mM	Millimolar
mmol	Millimol
min	Minute
MSCUR	Monoethylsuccinyl curcumin
nm	Nanometer
rpm	Revolutions per minute
sec	Second
PMSF	Phenylmethylsulfonyl fluoride
VEGF	Vascular endothelial growth factor
v/v	Volume-by-volume
w/v	Weight-by-volume

CHAPTER 1

INTRODUCTION

Hepatocellular carcinoma (HCC) is a growing health problem, which is the most common malignant tumor that accounts for nearly 80% of all liver cancer cases (Aravalli *et al.*, 2013). HCC is leading cause of cancer morbidity and mortality in men and women throughout developed countries. In Thailand, HCC has the first highest incidence and mortality rate in men and the third highest in women from cancer. (Chitapanarux and Phornphutkul, 2015; Thai Ministry of Public Health, 2011). Liver is an important organ which has various complex functions such as synthesizing, metabolism and chemical neutralizing. Although, several harmful substances are detoxified and eliminated by liver, some of chemical substances or metabolized form such as drugs, alcohol, aflatoxin, dimethylnitrosamine (DMN), diethylnitrosamine (DEN), herbicides, and pesticides as well as chronic hepatitis B and C infections can produced the generation of reactive oxygen species (ROS) leading to oxidative stress and chronic inflammation that can damage liver parenchyma, DNA, and activation of hepatic stellate cell and lead to necrosis. During this process, liver fibrosis and cirrhosis may also occur. It is one of the most important processing to the development of HCC (Aravalli *et al.*, 2013; Cabibbo *et al.*, 2010). The conventional cancer treatments, such as surgical resection, radiotherapy, and chemotherapy have been found to be ineffective or only minimally effective in patients with unresectable HCC and also, they have toxicity to normal cells and serious side effects (Aravalli *et al.*, 2013). Therefore, developing more effective and less toxic anti-cancer agents including natural bioactive compounds, is necessary to prevent or against the process of carcinogenesis, especially hepatocarcinogenesis. Evidence from epidemiological studies demonstrated that the consumption of vegetables and fruits at the adequate amount was significantly reduced the detriments of cancer (Reddy

et al., 2003). Vegetables, fruits including herbs and spices are rich of natural bioactive compounds such as curcuminoids, flavonoids, carotenoids and triterpenoids. They have been shown have anti-inflammatory, antioxidant and anticancer activities (Hooper and Cassidy, 2006).

Curcumin (1,7-bis(4-hydroxy-3-methoxy-phenyl)-1,6-heptadiene-3,5-dione; diferuloylmethane; **Figure 1**) is a major bioactive compound of turmeric (*Curcuma longa* L.) with no discernable toxicity (Epstein *et al.*, 2010), has been shown anti-inflammation (Nonn *et al.*, 2007; Basnet *et al.*, 2011), antioxidant (Lee *et al.*, 2010) and anti-cancer activities (Wu *et al.*, 2010).

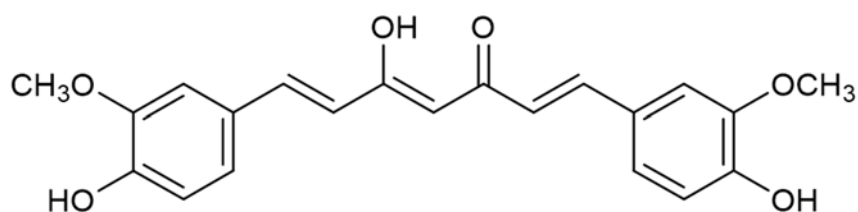


Figure 1 Structure of curcumin

The anti-cancer activities of curcumin, it shows anti-carcinogenic effects on leukemia, lymphoma, brain cancer, and colorectal epithelium cancers (Mimeault and Batra, 2011). It could inhibit tumor angiogenesis (Yoysungneon *et al.*, 2006) and is also a potential of tumor inhibitory agent with chemo-preventive effects against colon cancer (Kwon *et al.*, 2009). Curcumin has been reported to play a potent role in the regulation of proliferation and apoptosis in various types of cancer underlying mechanism the apoptosis induction and autophagy protection (Li *et al.*, 2017; Shu and Bu, 2017; Zhi-Dong *et al.*, 2014). Moreover, Curcumin has been used as a dietary supplement as well as a therapeutic agent in Chinese and Asian medicines for centuries. Although curcumin has varied of pharmacological activities, curcumin has a

limitation of drug development because of its poor absorption and instability in aqueous and basic solutions.

The use of a prodrug approach is a chemical and biochemical stabilization to overcome various barriers which can increase water solubility and stability. A curcumin prodrug, curcumin diethyl disuccinate (CurDD) (**Figure 2**) was synthesized by conjugation of curcumin with succinic acid via an ester bond. Previous study found that CurDD was more stable in phosphate buffer at pH 7.4 than curcumin and CurDD can also be hydrolyzed to curcumin by esterase enzymes in plasma (Wichitnithad *et al.*, 2011). These demonstrated that stability of curcumin can be increased and also, it can be released by CurDD. These make CurDD of interest as a prodrug of curcumin. Therefore, CurDD as a prodrug of curcumin may increase the pharmacological activities of curcumin such as anticancer activities after oral administration. However, the some physicochemical, biopharmaceutical properties and anticancer activities, especially anti-hepatocellular carcinoma of CurDD are unknown, and these required for drug development.

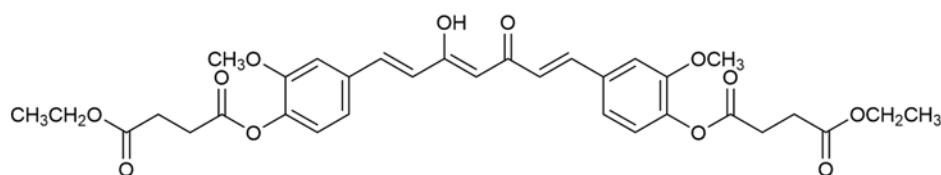


Figure 2 Structure of curcumin diethyl disuccinate (CurDD)

The objectives of this study are to study the physicochemical (partition coefficient and stability in simulated gastric and in intestinal fluid) and biopharmaceutical (cellular uptake and transport) properties of CurDD. Moreover, anti-hepatocellular carcinoma properties and mechanisms of CurDD was studied by investigation in hepatocellular carcinoma cell lines (HepG2) and implanted hepatocellular carcinoma in nude mice.

The main objectives of this research study are as followed:

1. To investigate physicochemical and biopharmaceutical properties of curcumin diethyl disuccinate.
2. To evaluate of *in vitro* and *in vivo* anti-hepatocellular carcinoma properties and mechanisms of curcumin diethyl disuccinate.

CHAPTER 2

LITERATURE REVIEW

2.1. Hepatocellular Carcinoma (HCC)

2.1.1. Incidence of HCC

HCC is one of the most malignant tumors in the world, representing the third leading cause of death from cancer and the fifth most prevalent malignancy worldwide, its incidence is increasing worldwide and mostly emerges in advanced fibrosis patients (Center *et al.*, 2011). In Thailand, HCC has the first highest incidence and mortality rate in men and the third highest in women from cancer and the third highest among cancers worldwide (Chitapanarux T. and Phornphutkul, 2015; Thai Ministry of Public Health, 2011). HCC is thought a pattern of the oxidative stress and chronic inflammation to chronic liver injury (Bataller *et al.*, 2005). The overabundance of extracellular matrix (ECM) accumulation distorts the architecture of hepatocytes by forming fibrotic scars and the consequent progression of nodules of regenerating hepatocytes defines liver cirrhosis (Hernandez-Gea, 2011). The clinical significance of liver cirrhosis is involved to the associated hepatocellular dysfunction and the increased resistance to blood flow in intrahepatic causing hepatic insufficiency and portal hypertension, respectively, following to the occurrence of hepatocellular carcinoma (Wong, 2011).

2.1.2. Risk Factors of HCC

HCC is a complex disease associated with many risk factors and cofactors. The major risk factor for the HCC development is cirrhosis of the liver from oxidative stress and chronic inflammation. Although, common causes of cirrhosis have been identified as key risk factors for HCC, approximately one-quarter of HCC cases diagnosis were not linked with any predisposing risk factors. Therefore, the major known risk factors for HCC can be divided into four categories: (I) viral

(hepatitis B and C), (II) toxic (aflatoxins and alcohol), (III) metabolic (diabetes and non-alcoholic fatty liver disease), (IV) hereditary hemochromatosis, and immune-related (primary biliary cirrhosis and autoimmune hepatitis) . The geographical variability in the incidence of HCC has been attributed to changes in the natural history and distribution of hepatitis B and C virus (HBV and HCV) infections. It has been estimated that HBV and HCV are responsible for 50-80% and 10-25%, respectively, of HCC cases worldwide (Chitapanarux and Phornphutkul, 2015; Block *et al.*, 2003)

2.1.3. Pathophysiology and Biomarkers of Hepatocellular Carcinoma

There is growing evidence to suggest that gradual accumulation of mutations and genetic changes in pre-neoplastic hepatocytes causes malignant transformation and leads to the HCC development. The tumor may consist of only a single lesion or could be multiple lesions within the liver, the latter being the most common. When the tumor is well differentiated , the neoplastic cells show features of normal hepatocytes, but in poorly differentiated tumors, the cells are large and are often indistinguishable from those of other metastatic tumors.

The normal liver lobule is formed by hepatocytes, cholangiocytes, and non-parenchymal cells (Kupffer cells, sinusoidal endothelial cells, and hepatic stellate cells (HSCs)). Intrahepatic lymphocytes and liver-specific natural killer (NK) cells are present in the sinusoidal lumen and perisinusoidal space of Disse.

The exposure to toxic substances such as alcohol, aflatoxin, DMN, DEN, and pesticides as well as chronic HBV and HCV infections and induction of immune response in liver can produce reactive nitrogen species (RNS) and reactive oxygen species (ROS) leading to chronic inflammation that can damage liver cells, DNA, and activation of hepatic stellate cell, cell proliferation, these lead to

the malignant tumor and HCC, respectively (Figure 3). (Fernandez *et al.*, 2009; Cabibbo *et al.*, 2010; Srisuttee *et al.*, 2011).

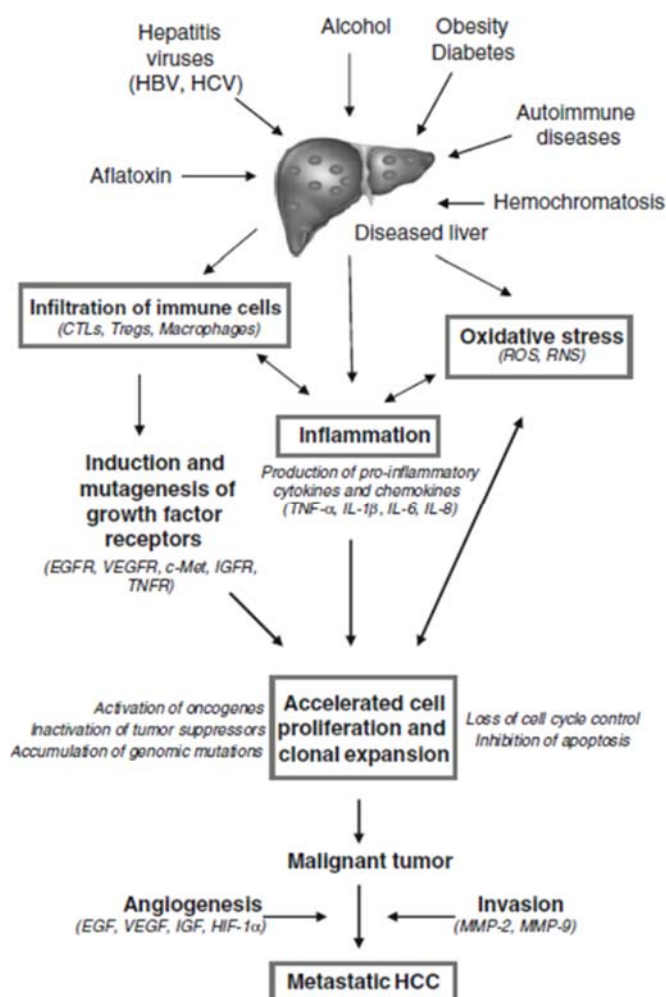


Figure3 Several of risk factors and cofactors of hepatocellular carcinoma development

2.1.4. Tumor Microenvironment

Carcinogenesis is a process that involves the transition of a normal cell into a pre-neoplastic lesion that develops into malignant tumor. In HCC, they are involved in tumour initiation and progression where they produce epidermal growth factor (EGF), hepatocyte growth factor (HGF), fibroblast growth factor (FGF),

interleukin 6 (IL-6), chemokine (C-X-C motif) ligand 12 (CXCL12), and matrix metalloproteases 3 and 9 (MMP-3 and MMP-9) (Pietras and Ostman, 2010).

2.1.5. Inflammation

Inflammation is the means by which the body deals with assault and injury, which may be caused by mechanically (pressure and foreign bodies), chemically (acidity, alkalinity, and toxins), and microorganisms (virus, bacteria, and parasites), internal processes (uremia), and physically (temperature), which is commonly separated into acute and chronic inflammation.

Acute inflammation is the immediate and early response to invaded agents and occurs before adaptive immunity becomes established. Its objects are elimination of invaded agent and suppress the extent of damaged tissues, which is able to be induced by a diversity of stimuli for example physical or chemical agents, penetrating trauma, immune reactions, and infection. The acute inflammation involves with three components including I) changes in structure of the microvascular simplifying to leaking out of plasma proteins and recruitment of leukocytes from the circulation, II) migration of leukocytes from the microcirculation, accumulation and activation of leukocytes within the damaged sites, III) changes in vascular caliber causing increase blood flow. The variety types of cells are involved in inflammation process comprising of endothelial cells lining in blood vessels, circulating leukocytes, connective tissue cells (fibroblasts, mast cell, lymphocytes and macrophages) and extracellular matrix such as fibrous proteins (elastin and collagen), adhesive glycoprotein, and proteoglycans. In biochemical reactions, the inflammatory mediators play a role in amplifying the initial response and influencing its evolution via regulation the following vascular and cellular responses. The first function of inflammatory response is to arrest the injurious effect of the demolish and pathology the injured tissues and dead cells by macrophages, by way of allowing

initiated tissue remodeling, repairing and healing (Medzhitov, 2008; Krishnamoorthy and Honn, 2006).

Chronic inflammation is a prolonged process and it may be weeks or even years. It may appear after a recurrent or progressive acute inflammatory process or from low-grade, smoldering reactions that are unsuccessful to emerge an acute reaction. Chronic inflammation is characterized by 1) attempts to repair by replacing connective tissues including small blood vessels proliferation (angiogenesis) and especially fibrosis, 2) infiltration with mononuclear cells, comprising of plasma, lymphocytes and macrophages cells, a reflection of a continued response against injury, and 3) destruction of injured tissue, largely triggered by secretion generated by the inflammatory cells. Consequently, deformity and scarring are formed that is normally more than those of acute inflammation (Medzhitov, 2008).

Inflammation of liver is able to occur with exposure to a number of agents including chemicals, alcohol, metabolites of drug, bacteria and viruses. If hepatic metabolism is impaired to some degree and fails to convert chemicals and drugs to nonreactive or non-immunogenic substances, the metabolic intermediates formed in hepatic tissues may cause damage of liver (Severi *et al.*, 2010). Chemokines and cytokines such as tumor necrosis factor alpha (TNF- α), interleukin 6 (IL-6), and interleukin 1-beta (IL-1 β), and are produced by Kupffer cells and other cell types that result in liver inflammation. Also, pro-inflammatory enzymes such as cyclooxygenase-2 (COX-2) and inducible nitric oxide synthase (iNOS) are produced by Kupffer cells and other immune cell types that result in the liver inflammation. This reaction coupled with deregulated hepatocyte proliferation can contribute to the pathogenesis of liver cancer (Aravalli *et al.*, 2013).

IL-6 is an important cytokine associated with increased risk of HCC, especially in the presence of cirrhosis (Nakagawa *et al.*, 2009). It has been well

documented that IL-6 is also involved in tumor cell proliferation by inhibiting apoptosis through the signal transducer and activator of transcription 3 (STAT3) activation. IL-6 also forms a critical link between cancer, obesity, and the gender disparity seen during HCC development is attributed to the suppression of IL-6 production in Kupffer cells by estrogen (Yu *et al.*, 2009).

TNF- α is secreted by Kupffer cells and other immune cells in response to tissue injury, modulates protein kinase B (Akt) and nuclear factor kappa B (NF- κ B) pathways, and is involved in tumor progression and development (Leonardi *et al.*, 2012).

IL-1 β is a pro-inflammatory cytokine in HCC, promotes the proliferation of hepatic stellate cells (HSCs), transdifferentiation and activation into the myofibroblastic phenotype. IL-1 β has also been shown to induce the TNF-related apoptosis-inducing ligand (TRAIL) expression in HCC cell lines (Hep3B, HuH7, HepG2) (Leonardi *et al.*, 2012).

COX-2 and iNOS are pro-inflammatory enzymes in HCC, which are produced from Kupffer cells, expressed in hepatocytes and involved in the development of HCC (Wu, 2006; Mann *et al.*, 2007). COX-2 appears to induce angiogenesis in several of tumors or to act as a biomarker of cancer (Yoysungnoen *et al.*, 2006). Previous study found that the expression of COX-2 was significantly correlated with the expression of vascular endothelial growth factor (VEGF) (Xiong *et al.*, 2003).

2.1.6. Oxidative Stress

Nomally, all life forms preserve a reducing cellular redox environment within their cells by a constant input of metabolic energy maintaining, a process controlled by enzymes with varying of cellular functions. The imbalance in the normal redox state can have toxic effects in the cell due to an increased the free radicals (reactive nitrogen species; RNS and reactive oxygen species; ROS) production,

which resulting in oxidative stress. RNS and ROS are products from both external sources and normal cellular metabolism (Severi *et al.*, 2010). During the cellular imbalance caused by ROS formation, highly reactive radicals can damage proteins, RNA, DNA, and lipid components, which this may lead to mutations or apoptosis (Severi *et al.*, 2010).

In the liver, Kupffer cells represent the main sources of free radicals are activated for RNS and ROS production by pro-inflammatory cytokine mediators and endotoxin. RNS and ROS are involved in the activation and transcription of growth factors, pro-inflammatory enzymes, chemokines and cytokines, thereby playing crucial roles in the progression and pathogenesis of HCC. Cells have developed mechanisms to counteract the oxidative stress that includes redox active antioxidant enzymes (superoxide dismutase (SOD), catalase (CAT), glutathione peroxidase (GPx), glutathione (GSH), and thioredoxin (TRX) (Severi *et al.*, 2010). Malondialdehyde (MDA) formed during lipid peroxidation was shown to accumulate in the serum of chronic hepatitis patients, serving as a potential biomarker of HCC (Aravalli *et al.*, 2013).

2.1.7. The mechanism of cell response to oxidative stress and inflammation

Cells were activated by inflammation and oxidative stress pass to the mitogen-activated protein kinases (MAP kinases) signalling such as p38 mitogen-activated protein kinases (p38), c-JUN N-terminal kinases (JNK) and extracellular signal-regulated kinases (ERK), cells were response to these in two pathways in **Figure 4**. First (number 1), NF- κ B pathway, it is a central role in regulation of transcription of pro-inflammatory mediators like chemokines and cytokines. The inactive form of NF- κ B in cytoplasm was activated to active form (NF- κ B) by MAP kinases activated from inflammation and oxidative. NF- κ B translocated to nucleus result in expression of pro-inflammatory mediators such as IL-6, TNF- α , iNOS and COX-2. Second, nuclear

erythroid 2-related factor 2 (Nrf2) pathways, it is a central role in regulation of transcription of antioxidant like antioxidant enzymes, non-enzymatic antioxidant and detoxifying enzymes. The inactive form of Nrf2 (Nrf2-keap1 complexes) in cytoplasm was activated to active form (NF- κ B) by activated-MAP kinases from oxidative stress and inflammation. Free form of Nrf2 translocated to nucleus result in expression of antioxidant enzymes (SOD, CAT and GPx), non-enzymatic antioxidant (glutathione; GSH) and detoxifying enzymes (glutathione S-transferase; GST, NAD(P)H dehydrogenase quinone 1; NQO1 and heme oxygenase 1; HO-1) (Aggarwal *et al.*, 2006; Gallego and Tunon, 2007).

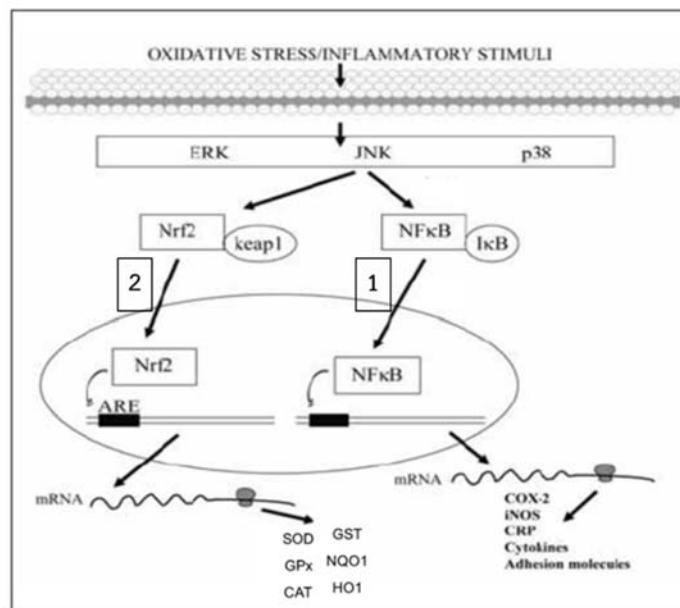


Figure 4 The mechanism of cell response to oxidative stress and inflammation

2.1.8. Histology of Hepatocellular Carcinoma

Histopathological progression of HCC present in **Figure 5**. After hepatocytes were injured by the several of factors such as alcohol, aflatoxin, chemical substances, HBV, HBC and drugs, there is necrosis followed by hepatocyte proliferation. The continuous cycle of this destructive is the cause of regenerative

process fosters a chronic liver disease condition which culminates in the liver cirrhosis. Cirrhosis is characterized by abnormal liver nodule formation surrounded by scarring and collagen deposition of the liver. Subsequently, hyperplastic nodules are observed, followed by dysplastic nodules and ultimately HCC, which can be further classified into poorly differentiated tumors, moderately differentiated and well differentiated (Farazi and Depinho, 2006).

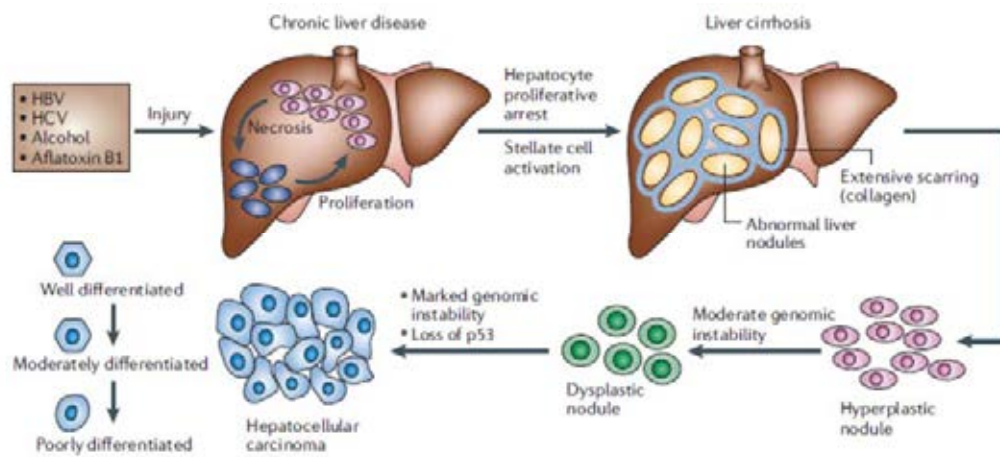


Figure 5 Histopathological progression of HCC

2.2. Apoptosis

Apoptosis is the natural mechanism of cells for programmed cell death. It is particularly critical in long-lived mammals as it plays a critical role in development as well as homeostasis. It serves to eliminate any unimportant or unwanted cells and is a highly regulated process. There are a wide several of conditions that will result in the pathway of apoptotic becoming activated including uncontrolled proliferation or DNA damage (Danial *et al.*, 2004). As soon as apoptosis is signaled, changes start to occur within the cell. These changes include activation of caspases which cleave cellular components required for normal cellular function such

cytoskeletal and nuclear proteins. As a result of caspase activity, apoptotic cells begin to shrink and undergo plasma membrane changes that signal the macrophage response (Elmore, 2007).

The apoptotic pathway is triggered by both intracellular and extracellular signals. There are two different pathways that lead to apoptosis: the intrinsic and extrinsic pathways (**Figure 6**) that correlate with the signal type. They are also referred to as the mitochondrial and death receptor pathways, respectively (Hassan *et al*, 2014). The intracellular signals include DNA damage, growth factor deprivation and cytokine deprivation, whereas the most common extracellular signals are death-inducing signals produced by cytotoxic T cells from the immune system in response to cells that are damaged or infected. The pathways converge at the executioner caspases (Elmore, 2007).

2.2.1. Apoptosis pathway

2.2.1.1. Intrinsic pathway

The intrinsic pathway is the apoptosis mechanism that uses the mitochondria and mitochondrial proteins (**Figure 6**). Oncogenes upregulated or DNA damaged can stimulate this pathway. In addition, stimulation of this pathway includes oxidant, growth factor deprivation, microtubule targeting drugs and DNA-damaging molecules (Hassan *et al.*, 2014). The overall pathway is controlled by the BCL-2 family of proteins. Several apoptotic stimuli result in the upregulation of BH3-only proteins, which then activate both BAX and BAK. BAX is regulated by p53, a tumor suppressor gene (Lopez *et al.*, 2015; Zaman *et al.*, 2014; Lomonosova *et al.*, 2008). Once activated, BAX and BAK, which leads to mitochondrial outer membrane permeabilization (MOMP). MOMP is the defining event of intrinsic apoptosis and is considered the point of no return. The permeabilization allows the release of intermembrane proteins namely, cytochrome c, second mitochondria-derived activator of caspase (SMAC) and Omi. Upon the release of cytochrome c, the

apoptosome is formed from cytochrome c, apoptotic protease-activating factor-1 (APAF-1) and procaspase-9 (Lopez *et al.*, 2015). Within the apoptosome, procaspase-9 is converted into caspase-9 (active form) which activation of the executioner caspases-3 and -7 (Hassan *et al.*, 2014; Zaman *et al.*, 2014). The executioner caspases quickly begin to break down proteins leading to cell death.

2.2.1.2. Extrinsic pathway

The extrinsic pathway uses extracellular signals to apoptosis induction (**Figure 6**). The signal of cell death, also known as death ligands, bind to tumor necrosis factor (TNF) family death receptors (Zaman *et al.*, 2014). Some death ligands include tumor necrosis factor (TNF), TNF-related apoptosis-inducing ligand (TRAIL), and Fas ligand (Fas-L) (Green *et al.*, 2015; Goldar *et al.*, 2015). An adaptor protein is selected to the death receptor; TNF receptor-associated death domain (TRADD) and adaptor proteins include Fas-associated death domain (FADD). Initiator procaspases-8 and -10 bind to the adaptor protein, forming the death-inducing signaling complex (DISC). The procaspases have a death effector domain (DED) that binds to the adaptor protein at its DED. Procaspases-8 and -10 are activated by DISC. Executioner caspases 3, -6 and -7 are then activated and begin the cleavage of proteins and the cytoskeleton leading to cell death. DISC is controlled by the c-FLIP inhibitor which is homologous to caspase-8 yet lacks caspase activity (Zaman *et al.*, 2014; Green *et al.*, 2015; Goldar *et al.*, 2015)

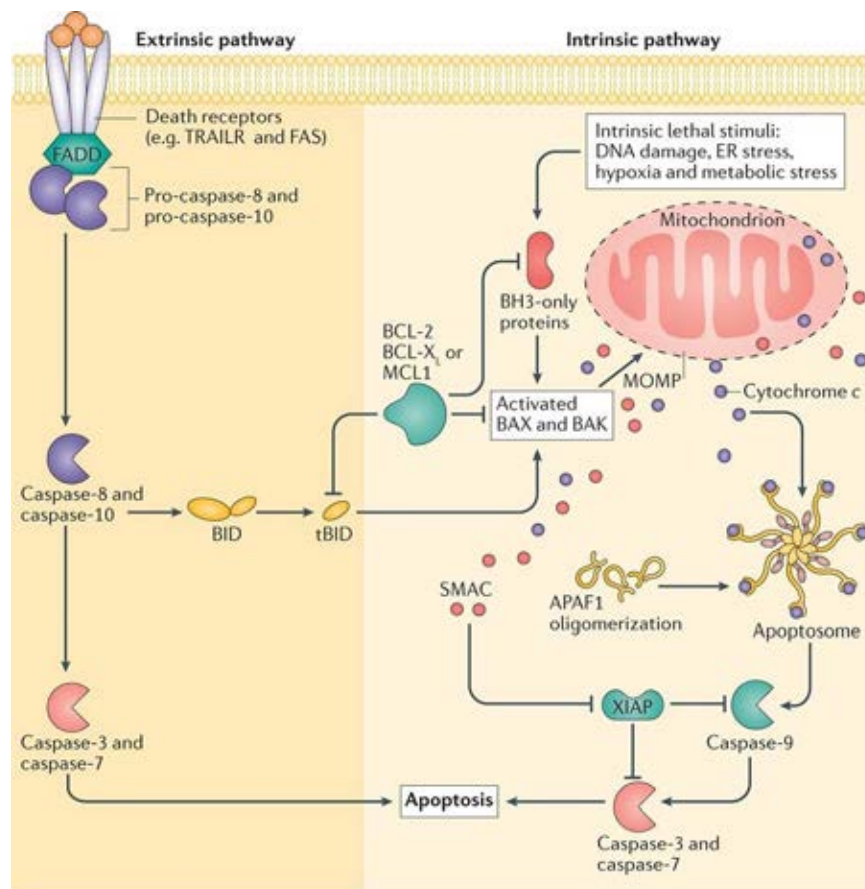


Figure 6 Intrinsic and Extrinsic Pathway of Apoptosis

2.2.2. Apoptosis and cancer

The main points of cancer are present in all cancer cells regardless of the cause or type; these include angiogenesis and apoptosis evasion, and uncontrolled growth, (Arbiser *et al.*, 2017; Xu *et al.*, 2015). Apoptosis is the main functions for prevention of cancer. Typically, it is the intrinsic pathway that is inhibited in cancer, however, there are a wide range of means to inhibit apoptosis. The loss of apoptotic control allows cancer cells to long survival and gives more time for the accumulation of mutations which can increase invasiveness during stimulate angiogenesis, tumor progression, interfere with differentiation and deregulate cell proliferation (Hassan *et al.*, 2014; Lopez *et al.*, 2015). There are varies ways in which cancer cells which evade apoptosis: the trigger for apoptosis can be disabled or

caspace function can be inhibited. Upregulation of anti-apoptotic BCL-2 proteins and loss of BAX and/ or BAK are the predominant strategy of evasion. BCL-2 is not considered an oncogene, but mutations in it enhance tumor onset. Many expression of BCL-2 proteins are present in over half of all cancers, regardless of type. This results in tumour cells that are resistant to any intrinsic and extrinsic apoptotic stimuli which includes some anticancer drugs (Lopez *et al.*, 2015).

Cancer cells can evade apoptosis through a several of mechanisms. Deviation from the normal pathways can either cause pro-apoptotic regulation or pro-survival regulation. While not classified as such, pro-survival genes are potentially oncogenic and can have mutations that increasing of their expression. On this same note, pro-apoptotic genes may act as tumor suppressors (Goldar *et al.*, 2015). All of the activators and inhibitors have been found outside their normal range of cancer cell lines expression. For example, in almost half of all cancers of human, Bcl-2 expression is promoted (Adam *et al.*, 1998; Yip and Reed, 2008). The vast majority of traditional anticancer drugs depend on mechanisms of Bcl-2/ Bax-dependent to kill cancer cells (Yip and Reed, 2008). This leads to the drugs failure if this mechanism is changed or disrupted in any way and forms an intrinsic chemoresistance. In addition, the threshold for radiotherapy or chemotherapy is raised due to apoptosis defects which leads to resistance to those therapies. Altered signaling pathways of apoptosis improve resistance to the immune system as the immune system depends on apoptosis (Hassan *et al.*, 2014).

2.2.3. Pro-apoptotic regulation in tumour cells

The regulation in tumour cells, there are several signals that can occur in cancer cells that quickly lead to apoptosis despite their typical evasion of apoptosis. Cancer cells are ‘primed for death’ meaning that they are closer to activating the apoptotic pathway than normal cells (Elkholi *et al.*, 2014). The sensitivity for apoptotic signals increases in these primed cells. Priming is due to the

dual upregulation of pro-apoptotic and anti-apoptotic proteins, which results in cells that undergo apoptosis more quickly and easily. If upregulation of the anti-apoptotic proteins is halted or disrupted, then the pro-apoptotic proteins can trigger apoptosis. Targeting primed cells with an inhibitor of anti-apoptotic proteins could result in the death of the tumour cell and apoptosis (Lopez *et al.*, 2015; Elkholi *et al.*, 2014).

In addition, cancer cells are more sensitive to apoptosis because of environmental stressors so that they endure low availability of hypoxia or nutrients. Normally, tumor cells are more sensitive to the extrinsic pathway than the intrinsic one, which suggests that the extrinsic pathway should be targeted for cancer therapy. Other tumour suppressors mediate, oncogenes or affect apoptosis which could be the cause for apoptotic evasion. The p53, tumor suppressor activates transcription of pro-apoptotic proteins from the Bcl-2 family (Elkholi *et al.*, 2014). If a tumor suppressor mutation is the cause of apoptotic evasion, then the apoptotic pathway would need to be activated in another manner. This knowledge can help predict the best and most effective mechanism to target in cancer treatment.

2.2.4. Pro-survival regulation in tumour cells

There are several inhibitors of both the apoptotic pathways that are overexpressed in tumours. Increased expression of anti-apoptotic proteins like Bcl-2 and decreased expression of pro-apoptotic proteins like BAX are two methods for cells to resist apoptosis (Hassan *et al.*, 2014). The defects in the apoptosis allow tumour cells to resist traditional treatment such as chemotherapy and radiotherapy. This is done by raising the threshold needed for cell death. In addition, this resistance to apoptosis can also promote resistance to the overall immune system as the immune system depends on the integrity of the apoptosis pathways (Danial *et al.*, 2004; Lopez *et al.*, 2015). The pro-survival proteins throughout the apoptotic pathway include BCL-xl, BCL-2, BCL-w, NR-13, mcl-1, A1, E1b-19K, BHRF1, ORF16,

LMW5-HL and KS-BCL-2 (Adam and Cory, 1998). Several of these proteins have been found overexpressed in cancer. For instance, BCL-2 has elevated gene expression in over half of all cancers and XIAP is overexpressed in many different tumours. The overexpression of these anti-apoptotic proteins inhibits apoptosis from a variety of signals including oxidative stress, growth factor deprivation and hypoxia (Yip *et al.*, 2008; Elkholi *et al.*, 2014).

While pro-survival proteins are overexpressed, the pro-apoptotic proteins are inhibited or under-expressed. Caspases, particularly the executioner caspases, are under-expressed in tumour cells (Elkholi *et al.*, 2014). Inactivation mutations or deletions in caspase genes have been observed in several cancers (Yip and Reed, 2008). A globin found preferentially in neurons, neuroglobin (NGB), associates with cytochrome c. This impairs its release into the cytosol and activation of the apoptosome. NGB has been found at higher concentrations in cancer cells which is believed to render cells insensitive to chemotherapy and radiotherapy due to its interference in the intrinsic apoptotic pathway. In addition, cancer cells have found ways to survive past MOMP. In order for an apoptotic response to occur, 15% of the cell's mitochondrial population must undergo MOMP. If cells are able to halt MOMP before 15% of the mitochondria are permeabilized, then the apoptotic response will not continue to propagate. This gives cancer cells more time to prevent a full apoptotic response (Yip and Reed, 2008; Elkholi *et al.*, 2014).

2.2.5. Apoptosis and cancer treatment

One way of cancer treatment is to gain control or possibly terminate the uncontrolled growth of cancer cells. Using the mechanism of cells for death is a highly effective strategy. In addition, targeting of apoptosis is the most successful non-surgical treatment. Apoptosis targeting is also effective for all types of cancer, as apoptosis evasion is a hallmark of cancer and is nonspecific to the cause or type of the cancer. There are many anticancer drugs that target various

stages in both the intrinsic and extrinsic apoptosis pathways (Liu *et al.*, 2017; Villa-Pulgarin *et al.*, 2017; Bao *et al.*, 2017). Two common methods for therapeutic targeting are inhibition of antiapoptotic molecules and stimulation of proapoptotic molecules. Some of the targets that have been researched include ligands for death-receptors, inhibitors for BCL-2, XIAP inhibition and alkylphospholipid analogs (APL) which act as apoptotic signals (Hassan *et al.*, 2014; Lopez *et al.*, 2015). Any stage in the pathways can be targeted for treatment, however, there is no indication of which target is most effective. As more apoptosis-inducing anticancer drugs are designed, the most effective targets will be determined.

2.3. Turmeric and bioactive compounds

Curcuma longa Linn (Turmeric) is a tropical plant native to south and southeast tropical Asia. It is a member of the ginger or *Zingiberaceae* family. Rhizome of turmeric is used as coloring, spice and flavoring in food. The chemical constituents of turmeric are protein (6.3%), lipid (5.1%), minerals (3.5%), carbohydrate (69.4%), moisture (13.1%), essential oil (5.8%), curcuminoids (3-4%), and volatile oil (7%) Ruby *et al.*, 1995. The bioactive compounds in turmeric can be divided into two groups (**Figure 7**): (1) volatile oils: aromatic turmerones such as α -turmerone and β -turmerone, and (2) curcuminoids or diarylheptanoids: curcumin (70-80%), demethoxycurcumin (15-25%) and bisdemethoxycurcumin (2.5-6.5%) (Anand *et al.*, 2008; Strimpakos and Sharma, 2008; Wichitnithad *et al.*, 2009)

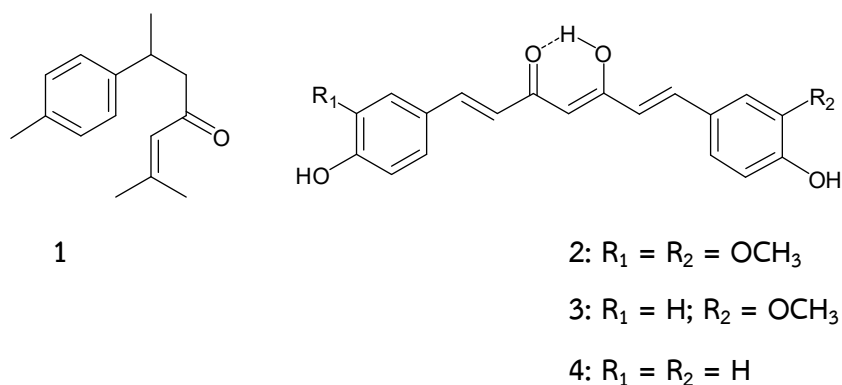


Figure 7 Structure of bioactive compounds in turmeric 1: turmerone, 2: curcumin, 3: demethoxycurcumin and, 4: bisdemethoxycurcumin

2.3.1. Pharmacological activities and limitation of curcumin

Curcumin (1,7-bis(4-hydroxy-3-methoxy-phenyl)-1,6-heptadiene-3,5-dione; diferuloylmethane) is a main bioactive compound of curcuminoids from turmeric, which not has been shown discernable toxicity (Epstein *et al.*, 2010). The several pharmacological activities of curcumin were reported, including antioxidant activities (Pinlaor *et al.*, 2009; Lee *et al.*, 2010), anti-inflammation (Nonn *et al.*, 2007; Buadonpri *et al.*, 2009), anti-cancer activities (Ajaikumar *et al.*, 2007; Wu *et al.*, 2010; Aziza *et al.*, 2014), anti-mutagenic activity (Anand *et al.*, 2008), anti-fungal (Mishra *et al.*, 2005), anti-bacterial activity (Reddy *et al.*, 2005) and hepatoprotective effect (Girish *et al.*, 2009).

2.3.2. Anti-cancer activities and mechanisms of curcumin

Curcumin shows anti-carcinogenic effects on leukemia, lymphoma, brain cancer, and colorectal epithelium cancers (Mimeault and Batra, 2011). It is also a potential of tumor-inhibitory agent with chemo-preventive effects against colon cancer (Kwon *et al.*, 2009). Moreover, dietary curcumin is show increases antioxidant defenses in lung and ameliorates radiation-induce pulmonary fibrosis and improves survival in mice (Lee *et al.*, 2010). The study in animal model found that curcumin

reduced the over-expression of COX-2 and serum VEGF in implanted hepatocellular carcinoma in nude mice, indicating that curcumin could inhibit tumor angiogenesis (Yoysungneon *et al.*, 2006). Curcumin play a potent role in the regulation of proliferation and apoptosis in various types of cancer underlying mechanism the apoptosis pathway by induction of the apoptosis (Karunakaran *et al.*, 2005). Curcumin also induces typical characteristics of apoptosis like cell shrinkage, chromatin condensation, and DNA fragmentation in immortalized mouse embryo fibroblast NIH 3T3 cells in a concentration and time dependent manner. The main of apoptotic signaling pathways have been characterized in mammalian cells which was the intrinsic or mitochondrial pathway. *In vitro* and *in vivo* experiments have shown the ability of curcumin to sensitize tumour cells to TRAIL induced apoptosis, inhibit NFκB activity, and downregulate expression of the antiapoptotic Bcl-2, Bcl-xL, and XIAP proteins which showed in **Figure 8** (Karunakaran *et al.*, 2005; Zhi-Dong *et al.*, 2014). Moreover, curcumin upregulates expression of P53, Bax, Bak, PUMA, Bim, NOXA and death receptors DR4 and DR5, triggering activation of caspase-3, -9, -7 which showed in **Figure 8** (Karunakaran *et al.*, 2005; Rodríguez *et al.*, 2013; Zhu and Bu, 2017).

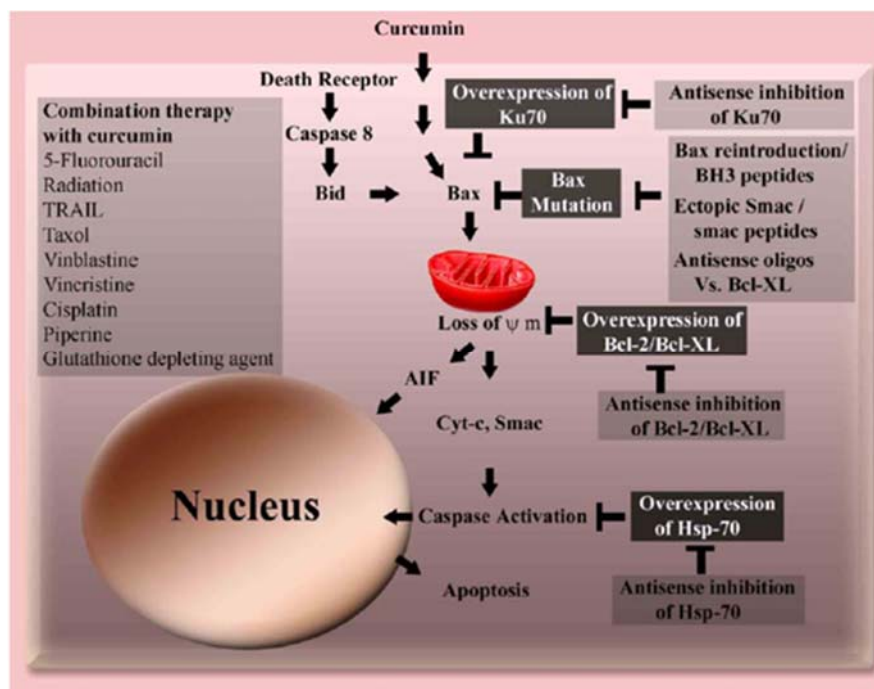


Figure 8 Potential strategies targeting curcumin-induced apoptotic pathway to overcome chemoresistance in cancers

2.4. Limitation of curcumin for anti-cancer agent development

Although curcumin has several pharmacological activities, especially anti-cancer activities and no discernable toxicity, curcumin is limited in development as a drug because of its low water solubility and instability in aqueous and basic solutions, especially in the intestine. The degradation pathways of Cur are depicted in **Figure 9**. The part of metabolism, Cur undergoes extensive metabolism in the alimentary tract especially in liver and intestine. The hepatocytic metabolism of Cur yields reduced metabolites including tetrahydroCur hexahydroCur and octahydroCur as major metabolites. The summarized metabolic pathways of CUR are illustrated in **Figure 10**.

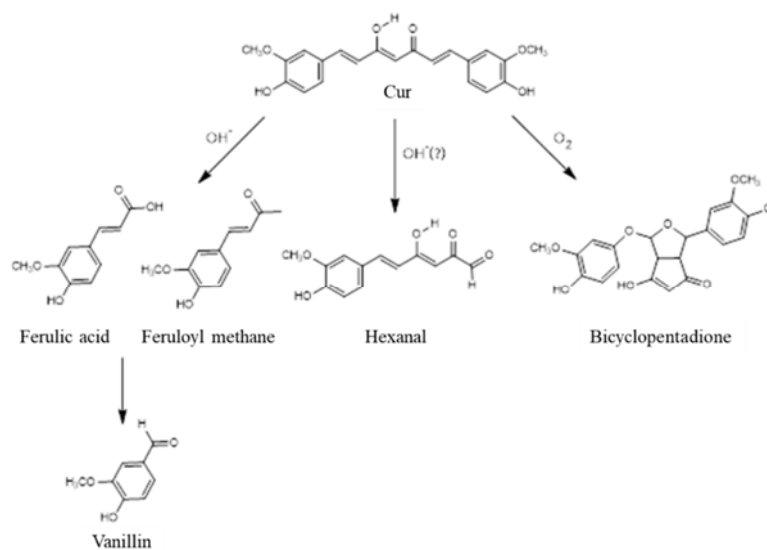


Figure 9 Degradation products of Cur from alkaline hydrolysis and autoxidation. The degradation pathway to hexanal (pathway with a question mark) has not been confirmed

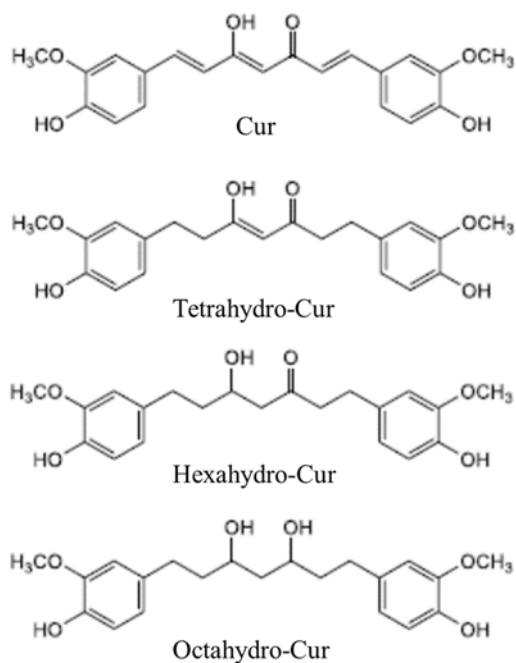


Figure 10 Chemical structures of Cur and its major reductive metabolites

These properties were cause poor absorption, rapid metabolism and elimination of curcumin, which leads to poor oral bioavailability (Sharma *et al.*, 2005; Anand *et al.*, 2007; Yang *et al.*, 2007). These problems of curcumin involve degradation of its phenolic groups (Wang *et al.*, 1997). Several methods are used to enhance the solubility, chemical stability and bioavailability of curcumin, including incorporation in micelles, liposomes and phospholipids (Zhang *et al.*, 2011). A prodrug approach can also be used for chemical and biochemical stabilization to overcome barriers that hinder drug delivery. Prevention of phenolic degradation of bioactive compounds is possible by conjugation of the phenol with compounds such as folic acid, fatty acid and amino acid via ester bonds (Singh *et al.*, 2010; Harish *et al.*, 2010).

2.5. Prodrugs of curcumin

Prodrug design is a process for modifying the structure of parent compounds by conjugation with a pro-moiety via covalent bond. The prodrug refers to a pharmacologically inactive compound that is transformed by enzymes such as esterases, phosphatases and carboxylases in the mammalian system into an active substance by chemical or metabolic means. The principle of prodrug design is that prodrugs are inactive compounds with improved physicochemical properties such as water solubility and stability, compared with parent compounds. Moreover, prodrugs can be transformed to the active compound in mammalian and biological systems.

Synthesis of curcumin prodrugs may improve the problems in development of curcumin as a drug, especially its low water solubility and instability in aqueous and basic solutions, which cause poor oral bioavailability. Previous curcumin prodrugs have been synthesized to improve the solubility and stability of curcumin by conjugation of the phenolic groups of curcumin with compounds such as glycosides, acetic acids, and amino acids via an ester bond.

2.5.1. Curcumin- β -diglucosides

Curcumin- β -diglucosides were synthesized using glycosides, which are soluble in water, via conjugation with the phenolic groups of curcumin through an ester bond. These curcumin- β -diglucosides had increased water solubility compared with curcumin. In *Staphylococcus aureus* and *Escherichia coli*, curcumin- β -diglucosides had antibacterial activity with minimum inhibitory concentrations (MICs) of 0.051 and 0.469 μ M, respectively, whereas, curcumin had MICs of 0.081 and 0.611 μ M, respectively (Parvathy *et al.*, 2009).

2.5.2. Acetoxy-curcumin

Acetoxy-curcumin was synthesized using acetic acid conjugated with the phenolic groups of curcumin via an ester bond. Acetoxy-curcumin has high solubility in PBS (pH 7.4) compared with curcumin, and has higher cytotoxicity in colon cancer cells, with a 50% effective concentration (EC_{50}) of 26.5 μ M compared to an EC_{50} of 42.4 μ M for curcumin (Kim *et al.*, 2012).

2.5.3. Curcumin-amino acids

Curcumin-amino acids were synthesized using amino acids such as glycine, serine, proline, alanine, leucine or cysteine conjugated with the phenolic groups of curcumin via an ester-bond. The curcumin-amino acid conjugates have high solubility in water, with the conjugates with glycine and proline displaying the highest solubility (10 mg/ml). Studies using the DPPH method found that curcumin-amino acids have significantly more potent antioxidant activities than curcumin (Parvathy *et al.*, 2010). Curcumin-amino acids also have significantly more potent antibacterial activities than curcumin (Dubey *et al.*, 2008).

2.5.4. Succinate ester prodrugs of Curcumin

Wichitnithad *et al.* synthesized six succinate ester prodrugs of curcuminoids and tested their cytotoxicity against Caco-2 cells (Wichitnithad *et al.*,

2011). Among the six prodrugs, CurDD, an ethyl succinyl ester prodrug of Cur, demonstrated the most potent cytotoxic activity with the IC_{50} value of 1.84 μ M. The encapsulation of CurDD in chitosan/alginate nanoparticles significantly enhances the cytotoxicity of CurDD against breast cancer (MDA-MB-231) cells (Bhunchu *et al.*, 2016). CurDD showed higher stability in phosphate buffer pH 7.4 in comparison with Cur (Wichitnithad *et al.*, 2011).

2.6. Experimental mouse models for hepatocellular carcinoma

2.6.1. Chemical-induced liver cancer in animal models

Exposure to chemicals that is toxic to the liver repeatedly as a way to cause of liver cancer. Thioacetamide (TAA), carbon tetrachlorides (CCl_4), diethylnitrosamine (DEN), are the most commonly used as toxicity agents for liver. First, the fibrosis development occurs in pericentral areas, building bridges between areas of central and the secondary fibrosis development occurs between central and portal areas ultimately bringing about to progression of cirrhosis. The models are simple to perform but complicate to operate in case of providing toxic agent ad libitum (diet or in drinking water). An absorption or metabolism of the toxic agent are affected such as the reaction of DEN or differences in drug metabolism between a genetically engineered animal and its wild-type regulate (Constandinou *et al.*, 2005; Bakiri and Wagner, 2013).

2.6.1.1. Dimethylnitrosamine (DEN)

DEN is used to HCC induction in rodents, and is the most widely used chemical to liver cancer induction in mice. The toxic metabolite of DEN is activated in hepatocytes by the cytochrome P450 enzyme family and acts as a complete carcinogen (Bakiri and Wagner, 2013). DEN is a DNA alkylating agent leading to the production of mutagenic DNA adducts. Additionally, activation of DEN by cytochrome P450 can produce ROS, which damage proteins, DNA and lipids which

lead to hepatocyte death. Similar to what occurs in patients, development of HCC in this model usually follows a slow multi-step sequence, where cycles of necrosis and regeneration promote neoplastic transformation. The progression from early dysplastic lesions to fully malignant tumors is associated with an increased occurrence of genomic alterations (Newell *et al*, 2008; Bakiri and Wagner, 2013).

2.6.1.2. Carbon tetrachloride (CCl₄)

CCl₄ is altered into a toxic trichloromethyl radical (CCl₃) radical by enzyme expressed in perivenular hepatocytes, CYP2E1. It activates an acute centrilobular necrosis which induce a wound healing response, by recruitment of inflammatory and phagocytic cells to clear necrotic zones. The activation of fibrogenesis and increased ECM, proliferation of non-parenchymal and parenchymal cells to supplant dead cells, which would reconstitute liver integrity. When the attack is repeated, successive rounds of wound healing occur prior to resolution of the previous one resulting in fibrosis formation and HCC development, respectively. (Constandinou, 2005).

2.6.1.3. Thioacetamide

Thioacetamide (TAA) is another toxic widely used for fibrosis-induction. It damages both zones 1 and 3 hepatocytes with periportal injury being more prominent than with other toxics. It is repeatedly injected (intraperitoneal i.p.) or administered in the drinking water (at a concentration adapted to water consumption). A long time is needed for significant fibrosis (Salguero *et al*, 2008), but this model is non-invasive and requires minimal handling of the animals. Cholangiocarcinoma and HCC have been described in rats after long time exposure to TAA (Newell *et al*, 2008).

2.6.2. Xenograft models

In xenograft models, the tumors are produced by injection of human cancer cells from a cell culture lab in immune deficient mice. Severe combined immune deficient (SCID) or nude mice are often used as hosts. Tumor xenografts can be established either by inoculation of human tumor cell lines or by direct implantation of biopsy material. Many kinds of xenograft models can be distinguished. First, the ectopic model, which tumours cells of human are injected subcutaneously in the flank of mice. Second, the orthotopic model, tumour cells are injected intrahepatically into the mice. The orthotopic xenograft model is more suitable for extrapolation to humans and gives information about the metastatic spread of the tumour. The advantage of xenograft mouse models is the short time span needed for the tumours development and the fact that it is an efficient way to show proof-of-principle when enough cell lines are used. This technique provides a model that allows investigation of aspects as pharmacokinetics, absorption, in vivo toxicity of a compound in a preclinical trial. Tumor phenotypes can vary remarkably between lines; it is therefore important to use different cell lines when using the xenograft model (Kerbel, 2003; Richmon and Su, 2008).

CHAPTER 3

RESEARCH METHODOLOGY

3.1. Cell lines, Media, Chemicals and Equipments

- 1) Human colorectal adenocarcinoma (Caco-2, ATCC No. HTB37), USA
- 2) Human hepatocellular carcinoma (HepG-2, ATCC), USA
- 3) Dulbecco's Modified Eagle Medium (DMEM) (Gibco, 12800), USA
- 4) Fetal bovine serum (FBS) (Gibco, 16000-044), USA
- 5) L-Glutamine 200 mM (100x) (Gibco, 25030-081), USA
- 6) Nonessential amino acids (Gibco, 11140-050), USA
- 7) Penicilin-Streptomycin (Gibco, 15140-122), USA
- 8) Sodium bicarbonate (NaHCO_3) (MW 84.01) (Sigma Co. S5761), USA
- 9) BCATM Protein Assay Reagent A (Thermo Scientific cat.no. 23223), USA
- 10) Bovine serum albumin (BSA), Sigma-Aldrich, USA
- 11) 30% Acrylamide/Bis solution, 29:1 (Bio-Rad, 1610156), USA
- 12) Trizma® base, Sigma-Aldrich, USA
- 13) Glycine, Bio-Rad, USA
- 14) Ammonium persulphate (APS), Sigma-Aldrich, USA
- 15) TEMED, Merck Millipore, Germany
- 16) Blocking Powder, Bio-Rad, USA.
- 17) Mouse VEGF ELISA kit (Sigma-Aldrich, RAB0510), USA
- 18) Mouse IL-6 ELISA kit (Biolegend, 431301), USA
- 19) Mouse ALT ELISA kit (Biocompare, MBS2022063), USA
- 20) Mouse AST ELISA kit (Biocompare, MBS2019147), USA
- 21) Bax (D2E11) Rabbit mAb (Cell Signaling, #5023), USA
- 22) Bcl-2 (D174C4) Rabbit mAb (Cell Signaling, #3498), USA
- 23) COX-2 Rabbit mAb (Cell Signaling, #4842), USA

- 24) Anti-rabbit IgG, HRP-linked Ab (Cell Signaling, #7074), USA
- 25) Annexin V-FITC Apoptosis detection kit (Merck Millipore, PF032), Germany
- 26) 37% Hydrochloric acid (HCl), Merck, Germany
- 27) Sodium chloride (NaCl), Sigma-Aldrich, USA
- 28) Sodium hydroxide, Merck, Germany
- 29) Western Blotting Reagent, Merck Millipore, Germany
- 30) Laminar flow hood, Model: BV-126 (Thermo Scientific), USA
- 31) CO₂ Incubator for cell culture (Thermo Scientific), USA
- 32) Mini-PROTEAN® Tetra Cell, Mini Trans-Blot® Module, and PowerPac™ HC Power Supply (Bio-Rad, #1658035), USA
- 33) Vortex mixer, Model: Vortex-Genie 2, Scientific Industries, USA
- 34) pH meter, Model: SevenEasy™, METTLER TOLEDO, Italy
- 35) Stirrer, Model: IKA® C-MAG HS-7
- 36) Centrifuge (Hettich instrument 1706-01 Rotina 380R Benchtop), USA
- 37) Gel Documentation system, Bio-Rad Laboratories Inc., Berkeley, California
- 38) Inverted microscope, Nikon model TMS, Japan
- 39) Microplate reader (CLARIOstar, BMG LABTECH, Germany).
- 40) Flow Cytometer (Guava®easyCyte Flow Cytometers, MerckMillipore, Germany).
- 41) Autoclave, Model: HA-3D, Hirayama, Japan
- 42) 6 and 96 well plate for cell culture (Corning), USA
- 43) 75 T-flask for cell culture (Corning), USA
- 44) Trans-well insert 6 well plate (ThinCerts™-TC Einsätze, Greiner Bio-one), Switzerland

Methodology of study

The methodology of this study was showed in **Figure 11**.

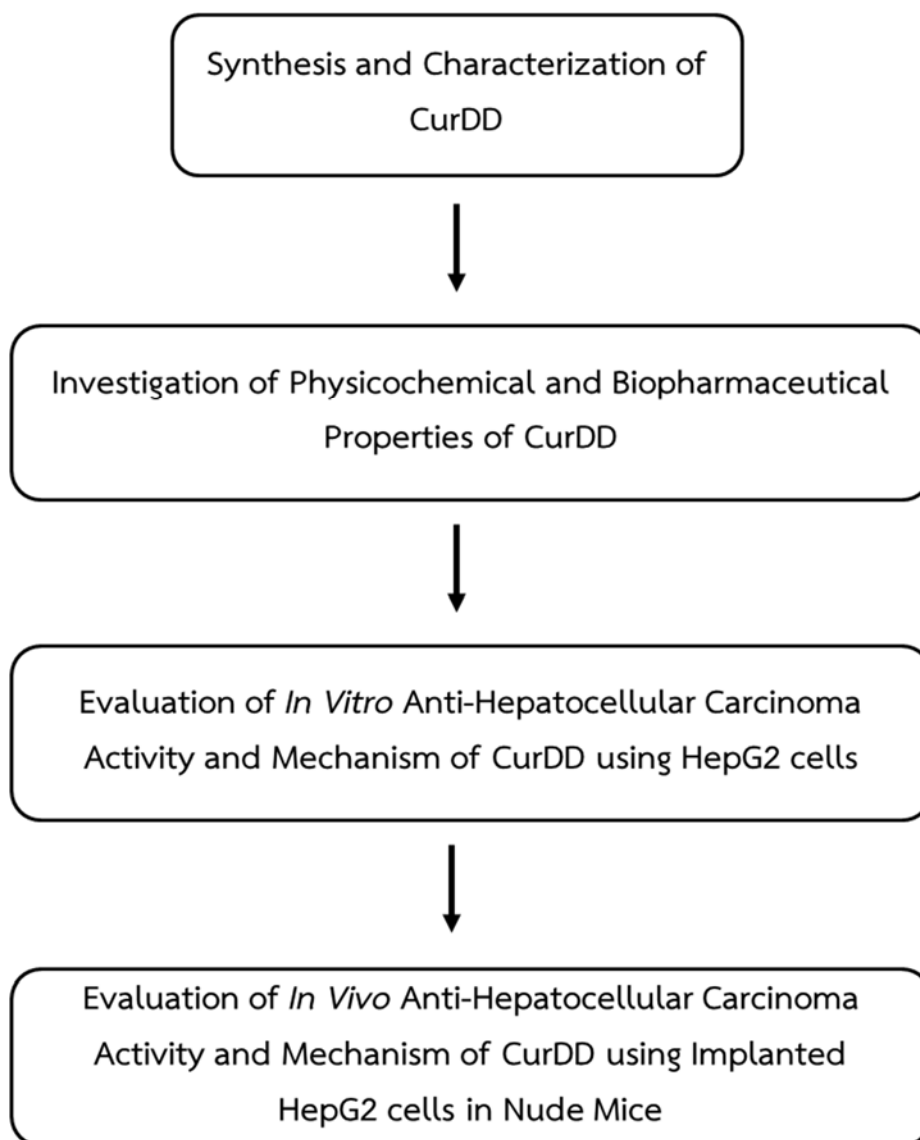


Figure 11 Methodology of study

3.2. Cur and CurDD

Cur (purity >98% by HPLC) and CurDD (purity >98% by HPLC) were synthesized and characterized using the previously reported method with some modification (Wichitnithad *et al.*, 2011). ¹H-NMR and mass spectrum, and chromatogram of Cur and CurDD were showed in Appendix A and B.

3.3. Investigation of physicochemical properties of Cur and CurDD

3.3.1. Investigation of water solubility of Cur and CurDD

The solubility study was performed using the standard flask method of the Organization for Economic Cooperation and Development (OECD) (OECD Guidelines for the Testing of Chemicals: Water Solubility; 1995). Cur or CurDD was added to a flask. Water was added and the flasks were capped. The samples were continuously shaken at 100 rpm for 24 h at 25°C. Then, the samples were centrifuged and the supernatant were collected for analysis of Cur or CurDD by a modified HPLC-UV method (Wichitnithad *et al.*, 2009; Wichitnithad *et al.*, 2011). Results were shown as solubility of Cur or CurDD.

3.3.2. Investigation of partition coefficient (log P) of Cur and CurDD

The partition coefficient study was performed using the shake-flask method of the Organization for Economic Cooperation and Development (OECD) (OECD Guidelines for the Testing of Chemicals: Partition Coefficient; 1995). Cur and CurDD was added to an erlenmeyer flask containing octanol and water. The mixture was shaken, and the octanol and water phases were analyzed. Experiments were performed in triplicate. The amounts of Cur or CurDD were determined at appropriate time intervals using a modified HPLC-UV method (Wichitnithad *et al.*, 2009; Wichitnithad *et al.*, 2011). The partition coefficient was calculated by:

$$\text{Partition Coefficient} = \frac{\text{Concentration of compound in octanol}}{\text{Concentration of compound in water}}$$

3.3.3. Investigation of stability of Cur and CurDD in buffer solution

Stock methanolic solutions of Cur and CurDD were separately prepared in buffer solution pH 7.4 and then diluted with the same buffer to give a final concentration of 1.5 μM . The solution was left to stand at 37 °C for 15, 30, 60, 120 and 240 min. The amount of Cur and CurDD was determined at appropriate time intervals using a previously reported HPLC method with modifications (Wichitnithad *et al.*, 2009; Wichitnithad *et al.*, 2011).

3.3.4. Investigation of stability in simulated gastric and intestinal fluid of CurDD

The simulated gastric and intestinal fluids were prepared according to USP (United States Pharmacopoeia 38/ National Formulary 33, 2015) specification and performed using the previously studied (Asafu-Adjaye *et al.*, 2007). For simulated gastric fluid (SFG), 2 g of sodium chloride and 3.2 g of pepsin (from porcine stomach mucosa) was dissolved in 7 mL of hydrochloric acid and a sufficient volume of water to make 1000 mL. The pH of SGF was adjusted about 1.2. For simulated intestinal fluid (SIF), 6.8 g of monobasic potassium phosphate was dissolved in 250 mL of water. To this, 77 mL of 0.2 N sodium hydroxide and 500 mL of water was added and mixed along with 10 g pancreatin (from porcine pancreas). The SIF solution was adjusted to pH 6.8 ± 0.1 with either 0.2 N of sodium hydroxide or 0.2 N of hydrochloric acid and then diluted with water to 1000 mL.

Cur and CurDD at concentration 0.4 mg/mL was prepared in SGF and SIF. Aliquots of these solutions were pipetted into glass tubes, and placed in a 37 °C shaking water bath. At time points 5, 15, 30, 45 and 60 min for the gastric stability experiment and at 15, 30, 60, 120 and 180 min for the intestinal stability

experiment. Experiments were performed in triplicate. The amounts of Cur or CurDD were determined using a modified HPLC-UV method (Wichitnithad et al, 2009; Wichitnithad et al, 2011). Results were presented as % Cur or CurDD remained which was calculated in the following equation:

$$\% \text{ Cur or CurDD remained} = (C_s / C_0) \times 100$$

where C_0 is the amount of Cur or CurDD found at the zero-time point and C_s is the amount found at the end of incubation. It gives a measure of the extent of any degradation of the Cur or CurDD in the presence of the gastric and intestinal fluids.

3.4. HPLC condition for Cur and CurDD determination

3.4.1. HPLC instrumentation

HPLC analysis was performed using a Shimadzu-VP system (Shimadzu, Japan) consisting of an SCL-10A VP system controller, an LC-10AD VP pump, an SIL-10AD VP auto-injector, a DGU-14A degasser, an SPD-10A VP UV-VIS detector, Chromeleon (c) Dionex software and an HALO® C8 column (50 × 4.6 mm, 2.7 μm).

3.4.2. Chromatographic condition

A reverse-phase HPLC assay was carried out using an isocratic system with a flow rate of 1.0 mL/min, a column temperature of 33°C. a mobile phase of acetonitrile and 2% acetic acid (38:62, v/v), and a detection wavelength of 400 nm. The injection volume was 10 μL. Solutions were filtered through a 0.45 μm nylon membrane prior to HPLC injection. The total chromatographic analysis time was 3.5 min per sample, with Cur, Dimethyl curcumin (DMC; internal standard) and CurDD eluting at retention times of 0.7, 1.3 and 2.6 min, respectively.

3.5. Determination of biopharmaceutical properties of Cur and CurDD

3.5.1. Cellular Uptake and Transport of Cur from Cur or CurDD

Determination of cellular uptake and transport of Cur from Cur or CurDD was performed using human colorectal adenocarcinoma (Caco-2, ATCC No. HTB37) cells which were obtained from the American Type Culture Collection (ATCC, Rockville, MD, USA). The medium for Caco-2 cells were cultured with complete medium containing 15% (v/v) heat inactivated fetal bovine serum (FBS), 1% (v/v) L-glutamine, 1% (v/v) nonessential amino acids, 1% (v/v) penicillin-streptomycin (antibiotic), 0.2% (v/v) fungizone (antifungal) and basal media (DMEM).

3.5.2. Cytotoxicity of Cur and CurDD

Cytotoxicity was evaluated prior to the cellular uptake and transport of Cur or CurDD. Cells were seeded in 96-well plates at a density of 1×10^4 cells/well and incubated at 37°C in a humidified atmosphere of 95% air : 5% CO₂ for 24 h. Cells were divided into three groups:

- Group 1: Control group was treated only with DMSO
- Group 2: Cells were treated with Cur
- Group 3: Cells were treated with CurDD

Cells were washed with serum free media and then 200 µL of serum free media was added in each well prior to addition of 2 µL of DMSO or samples by preparing Cur or CurDD at concentrations of 5,000, 1,000, 500, 100 and 10 µM to final concentrations at 50, 10, 5, 1, and 0.1 µM. Treated cells were incubated at 37°C in humidified atmosphere of 95% air; 5% CO₂ for 4 h. Then, cells were washed with serum free media and then 200 µL of serum free media were added prior to adding 20 µL of MTT solution (5 mg/mL in PBS) at each well and incubated for 4 h. Culture medium was removed prior to adding DMSO (200 µL) to ensure cell lysis and dissolving of formazan crystals. The absorbance of formazan was measured at 540 nm. Experiments were performed in four replicates. Results were presented as

% cell viability which was calculated in the following equation:

$$\% \text{ Cell viability} = \frac{\text{Absorbance of sample} \times 100}{\text{Absorbance of control}}$$

The concentration of Cur and CurDD which no difference of cell viability when compared to the control group, it was used for the study of the cellular uptake and transport of Cur from Cur or CurDD.

3.5.3. Cellular Uptake of Cur from Cur or CurDD

Caco-2 cells were seeded in 6-well plates at a density of 4×10^4 cells/ 2 mL of complete medium /well and incubated at 37°C in a humidified atmosphere of 95% air: 5% CO₂ until confluences (about 5-7 days). The serum (FBS) content of the complete medium was decreased to 7.5% once the cultures reached confluency. The complete medium was changed every other day. At 11-14 days after confluence, cells were divided into three groups:

- Group 1: Control group was treated only with DMSO
- Group 2: Cells were treated with Cur
- Group 3: Cells were treated with CurDD

Cells were washed with serum free media and then 2 mL of basal media and added to each well prior to addition of 20 µL of DMSO or samples by preparing Cur or CurDD at the maximum concentration which no toxicity from section 3.5.2 into each well and incubated as above for 15, 30, 60, 120, and 240 min. Experiments were performed in four replicates. Cells were then collected for extraction and analysis of Cur at section 3.6. The amounts of Cur were determined at appropriate time intervals using a modified HPLC-UV method (Wichitnithad *et al.*, 2009; Wichitnithad *et al.*, 2011) at section 3.4.

3.5.4. Transport of Cur from Cur or CurDD

Caco-2 cells werer seeded in trans-well inserts of 6-well plate (ThinCerts™-TC Einsätze, Greiner Bio-one, Switzerland) at a density of 2.5×10^4

cells/well in apical compartment, basolateral compartment was added 2 mL of serum free media free phenol red, and incubated at 37°C in a humidified atmosphere of 95% air: 5% CO₂. The serum (FBS) content of the complete medium was decreased to 7.5% once the cultures reached confluency. The complete medium was changed every other day. At 21-24 days after confluence with the trans epithelial electrical resistance (TEER) between 500-700 Ω/cm^2 . Cells were divided into three groups:

- Group 1: Control group was treated only with DMSO
- Group 2: Cells were treated with Cur
- Group 3: Cells were treated with CurDD

The differentiated monolayers were washed with serum free medium before adding 2 mL of serum free medium containing Cur or CurDD which no toxicity from section 3.5.2 at the apical compartment. The 2 mL of serum free media free phenol red were added at the basolateral compartment. The plates were returned to an incubator at 37°C. The medium in the apical and basolateral compartments of treated samples was collected at 15, 30, 60, 120, and 240 min. The solution of apical and basolateral compartments was collected for extraction and analysis of Cur at section 3.6. Experiments were performed in four replicates. The amounts of Cur were determined at appropriate time intervals using a modified HPLC-UV method (Wichitnithad *et al.*, 2009; Wichitnithad *et al.*, 2011) at section 3.4.

3.6. Extraction of Cur

3.6.1. Extraction of Cur from cells

Cur extraction from Caco-2 cells was performed using the method of Wichitnithad *et al.* (Wichitnithad *et al.*, 2011). Cell pellets were thawed. Cell pellets were added with 0.5 mL of protease solution (10 mg protease/1 mL PBS) and were incubated in a 37°C shaking water bath for 30 min. After that, 1 mL of 1% sodium

dodecyl sulfate (SDS) in ethanol solution was added, and vortexed for 1 min. Cur in each sample was extracted by addition of 2 mL of ethyl acetate, sonicated for 10 min and vortexed for 2 min. Then, the extracted sample was centrifuged (DYNAC® sparks, MD 21152, USA) at 6,000 rpm for 10 min. The organic layer was collected into a 10 mL vial. The extraction was repeated twice and the organic layers were combined and dried under nitrogen gas blowing. The residue was reconstituted with a mobile phase prior to HPLC analysis in section 3.4.

3.6.2. Extraction of Cur from solution of apical and basolateral compartments

The solution of apical and basolateral compartments were thawed. A 2 mL of each solution was transferred into a 15-mL centrifuge tube and mixed with 2 mL of 0.1 M potassium phosphate buffer pH 7.1 containing 100 U of β -glucuronidase and 0.1 U of sulfatase. The mixture was incubated in a shaking water bath for 3 h at 37°C. Then, 1 mL of 1% SDS was added to the mixture in ethanol and subsequently vortexed for 1 min. Ethyl acetate was added to the mixture at the ratio of 1:1, sonicated for 10 min, vortexed for 2 min and centrifuged (DYNAC® sparks, MD 21152, USA) at 6,000 rpm for 10 min. The organic layer was collected into a 10 mL vial. The extraction was repeated twice and the organic layers were combined and dried under nitrogen gas blowing. The residue was reconstituted with a mobile phase prior to HPLC analysis in section 3.4.

3.7. Evaluation of *in vitro* anti-hepatocellular carcinoma activity and mechanism of bioavailable fraction of Cur or CurDD using HepG2 cells

3.7.1. Preparation of bioavailable fraction of Cur or CurDD

Caco-2 cells were seeded in trans-well inserts of 6-well plate (ThinCerts™-TC Einsätze, Greiner Bio-one, Switzerland) at a density of 2.5×10^4 cells/well in apical compartment, basolateral compartment was added 2 mL of

serum free media free phenol red, and incubated at 37°C in a humidified atmosphere of 95% air: 5% CO₂. The serum (FBS) content of the complete medium was decreased to 7.5% once the cultures reached confluency. The complete medium was changed every other day. At 21-24 days after confluence with the trans epithelial electrical resistance (TEER) between 500-700 Ω/cm². Cells were divided into three groups:

- Group 1: Control group was treated only with DMSO
- Group 2: Cells were treated with Cur
- Group 3: Cells were treated with CurDD

The differentiated monolayers were washed with serum free medium before adding 2 mL of serum free medium containing Cur or CurDD which no toxicity from section 3.1.4.2 at the apical compartment. The 2 ml of serum free media free phenol red were The plates were returned to an incubator at 37°C. The medium in the basolateral compartment of treated samples was collected at 4 h. Experiments were performed in four replicates. The collected BF were blanked with nitrogen gas and stored at -80°C for evaluation of anti-hepatocellular carcinoma activity and mechanism *in vitro*.

3.7.2. Evaluation of *in vitro* anti-hepatocellular carcinoma activity and mechanism of bioavailable fraction of Cur or CurDD

Human hepatocellular carcinoma (HepG2) cells were obtained from the American Type Culture Collection (ATCC, Rockville, MD, USA). HepG2 cells (passage 50 – 60) were cultured in complete medium [DMEM supplemented with 10 % FBS (v/v) and 1% penicillin and streptomycin (v/v)] and seeded at a density of 1x10⁴ cells/well in 96-well plates for cytotoxicity test and at a density of 1.0x10⁵ cells/well in 6-well plates for investigation of apoptosis induction. The cells were

incubated at 37°C in a humidified atmosphere of 95% air/5% CO₂ for 24 h. Cells were divided into three groups:

- Group 1: Control group was treated with bioavailable fraction without sample
- Group 2: Cells were treated with bioavailable fraction of Cur
- Group 3: Cells were treated with bioavailable fraction of CurDD

3.7.2.1. Cell viability test

HepG2 cells in the 96-well plates were washed with serum free medium before adding 200 µL of sample (bioavailable fraction of Cur or CurDD) and were incubated for 24 h. Then, the viability of treated cells was determined by MTT assay using a microplate reader (CLARIOstar, BMG LABTECH, Germany). Experiments were performed in four replicates. DMSO was used as a negative control. Results are presented as % cell viability in comparison with the control.

3.7.2.2. Apoptosis test

Cells in the 6-well plate were washed with serum free medium, then 2 mL of samples (bioavailable fraction of Cur or CurDD) were added and incubated for 24 h. Then, the cells were trypsinised by adding 1 mL of trypsin and incubated at 37°C for 5 min. Following addition of 1 mL of 10% FBS in DMEM, cells were transferred into a 15-mL centrifuge tube and centrifuged at 800 rpm at 37°C for 5 min. Cell pellets were resuspended in serum free medium and stained with Annexin V (Guava® Nexin Reagent, MerckMillipore, Germany) at the ratio 1:1 before flow cytometric analysis (Guava®easyCyte Flow Cytometers, MerckMillipore, Germany).

3.7.2.3. Determination of caspase-3 and -9 activities

The method for determining caspase activation was performed as described with some modifications (Hwang et al., 2011). Briefly, HepG2 cells were seeded at 1×10^6 cells/mL in 6-well culture plates. After incubation for 24 h, the cells were treated with the BF of Cur or CurDD for 24 h. The treated cells were lysed in a hypotonic buffer (20 mM Tris-HCl pH 7.5, 1 mM EDTA, 100 μ M PMSF, 2 μ g/mL aprotinin, pepstatin, and leupeptin). The supernatant was collected and incubated at 37°C for 1 h with 100 μ M DEVD-pNA or LEHD-pNA as a specific substrate of caspase-3 and 9, respectively. The absorbance at 405 nm was measured using the microplate reader (CLARIOstar, BMG LABTECH, Germany).

3.7.2.4. Western blot analysis

HepG2 cells were seeded at 1×10^6 cells/mL in a 6-well culture plate. After 24 h for incubation, the cells were washed with the serum free medium (no phenol red) and treated with the BF of Cur or CurDD for 24 h. The treated cells in the 6-well plate were resuspended in an ice-cold lysis buffer for 30 min at 4°C and centrifuged at 13,500g at 4°C for 5 min. Equal amounts (40 μ g) of each protein sample were applied to 10% SDS-PAGE gels, transferred to a pure nitrocellulose membrane (Amersham™Protran®, Sigma Aldrich), and blocked with 5% dry milk. The membrane was incubated with antibodies against Bax (1:1000), Bcl-2 (1:1,000), or β -actin (1:5,000) at 4°C overnight. Then, membranes were washed with TBST and incubated with species-specific HRP conjugated secondary antibody reacted with Super Signal solution (Endogen Inc, Rockford, IL, USA) for 2 min. The membrane was exposed to an X-ray film, stripped off the bound antibody and re-probed with anti- β actin antibody to confirm the equal loading of protein. The density of target bands was quantified with the Image J program (downloaded from <http://rsb.info.nih.gov/ij/>). Results were expressed as a relative ratio of band intensity

of the target proteins and β -actin.

3.8. Evaluation of *in vivo* anti-hepatocellular carcinoma activity and mechanism of Cur or CurDD

This animal study was approved by the Experimental animal care and use committee, Chulalongkorn University (protocol approval; 01/2560) in Appendix J. BALB/c-nude mice weighing 20 –25 g was obtained from Nomura Siam International, Thailand. and maintained in an environmentally controlled room ($23\pm 2^{\circ}\text{C}$, $50\pm 20\%$ humidity) with a 12-hour light/dark cycle. All animals were allowed food and water *ad libitum* and the 1-week acclimation period prior to the experiment. The nude mice were divided into ten groups (n = 8/group) in **Figure 12**:

- Group 1: Control group without any treatment, they were gavaged with corn oil every day for 3 weeks.
- Group 2: Nude mice were received Cur in corn oil at 300 mg/kg body weight (BW) by gavage every day for 3 weeks.
- Group 3: Nude mice were received Cur in corn oil at 3000 mg/kg body weight (BW) by gavage every day for 3 weeks.
- Group 4: Nude mice were received CurDD in corn oil at 500 mg/kg body weight (BW) (equivalent of Cur 300 mg/kg BW) by gavage every day for 3 weeks.
- Group 5: Nude mice were received Cur in corn oil at 5000 mg/kg body weight (BW) (equivalent of Cur 3000 mg/kg BW) by gavage every day for 3 weeks.
- Group 6: Nude mice were injected one time with 100 μl of single cell suspension containing 5×10^6 of HepG2 cells by subcutaneously for 1 week before they were treated with corn oil by gavage every day for 3 weeks.

- Group 7: Nude mice were injected one time with 100 μ l of single cell suspension containing 5×10^6 of HepG2 cells by subcutaneously for 1 week before they were treated with Cur in corn oil at 300 mg/kg body weight (BW) by gavage every day for 3 weeks.
- Group 8: Nude mice were injected one time with 100 μ l of single cell suspension containing 5×10^6 of HepG2 cells by subcutaneously for 1 week before they were treated with Cur in corn oil at 3000 mg/kg body weight (BW) by gavage every day for 3 weeks.
- Group 9: Nude mice were injected one time with 100 μ l of single cell suspension containing 5×10^6 of HepG2 cells by subcutaneously for 1 week before they were treated with CurDD in corn oil at 500 mg/kg body weight (BW) by gavage every day for 3 weeks
- Group 10: Nude mice were injected one time with 100 μ l of single cell suspension containing 5×10^6 of HepG2 cells by subcutaneously for 1 week before they were treated with CurDD in corn oil at 5000 mg/kg body weight (BW) by gavage every day for 3 weeks

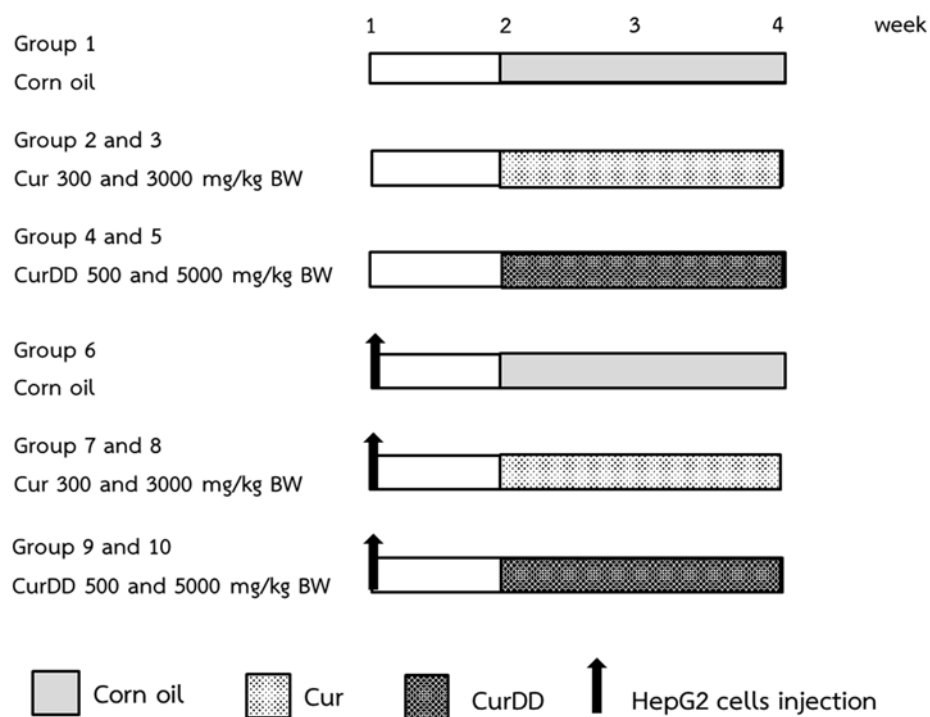


Figure 12 Experimental design for the evaluation of anti-hepatocellular carcinoma activity and mechanism of Cur or CurDD *in vivo*

Tumour size was measured every three days with vernier caliper. At the end of 4 weeks, all nude mice were fasted overnight and sacrificed. Blood samples were drawn by cardiac puncture and collected in a micro-centrifuge tube. After that it was allowed to clot for half an hour, it was centrifuged at 5,000 rpm for 10 minutes. The serum was separated collected and stored at -80 °C for determination of hepatotoxicity markers (AST and ALT) and angiogenesis markers (VEGF). Tissue samples were dissected out and washed immediately with 0.9% normal saline to remove as much blood as possible and weighted. After that tissue was immediately dipped into liquid nitrogen and stored at -80 °C for measurement of protein expression and protein content.

3.8.1. AST, ALT and VEGF determination

Blood samples were obtained by cardiac puncture and collected in a microcentrifuge tube. After allowing to clot for half an hour, the blood samples were centrifuged at 5000 rpm for 10 minutes. The sera were separated and stored at -20°C until the analysis was performed using AST, ALT (Biocompare, South San Francisco, USA) and VEGF kits (Sigma-Aldrich, Louis, MO, USA)).

3.8.2. Western blot analysis

Tumour tissues were excised from the dorsal skin-fold chamber and washed with cold PBS. The tissue samples were cut with medium-sized scissors on ice block, containing tissue lysis buffer (RIPA buffer supplemented with proteases inhibitors). Then, the tissue fragments were homogenized in an ice bath using a homogenizer at 10,000 rpm for 5 minutes. To remove the tissue debris, homogenates were centrifuged at 3500 rpm 4°C for 40 min. The supernatant was collected and aliquoted into sterile microcentrifuge tubes, kept at -80°C until it was used. Samples containing 50 μg of protein were added into 10% SDS-PAGE, transferred to a pure nitrocellulose membrane (Amersham™ Protran®, Sigma Aldrich), and blocked with 5% dry milk. The membrane was incubated with antibodies against Bax (1:1000), Bcl-2 (1:1,000), COX-2 (1:1000) or β -actin (1:5,000) at 4°C overnight. Then, membranes were washed with TBST and incubated with species-specific HRP conjugated secondary antibody reacted with Super Signal solution (Endogen Inc, Rockford, IL, USA) for 2 min. The membrane was detected band density with Chemi-luminescence documentation (ImageQuant LAS 4000, GE Healthcare Bio-Sciences, Sweden) and then, stripped off the bound antibody and re-probed with anti- β actin antibody to confirm the equal loading of protein. Results were expressed as a relative ratio of band intensity of the target proteins and β -actin.

3.9. Statistical analysis

All experiments were performed at least in four replicates unless indicated otherwise. Statistical analysis was performed using SPSS version 13.0 (SPSS Inc., USA). Data are presented as mean \pm standard deviation (SD). Means were compared by one-way analysis of variance (ANOVA) with Scheffe and Duncan's post hoc test. Differences were considered significantly at $p < 0.05$.

CHAPTER 4

RESULTS

4.1. Investigation of physicochemical properties of Cur and CurDD

4.1.1. Investigation of water solubility of Cur and CurDD

The water solubility of Cur and CurDD from the standard flask method is 0.068 and 0.059 $\mu\text{g/ml}$, respectively as shown in **Table 1**.

4.1.2. Investigation of partition coefficient of Cur and CurDD

The partition coefficient ($\log p$) indicates lipophilicity of compounds. For Cur and CurDD, their $\log P$ values were found to be 2.19 and 2.55, respectively, as shown in **Table 1**.

Table 1 Water solubility and partition coefficient ($\log p$) of curcumin (Cur) and curcumin diethyl disuccinate (CurDD)

Sample	Water Solubility $\mu\text{g/ml}$	Partition coefficient ; \log P
Cur	0.068	2.19
CurDD	0.059	2.55

4.1.3. Investigation of stability of Cur and CurDD in buffer solution pH

7.4

The investigation of stability of Cur and CurDD was studied in phosphate buffer solution pH 7.4 which was the physiological pH. The results, presented as % remained of Cur and CurDD in **Figure 13**. The amount of Cur in buffer solution pH 7.4 decreased in the time dependent. More than 80% Cur degraded in basic solution at 2 h, whereas CurDD degraded only 10% at 2 h and remained about

80% at 4 h. These results indicate that succinylation significantly enhanced the chemical stability of Cur against hydrolytic degradation at pH 7.4.

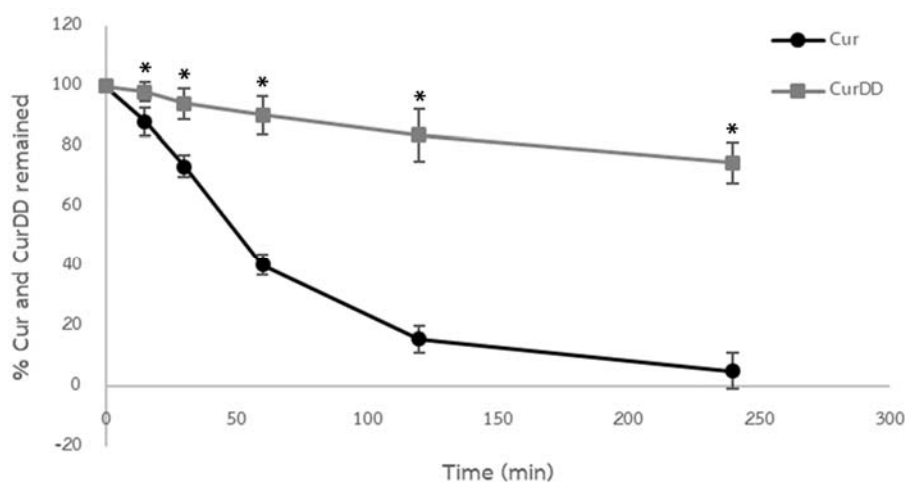


Figure 13 Chemical stability of Cur and CurDD in phosphate buffer solution pH 7.4 for 15, 30, 60, 120 and 240 min. Data presented is mean \pm SD values of triplicates, * $p < 0.05$ indicates significant differences from the Cur.

4.1.4. Investigation of stability of Cur and CurDD in simulated gastric and intestinal fluid

The investigation of stability of Cur and CurDD was studied in simulated gastric (SGF) and intestinal fluid (SIF). The results, presented as % remained of Cur and CurDD in **Figure 14** and **Figure 15**.

The amount of Cur and CurDD in SGF decreased in a time-dependent manner. The CurDD remained about 40% at 60 min, whereas Cur remained about 80% at 60 min (**Figure 14**).

The amount of Cur and CurDD in SIF decreased in a time-dependent manner. The decrease of CurDD in SIF was not different compared to Cur. Both Cur and CurDD remained about 50% at 180 min (**Figure 15**).

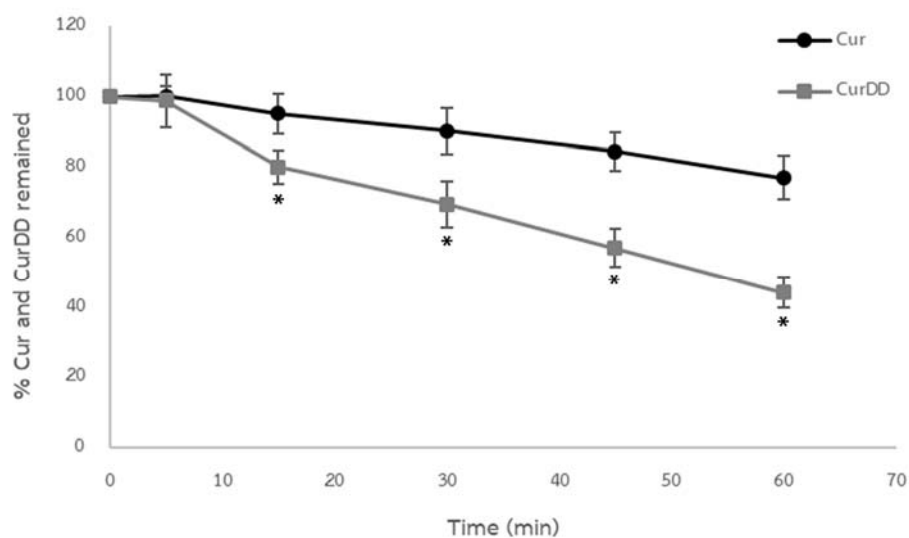


Figure 14 Cur and CurDD stability in SGF for 5, 15, 30, 45 and 60 min. Data presented is mean \pm SD values of triplicates, * $p < 0.05$ indicates significant differences from the Cur.

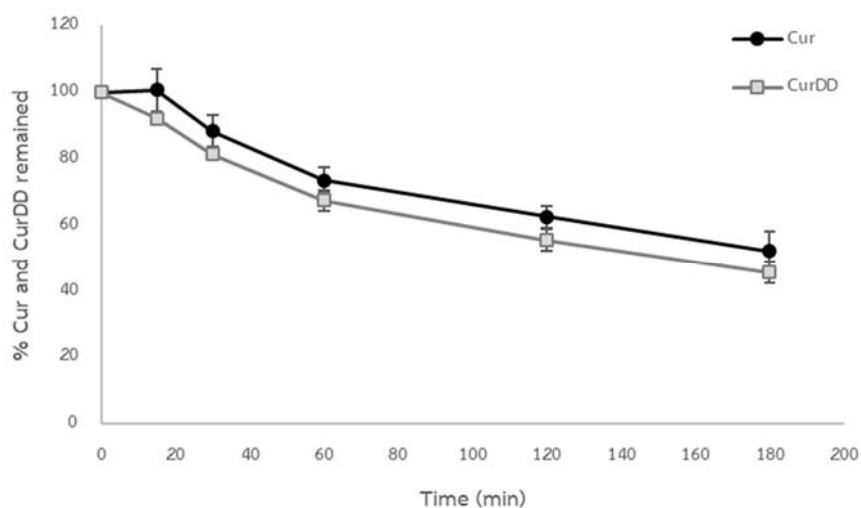


Figure 15 Cur and CurDD stability in SIF for 15, 30, 60, 120 and 180 min. Data presented is mean \pm SD values of triplicates.

4.2. Determination of biopharmaceutical properties of Cur and CurDD

4.2.1. Cytotoxicity of Cur and CurDD in Caco-2 cells

The determination of cytotoxicity of Cur and CurDD was performed on Caco-2 cells prior to the cellular transport study. The results, presented as % cell viability in **Figure 16**, indicated that the maximum concentrations of Cur and CurDD for which there was no difference in cell viability of Caco-2 compared with the control group were 5 μ M and 20 μ M, respectively. Therefore, the concentration of Cur and CurDD used for subsequent studies was 5 μ M.

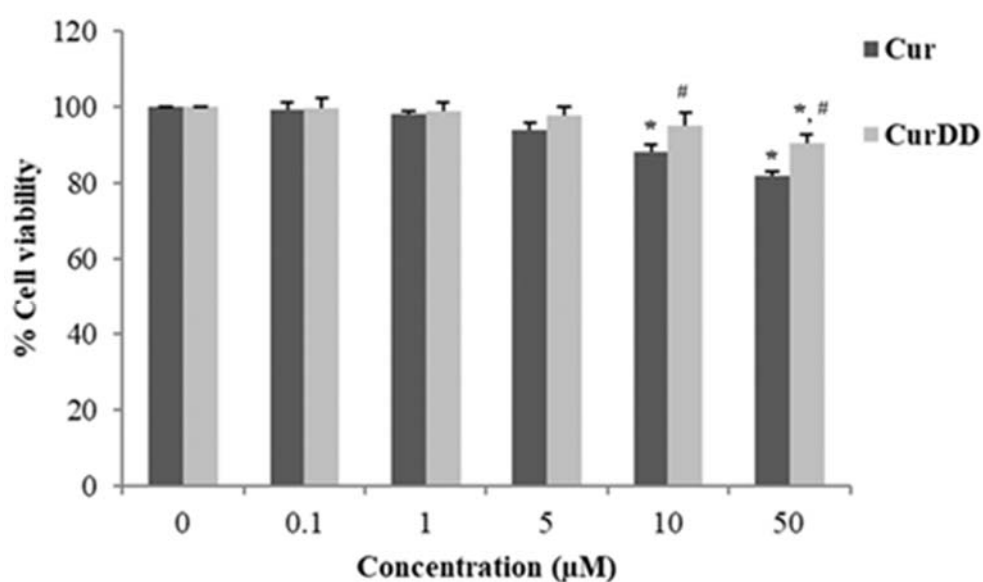


Figure 16 Cell viability of Caco-2 cells incubated with Cur or CurDD at various concentrations (0.1-50 μ M) for 4 h. Data presented is mean \pm SD values of four replicates * $p < 0.05$ indicates significant differences from the control group; # $p < 0.05$ indicates significant differences from the Cur group.

4.2.2. Cellular Uptake of Cur from Cur or CurDD

The study on cellular uptake of Cur and CurDD was studied in Caco-2 cells. Cells were culture in medium containing 5 μ M of Cur or CurDD. Cells were incubated at 0, 15, 30, 60, 120 and 240min. Then, cells were collected and extracted for determination of Cur. The quantities of Cur from cells are showed in **Figure 17**.

The amount of Cur in Caco-2 cells after treating with 5 μ M of Cur were 2,000 ng/mg proteins at 15 min and the amount of Cur in Caco-2 cells decreased significantly ($p<0.05$) over time. The quantity of Cur in Cur-treated group at 240 min was 70 ng/mg proteins. The quantity of Cur in Caco-2 cells after treating with 5 μ M of CurDD were 180 ng/mg proteins at 15 min and the quantity of curcumin increased significantly ($p<0.05$) in time dependent manner. The level of curcumin in Caco-2 cells treating with CurDD achieved the maximum concentration at 60 min with the concentration of 500 ng/ mg proteins. The quantity of Cur decreased significantly ($p<0.05$) after reaching maximum concentration. The remaining quantity of Cur in Caco-2 cells treated with CurDD at 240 min was 200 ng/mg proteins, which is higher than treating Caco-2 cells with Cur. The chromatogram of cellular uptake of Cur from Cur and CurDD were showed in Appendix H.

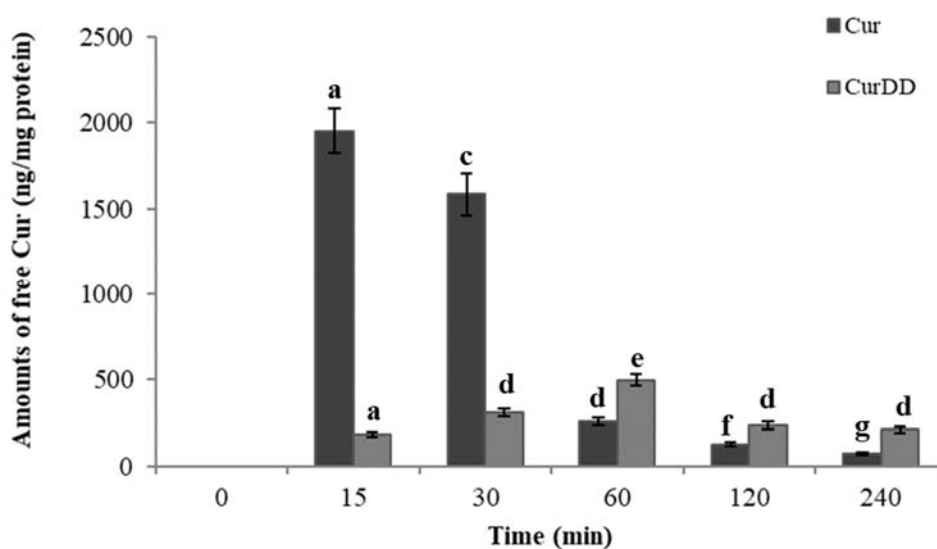


Figure 17 Amounts of free Cur from uptake of Caco-2 cells derived from 5 μ M of Cur or CurDD at different time intervals. Data presented is mean \pm SD values of four replications. Columns with different superscript letters (a-g) are significantly different ($p < 0.05$, N=4).

4.2.3. Cellular Transport of Cur from Cur or CurDD

The time profiles of Cur derived from Cur or CurDD (final concentration 5 μ M) permeating across the Caco-2 cells are depicted in **Figure 18**. The amount of Cur from the BF of the Cur-treated group at 15 min was 0.029 μ M. The amount of Cur increased over time to the maximum of 0.125 μ M at 60 min and decreased steadily after that. The remaining amount of Cur at 4 h in the BF of the Cur-treated group was only 0.082 μ M. Although CurDD showed a similar transport profile to that of Cur, the amount of free Cur found in the BF of CurDD was significantly different. Thus, at 15 min, the amount of free Cur was 0.015 which was about 2 times lower than in the Cur-treated group. The amount of Cur in the BF of CurDD reached the maximum of 0.379 μ M at 120 min. This maximum amount of Cur in the BF of CurDD-treated group was 3 times higher than the maximum amount of

Cur resulting from the BF of Cur. The remaining amount of free Cur at 4 h in the BF of CurDD-treated group was 0.321 μM , which was 4 times higher than the remaining amount of free Cur at 4 h in the BF of Cur-treated group. The chromatogram of transport of Cur from Cur and CurDD were showed in Appendix I.

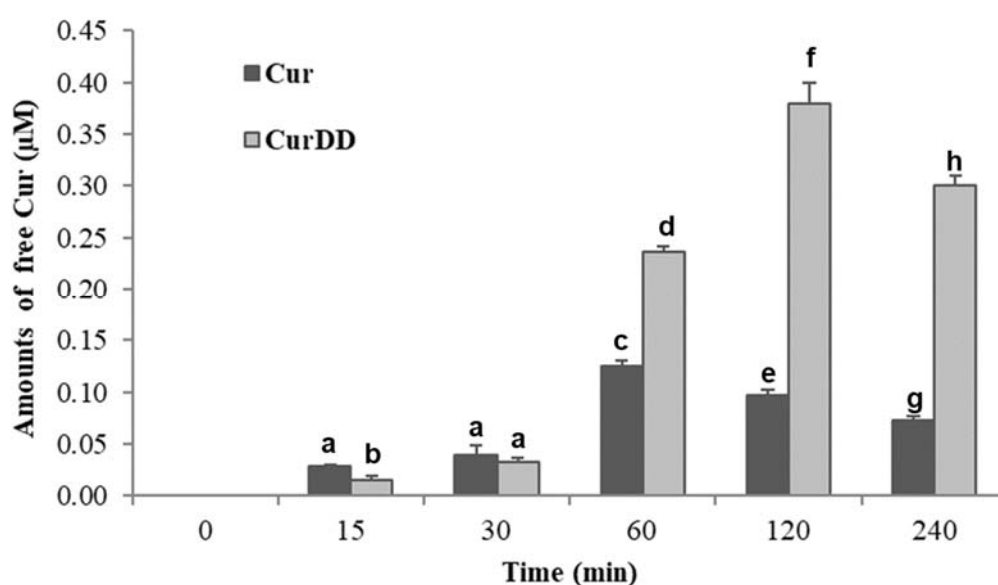


Figure 18 Amounts of free Cur from transport across Caco-2 cells derived from 5 μM of Cur or CurDD at different time intervals. Data presented is mean \pm SD values of four replications. Columns with different superscript letters (a-f) are significantly different ($p < 0.05$, $N=4$).

4.3. Evaluation of *in vitro* anti-hepatocellular carcinoma activity and mechanism of bioavailable fraction of Cur or CurDD using HepG2 cells

The anti-hepatocellular carcinoma activity of the bioavailable fraction (BF) of Cur and CurDD was determined based on cytotoxicity tests and apoptosis assays. The cytotoxic effects of the BF of Cur and CurDD against HepG2 cells are presented as % cell viability in **Figure 19**. The % cell viability values of HepG2 cells after treating

with the BF of Cur and CurDD were 85 and 67%, respectively. The outcomes of the apoptotic induction by the BF of Cur and CurDD in HepG2 cells are shown in **Figure 20**, indicating that HepG2 underwent early and late apoptosis. The % cell population in the early and late of apoptosis after incubating HepG2 cells with the BF of Cur for 24 h was found at 2.82% and 28.86%, respectively. The BF of CurDD also induced apoptosis in HepG2 cells with the % cell population in the early and late of apoptosis of 14.61% and 42.98%, respectively. These results indicated that the BF of CurDD-induced hepatocellular carcinoma apoptosis at significantly higher levels than that of Cur. The amount of Cur in the BF was subsequently determined to confirm that the difference in the anti-hepatocellular activity between the BF of Cur and CurDD resulted from the different amount of Cur being actively transported.

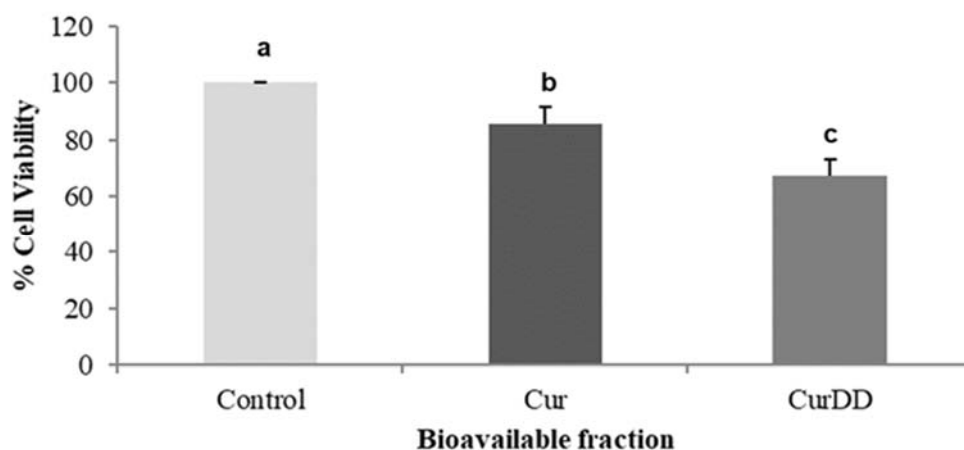


Figure 19 Cell viability of HepG2 cells incubated with the respective bioavailable fraction of Cur or CurDD for 24 h. Data presented is mean \pm SD values of four replications. Columns with different superscript letters (a-c) are significantly different ($p < 0.05$, $N=4$).

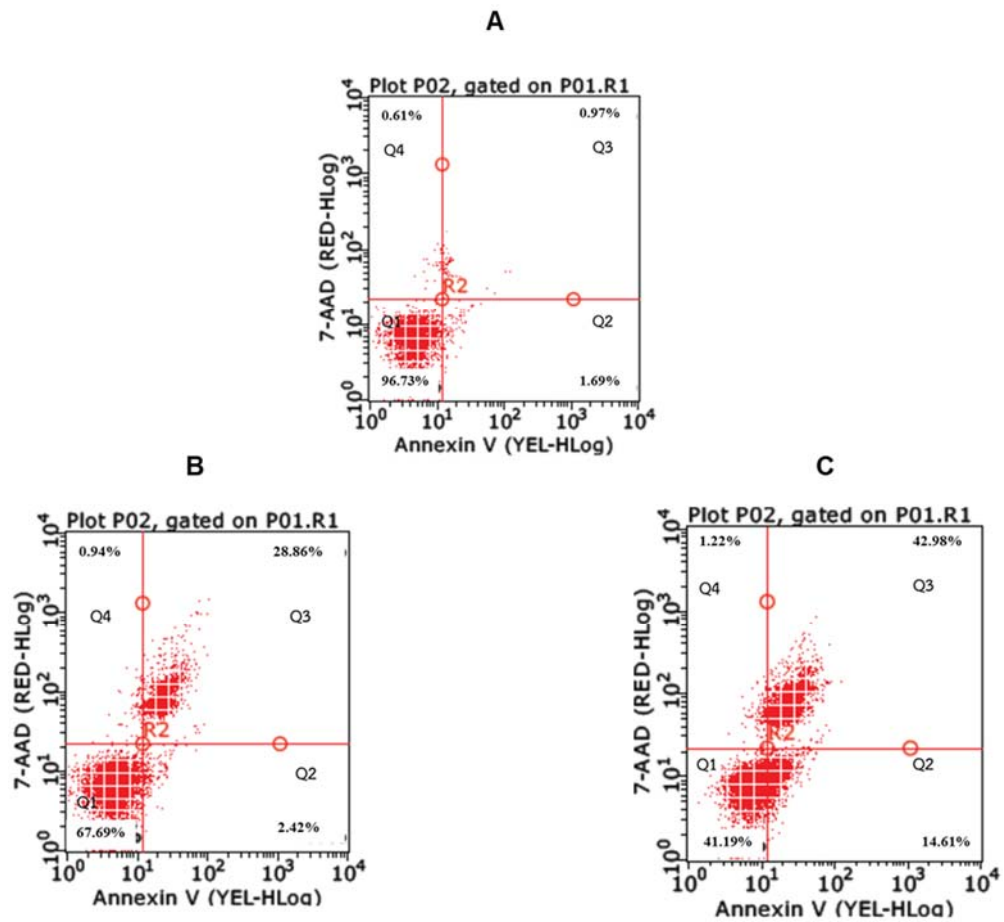


Figure 20 Flow cytometry results of HepG2 cells after treating with bioavailable fractions of Cur or CurDD. (A) Control group; (B) Treated with bioavailable fraction of Cur; (C) Treated with bioavailable fraction of CurDD. Q1 = Live cells, Q2 = Early apoptosis, Q3 = Late apoptosis and Q4 = Necrosis.

4.3.1. Effects of the BF of Cur and CurDD on caspase-3 and -9 activities

The profiles of caspase-3 and -9 activities after incubating HepG2 cells with the BF of Cur and CurDD are shown in **Figure 21**. Incubation of HepG2 cells with the BF of Cur increased caspase-3 and -9 activities by 1.8 and 1.5 times, respectively. The BF of CurDD also increased the caspase-3 and -9 activities by 6.1 and 5.3 times, respectively. The apoptosis induction effect of the BF of CurDD was thus significantly higher than that of Cur in relation to both induced caspase-3 and -9 activities.

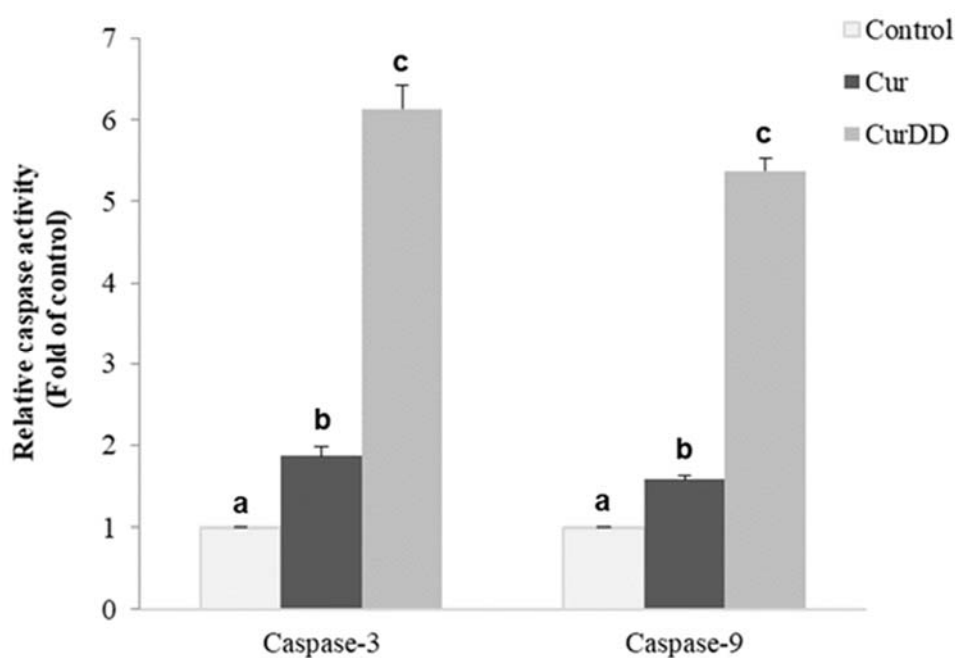


Figure 21 Effect of bioavailable fraction (BF) of Cur and CurDD on caspase-3 and -9 activities in HepG2 cells. Values represent means \pm SD of three independent experiments performed in triplicate. The different superscript letters (a, b and c) are significantly different ($p < 0.05$, $N=4$).

4.3.2. Effects of the BF of Cur and CurDD on Bax and Bcl-2 protein expression

Exposure of HepG2 cells to the BF of Cur and CurDD increased Bax (pro-apoptotic) protein by 15 and 35% , respectively, while decreasing Bcl-2 (anti-apoptotic) protein expression protein by 16 and 50% times, respectively (**Figure 22**). These results indicated that treatment of HepG2 cells with the BF of CurDD increased and respectively decreased the expression of Bax and Bcl-2 proteins, to a higher extent than in the case of the BF of Cur.

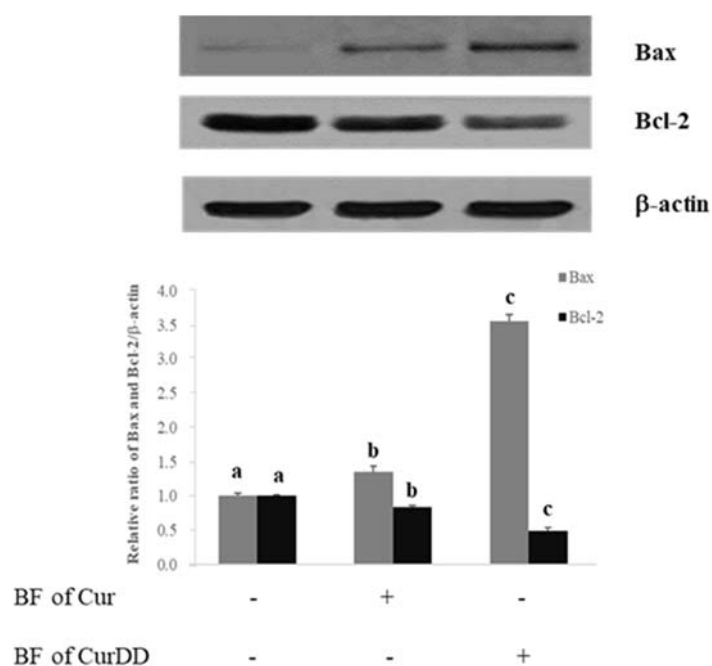


Figure 22 Effect of bioavailable fraction (BF) of Cur and CurDD on Bax and Bcl-2 expression in HepG2 cells. Values represent means \pm SD of three independent experiments performed in triplicate. The different superscript letters (a, b and c) are significantly different ($p < 0.05$, $N=4$).

4.4. Evaluation of *in vivo* anti-hepatocellular carcinoma activity and mechanism of Cur or CurDD

4.4.1. Effects of Cur and CurDD on tumour volume and tumour size

One week after inoculation of the nude mice with HepG2 cells, a tumour bud could be observed and enlarged continuously over time as shown in **Figure 23 and 24**. The tumour volume of Cur300 was not significantly different compared to the HepG2 group while the tumour volume of Cur3000, CurDD500 and CurDD5000 groups was significantly smaller than the tumour volume of the HepG2 group ($p < 0.05$) at day 15 after treatment. Furthermore, at day 21 after treatment, the tumour volume of the CurDD500 and Cur5000 groups was significantly smaller than the tumour volume of the HepG2 group ($p < 0.05$). Also, the tumour volume of the CurDD500 and Cur5000 groups was significantly less than that of the Cur300 and Cur3000 groups ($p < 0.05$). These results indicated that the treatment of CurDD could inhibit or delay the growth of hepatocellular carcinoma better than Cur in a dose dependent manner.

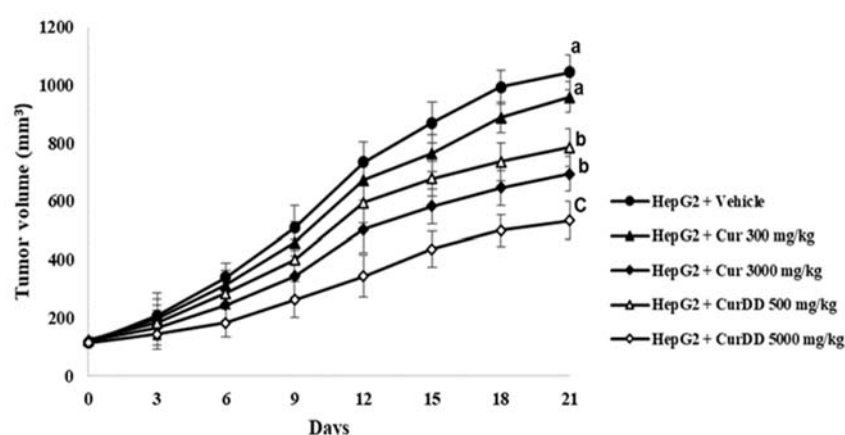


Figure 23 Effects of Cur and CurDD on tumour volume of HepG2-transplanted tumours in nude mice and in treatment groups at 21 days after treatment. Values represent means \pm SD. The different superscript letters (a, b and c) are significantly different ($p < 0.05$).

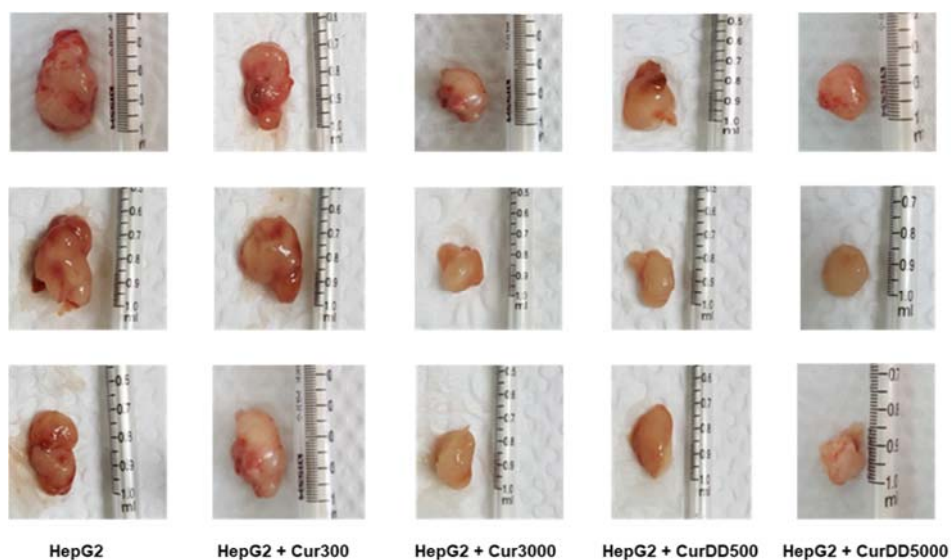


Figure 24 Effects of Cur and CurDD on tumour size of HepG2-transplanted tumours in nude mice and in treatment groups at 21 days after treatment.

4.4.2. Effects of Cur and CurDD on body weight, AST and ALT activities

The mean body weight, AST and ALT activities of the nude mice in the treatment groups was slightly smaller than that of the control group throughout the study period but not statistically significant (**Figure 25 and 26**). The mean body weight of the HepG2-induced tumour mice group was significantly decreased compared to the control group ($p < 0.05$). It was also noted that the HepG2-induced tumour had an effect on the mean body weight (**Figure 25**). The AST and ALT activities of nude mice in the test groups did not significantly differ from those of the control group throughout the study period (**Figure 26**). The results indicated that Cur, CurDD and HepG2 implantation did not affect the AST and ALT activities.

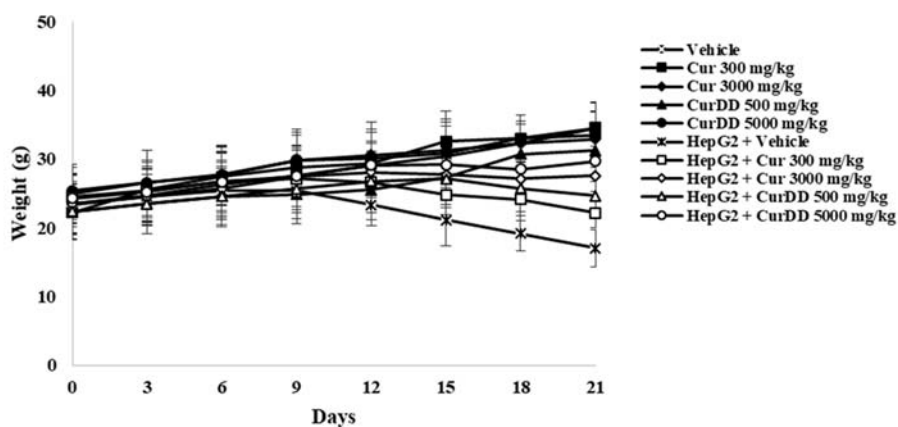


Figure 25 Effects of Cur and CurDD on body weight of HepG2- transplanted tumours in nude mice and treatment groups at 21 days after treatment. Values represent means \pm SD (N=8).

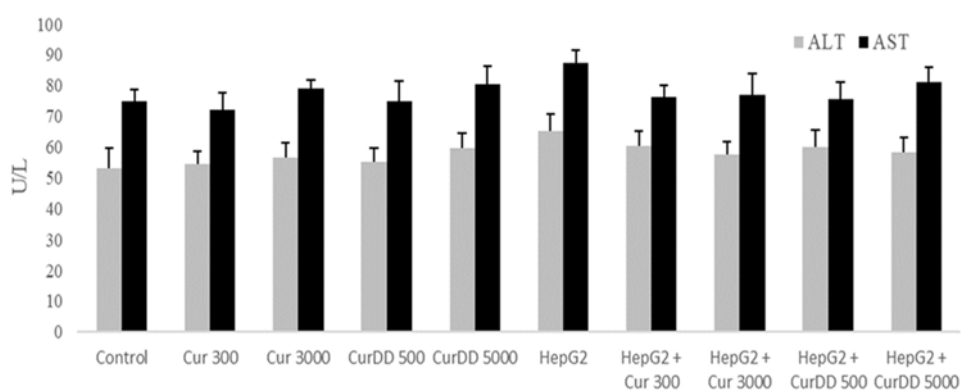


Figure 26 Effects of Cur and CurDD on AST and ALT activities of HepG2- transplanted tumours in nude mice and treatment groups at 21 days after treatment. Values represent means \pm SD (N=8).

4.4.3. Effects of Cur and CurDD on Bax and Bcl-2 expression

As shown in **Figure 27**, the expression of Bax protein increased by 25%, 20% and 40% after the treatment of Cur3000, CurDD500 and CurDD5000 for 21 days, respectively, in HepG2-induced tumour mice. In contrast, the treatment of Cur3000, CurDD500 and CurDD5000 in HepG2-induced tumour mice decreased the Bcl-2 expression by 20%, 15% and 35%, respectively. The suppressive effect of the CurDD was significantly higher than that of Cur ($p < 0.05$). These results indicated that the treatment of HepG2-induced tumour mice with CurDD increased and respectively decreased the expression of Bax and Bcl-2 protein to a higher extent than Cur.

4.4.4. Effects of Cur and CurDD on serum VEGF and COX-2 expression

Figure 28 and 29 show the results of the quantification of VEGF secretion and COX-2 expression in HepG2-induced tumour mice in comparison with the control group. The treatment with Cur300, CurDD500 and CurDD5000 significantly decreased the VEGF secretion and COX-2 expression in comparison with the HepG2-induced tumour mice group ($p < 0.05$). These results indicated that the treatment of CurDD could suppress the VEGF secretion and COX-2 expression in HepG2-induced tumour mice in a dose dependent manner better than Cur.

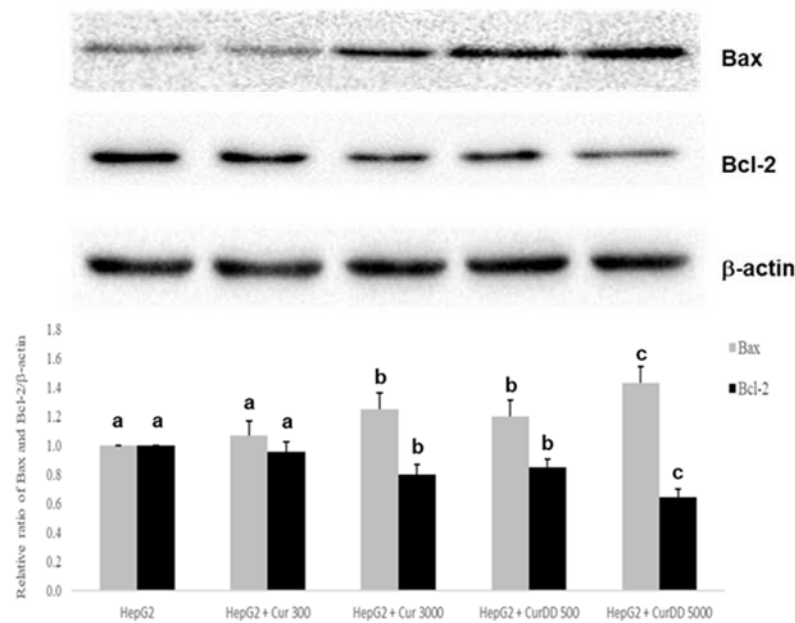


Figure 27 Effects of Cur and CurDD on Bax and Bcl-2 expression from tumour tissue of HepG2-transplanted tumour in nude mice and in the treatment groups at 21 days after treatment. Values represent means \pm SD (N = 8). Columns with different superscript letters (a-c) are significantly different ($p < 0.05$).

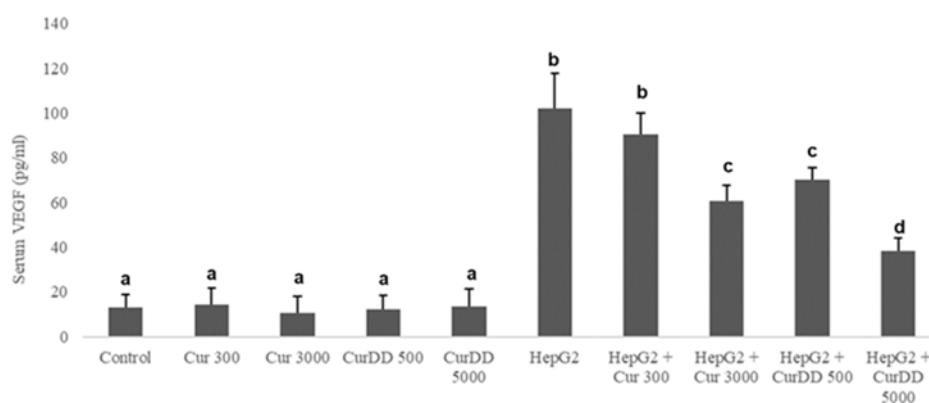


Figure 28 Effects of Cur and CurDD on serum VEGF secretion of HepG2-transplanted tumour in nude mice and in the treatment groups at 21 days after treatment. Values represent means \pm SD (N = 8). Columns with different superscript letters (a-d) are significantly different ($p < 0.05$).

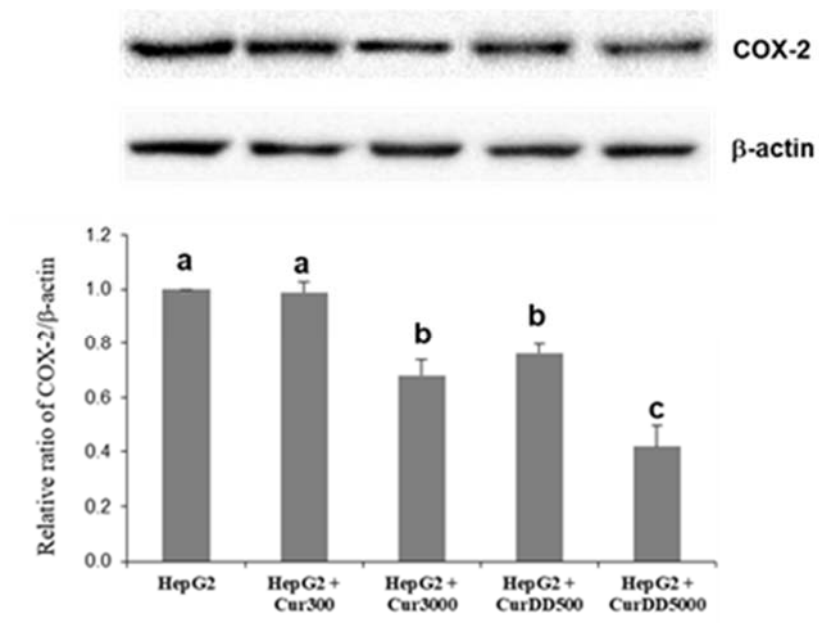


Figure 29 Effects of Cur and CurDD on (COX-2 expression from tumour tissue of HepG2-transplanted tumour in nude mice and in the treatment groups at 21 days after treatment. Values represent means \pm SD (N = 8). Columns with different superscript letters (a-d) are significantly different ($p < 0.05$).

CHAPTER 5

DISCUSSION AND CONCLUSION

Curcumin, the bioactive compound from turmeric, has numerous pharmacological properties with a good safety profile. However, curcumin has limitation to be developed as a drug because of its low water solubility and instability in aqueous solutions, resulting in poor oral bioavailability. A curcumin prodrug, CurDD is synthesized which is more stable than Cur and it can also be converted to curcumin in plasma which makes CurDD of interest as a curcumin prodrug in particular, therapeutic agents for anti-cancer. The aims of the present study were to determine the physicochemical, biopharmaceutic and anti-hepatocellular effects and mechanisms of CurDD, a succinate ester prodrug of Cur, both in vitro and in vivo in comparison with Cur.

The physicochemical properties of CurDD, we found that the solubility and of CurDD was not different compared to Cur (Table 1). CurDD had more partition coefficient than Cur (Table 1). Partition coefficient ($\log P$) is used in the pharmaceutical/biotech industries to understand the behavior of drug molecules in the body and present to lipophilicity of drugs. Drug candidates are often screened according to $\log P$, among other criteria, to help guide drug selection and analog optimization. This is because lipophilicity is a major determining factor in a compound's absorption, distribution in the body, penetration across vital membranes and biological barriers, metabolism and excretion (ADME properties) (Leo *et al.*, 1971). The results indicated that CurDD should be better permeability to cell membrane than Cur due to CurDD had more lipophilicity than Cur. The part os stability, CurDD had more stability than Cur in the phosphate buffer solution pH 7.4 which was the physiological pH. The amount of CurDD remained more than 80% at 4 h, whereas the amount of Cur remained less than 5 (Figure 13). These results indicate

that succinylation significantly enhanced the chemical stability of Cur against hydrolytic degradation at pH 7.4. The part of stability of Cur and CurDD in SGF and SIF, we found that CurDD in SGF was less the stability than Cur (Figure 14). The pH 1.2 of SGF had slightly affect to stability of Cur and CurDD, the remaining amount of Cur and CurDD in buffer pH 1.2 without pepsin at 60 min was 90 and 85% , respectively (Kumavat *et al.*, 2013; Pahweenvaj, 2018). The decrease of CurDD in SGF was more pronounced than that of Cur which could be derived from the presence of pepsin. Pepsin belongs to hydrolase superfamily, which it may have some capability to hydrolyze CurDD in the SGF (Hosokawa, 2008). The stability of Cur and CurDD in SIF, the remaining amount of Cur and CurDD in SIF at 180 min was 50% which not differrent between Cur and CurDD (Figure 15). The pH 6.8 in SIF had affect to stability of Cur and CurDD, the remained of Cur and CurDD in buffer pH 6.8 without pancreatin at 180 min was 50 and 75% , respectively (Kumavat *et al.* , 2013; Pahweenvaj, 2018). At the 180 min of SIF, the remaining amount of CurDD was 50% which was not different compared to Cur because pancreatin in SIF, it may have some capability to hydrolyze CurDD in the SIF (Hosokawa, 2008). The cellular uptake, we found that the remaining quantity of Cur in Caco-2 cells treated with CurDD for 4 h was higher than treating Caco-2 cells with Cur in a significance ($p < 0.05$) (Figure 16), and also the cellular transport, the remaining quantity of Cur in BF from CurDD for 4 h was higher than treating Caco-2 cells with Cur in a significance ($p < 0.05$) (Figure 17). These results indicate that CurDD enhanced the chemical stability of Cur against hydrolytic degradation at pH 7.4 which is the pH of culture media. The underlying properties for the cellular uptake and transport in Caco-2 cells might be the result of the enhancing of lop and stability of CurDD.

We show that, after passing across the Caco-2 monolayers, which served as an *in vitro* intestinal absorption model, the BF of CurDD exhibited better cytotoxic effects against HepG2 cells compared to those of Cur. This could be due to the

higher concentration of Cur found in the BF of CurDD compared to that resulting from administration of unmodified Cur. The differences in anti-hepatocellular carcinoma activities and the amounts of Cur found in the BF of Cur and CurDD might relate to the biotransformation in Caco-2 cells. Cur has been shown that it is extensively metabolized to several reduced and conjugated metabolites while being transported across Caco-2 cells (Dempe *et al.*, 2013; Zeng *et al.*, 2017). Hence, the low amounts of Cur found after permeating across the Caco-2 monolayers detected in our study. On the other hand, CurDD is subjected to hydrolysis by intracellular esterase(s) and releases Cur. The presence of two ethyl succinyl groups might allow the released Cur to circumvent the reductive and conjugative metabolic reactions in Caco-2 cells, resulting in the significantly higher amounts of Cur found in the BF of CurDD.

Of note is the fact that the concentration of Cur in both BF is very low (less than 1 μM) but despite this it could exert the significant cytotoxicity against HepG2 cells compared to the non- treated control ($p < 0.05$). The observed cytotoxicity may be due to the metabolites of Cur resulting during cellular transport. Possible metabolites of Cur include reductive metabolites tetrahydroCur, hexahydroCur and octahydroCur, as well as their sulfate and glucuronide conjugates. These metabolites were previously reported to possess various biological activities with different extent of their potency (Dempe *et al.*, 2013). We therefore suggest that, in addition to Cur, the cytotoxic effect might be derived from the Cur metabolites generated during the transport across Caco-2 monolayers. The previous studies showed that tetrahydroCur had the cytotoxic effect to cancer cells through apoptosis induction and anti-angiogenesis (Kang *et al.*, 2014; Zhang *et al.*, 2017). Cur has been shown to induce apoptosis in various cancer cells like leukemia, breast, lung, colon and hepatocellular carcinomas (Karunagaran *et al.*, 2005; Ravindran *et al.*, 2009). Cur could induce apoptosis in tumor or cancer cells by downregulation of anti-apoptotic Bcl-2, Bcl-xL,

and XIAP proteins expression (Karunakaran *et al.*, 2005; Zhi-Dong *et al.*, 2014). Moreover, Cur upregulates expression of P53, Bax, Bak, PUMA, Bim, NOXA and death receptors DR4 and DR5, triggering activation of caspase-3, -9, -7 which showed in Figure 6 (Karunakaran *et al.*, 2005; Rodríguez *et al.*, 2013; Zhu and Bu, 2017). In this study, we investigated and compared the patterns of apoptosis induction of Cur and CurDD using the BF of Cur and CurDD. The flow cytometric analysis showed that the BF of CurDD shifted HepG2 cells to early and late apoptosis to a higher extent than that of Cur (Fig. 20). CurDD had cytotoxicity effect to HepG2 cells by induction of apoptosis through mitochondria-mediated apoptotic pathway (Fig. 6). These findings could be explained by an increase in caspase activities and an alteration of the apoptotic protein expression. The BF of CurDD induced a 3-fold enhancement of the caspase-3 and -9 activities in comparison with the BF of Cur (Fig. 21). Bax and Bcl-2 proteins are apoptotic and anti-apoptotic proteins, respectively, which are regulated by caspase-3 and -9. The substantial increase in Bax protein expression (3.5 times vs control; 2.8 times vs Cur) and down regulation of Bcl-2 protein after treating HepG2 cells with the BF of CurDD are in agreement with the change in caspase activities (Fig. 22). These data indicated that BF from both Cur and CurDD can induce apoptosis in HepG2, with the BF of CurDD having greater effects. The propose mechanism of BF of CurDD induced apoptotic cell death in hepatocellular carcinoma was shown in Figure 30. CurDD was chaged to Cur by esterases from enterocyte and then the both of Cur and CurDD remained were transpoted to hepatocyte. CurDD could be changed to Cur again by esterases from enterocyte. Cur from CurDD activated and suppressed Bax (pro-apoptotic) and Bcl-2 (anti-apoptotic) expression in mitochondria, respectively. Cytochrome c from mitochondria is released into the cytosol resulting in its high affinity interaction with Apaf-1 and subsequent activation of caspase-9. The active caspase-9 activates caspase-3 which is effector caspases that mediate the execution phase exhibiting characteristic features of apoptosis, several of which

reflect the proteolytic cleavage of various intracellular proteins ensuring peaceful elimination of the cell. Caspase-3 is a frequently activated death protease, catalyzing the specific cleavage of many key cellular proteins (Porter and Janicke, 1999; McIlwain *et al.*, 2013).

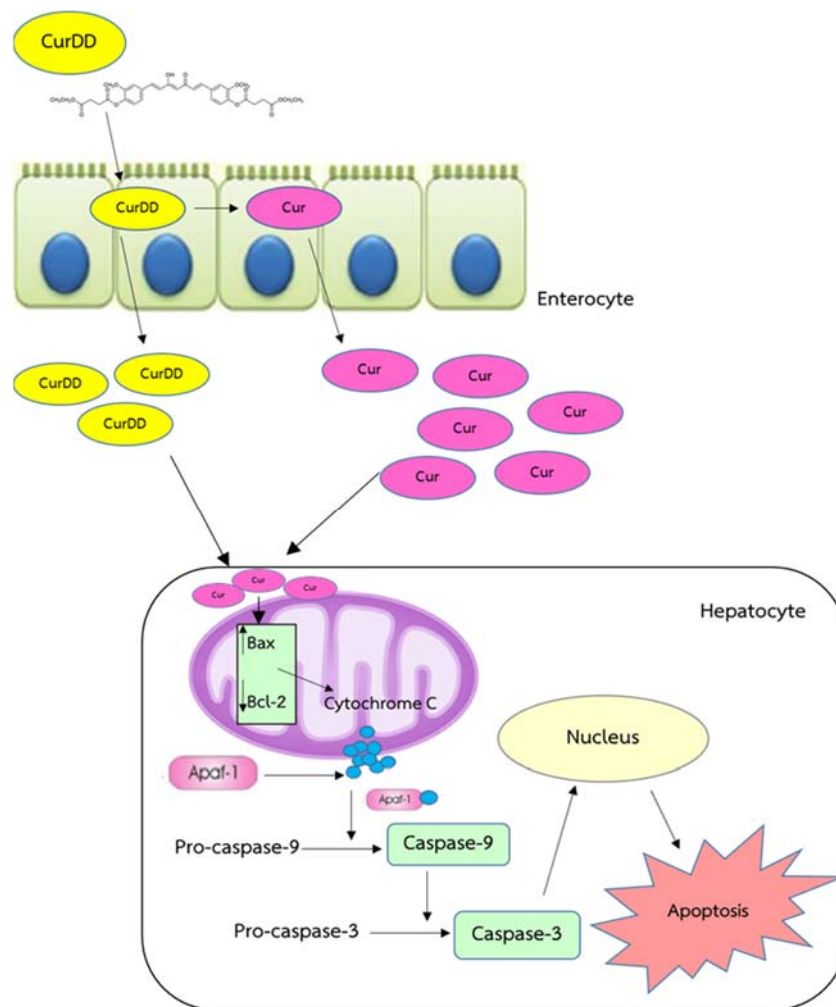


Figure 30 The propose mechanism of BF of CurDD induced apoptotic cell death in hepatocellular carcinoma

We also evaluated the anti-hepatocellular carcinoma activities and mechanisms of Cur and CurDD in the HepG2-induced nude mice. The *in vivo* study shows the similar trend to that observed *in vitro*. At the same equimolar doses, CurDD could delay the progression of tumour better than Cur, which could be a consequence of enhanced intestinal absorption of Cur derived from CurDD as demonstrated by the Caco-2 model. The underlying mechanisms for the anti-hepatocellular carcinoma activities in HepG2-induced nude mice might be the result of the reduction of serum VEGF and COX-2 expression (Fig. 28 and 29). VEGF plays an important role in angiogenesis by promoting endothelial cell proliferation, migration and differentiation while COX-2 appears to induce angiogenesis in a variety of tumours and is used as a biomarker of cancer (Yoysungnoen, *et al.*, 2006; Harris R. E., 2009). The reduction of VEGF secretion and COX-2 expression might be the result of the suppression of the mitogen-activated protein kinase (MAPK) and the nuclear factor kappa B (NF- κ B) signaling pathway. Potential anti-angiogenesis effects of Cur and CurDD may underpin the increased apoptosis of the tumour as suggested by the activation of caspase-3 and -9 pathways, the increase of Bax expression and the down regulation of Bcl-2 protein. Importantly, although the mice were fed with high doses of Cur and CurDD (3000 and 5000 mg/kg BW, respectively), the level of serum AST and ALT were not different from those of the control group. These data further indicate that Cur and CurDD do not lead to liver toxicity and can therefore be used safely. Moreover, the CurDD at 500 mg/kg BW could decrease the tumour volume, tumour size, serum VEGF, Bax (pro-apoptotic protein) and COX-2 expression, and increase Bcl-2 (anti-apoptotic protein) was not different compared to Cur at 3000 mg/kg BW. These results indicated that CurDD is an interesting prodrug of Cur which has the potential to be further developed as a therapeutic agent especially, anti-cancer agent. The overall of underlying mechanism of CurDD on *in vitro* and *in vivo* anti-hepatocellular carcinoma activities were showed in Figure 32. CurDD had *in vitro*

and *in vivo* anti-hepatocellular carcinoma activities through mitochondria-mediated apoptotic, mitogen-activated protein kinase (MAPK) and the nuclear factor kappa B (NF- κ B) signaling pathway.

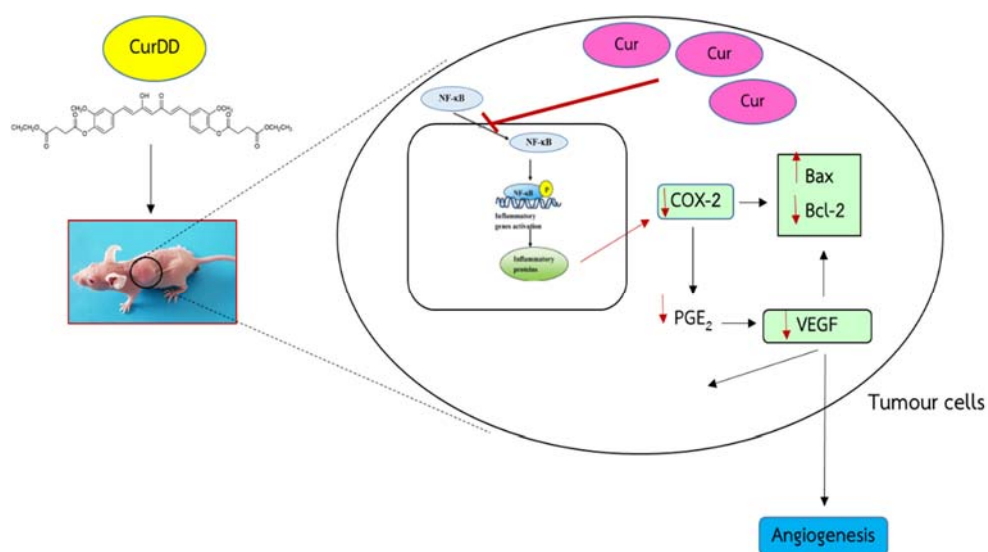


Figure 31 The underlying mechanisms of CurDD for the anti-hepatocellular carcinoma activities in HepG2-induced nude mice

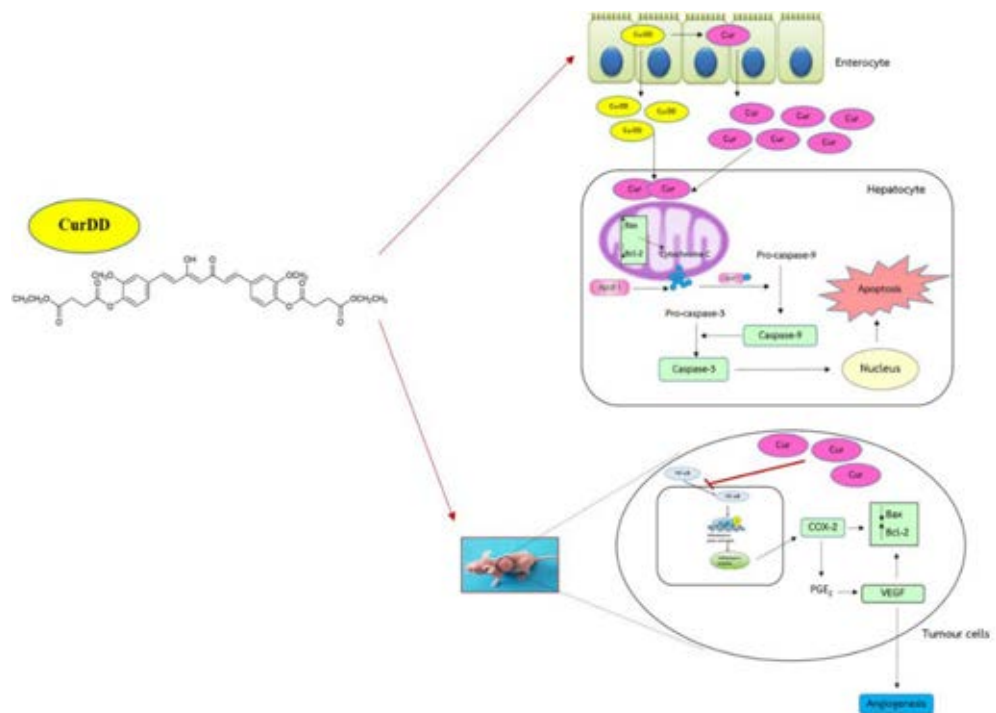


Figure 32 The underlying mechanisms of CurDD for the *in vitro* and *in vivo* anti-hepatocellular carcinoma activities

In summary, CurDD is an ester prodrug of curcumin that enhances the anti-hepatocellular activity of Cur. The enhanced anti-hepatocellular carcinoma effect could be derived from the higher intestinal absorption, which in turn might be due to its superior metabolic stability. CurDD has pro-apoptotic effects, possibly linked to anti-angiogenesis activity, resulting in delayed tumour progression in the HepG2-induced nude mice model. The results suggest that CurDD is a promising prodrug of Cur and has the potential to be further developed as a therapeutic agent or an adjuvant for the treatment of hepatocellular carcinoma.

REFERENCES

- Adams, J. M., and Cory, S. (1998). The BCL-2 protein family: Arbiters of cell survival. *Science*, 281, 1322–1326.
- Allegra, A., Innao, V., Russo, S., Gerace, D., Alonci, A., & Musolino, C. (2017). Anticancer Activity of Curcumin and Its Analogues: Preclinical and Clinical Studies. *Cancer Investigation*, 35, 1-22.
- Asafu-Adjaye, E. B., Faustino, P. J., Tawakkul, M. A., Anderson, L. W., Yu, L. X., Kwon, H. and Volpe, D. A. (2007). Validation and application of a stability-indicating HPLC method for the in vitro determination of gastric and intestinal stability of venlafaxine. *Journal of Pharmaceutical and biomedical analysis*, 43, 1854-1859.
- Aggarwal, B., Shishodia, S., Sandur, K., Pandey, K., and Sethi, G. (2006). Inflammation and cancer: How hot is the link? *Biochemical Pharmacology*, 72(11), 1605-1621.
- Ak, T. and Gulcin, L. (2008). Antioxidant and radical scavenging properties of curcumin. *Chemico-Biological Interactions*, 174, 27-37.
- Anand, P., Kunnumakkara, A. B., Newman, R. A. and Aggarwal, B. B. (2007). Bioavailability of curcumin: problems and promises. *Molecular pharmaceutics*, 6, 807-818.
- Anand, P., Thomas, S. G., Kunnumakkara, A. B., Sundaram, C., Harikumar, K. B., Sung, B., Tharakan, S. T., Misra, K., Priyadarsini, I. K., Rajasekharan, K. N. and Aggarwal, B. B. (2008). Biological activities of curcumin and its analogues (Congeners) made by man and Mother Nature. *Biochemical pharmacology*, 11, 1590-1611.
- Aravalli, R. N., Cressman, E. N. K., and Steer, C. (2013). Cellular and molecular mechanisms of hepatocellular carcinoma: an update. *Archives of Toxicology*, 87, 227-247.
- Arbiser, J. L., Bonner, M. Y., Gilbert, L. C. (2017). Targeting the duality of cancer. *NPJ Precis, Oncol*, 1.

- Bakiri, L., and Wagner, E. F. (2013). Mouse models for liver cancer. *Molecular Oncology*, 7, 206-223.
- Bangphumi, K., Kittiviriyakul, C., Towiwat, P., Rojsitthisak, P., & Khemawoot, P. (2016). Pharmacokinetics of Curcumin Diethyl Disuccinate, a Prodrug of Curcumin, in Wistar Rats. *European Journal of Drug Metabolism and Pharmacokinetics*, 41, 777-785.
- Bao, H., Zhang, Q., Zhu, Z., Xu, H., Ding, F., Wang, M., Du, S., Du, Y., and Yan, Z. (2017). BHX, a novel pyrazoline derivative, inhibits breast cancer cell invasion by reversing the epithelial-mesenchymal transition and down-regulating Wnt/ β -catenin signaling. *Sci. Rep*, 7, 9153.
- Basnet, P. and Basnet, N. S. (2011). Curcumin: An Anti-Inflammatory molecule from a curry spice on the path to cancer treatment. *Molecules*, 16, 4567-4598.
- Battaller, R. and Brenner, D. A. (2005). Liver fibrosis. *Journal of Clinical Investigation*, 115, 209-18.
- Block, T. M., Mesta, A. S., Fimmel, C. J., and Jordan, R. (2003). Molecular viral oncology of hepatocellular carcinoma. *Oncogene*, 22, 5093-5107.
- Bhunchu, S., Rojsitthisak, P., Muangnoi, C., and Rojsitthisak, P. (2016). Curcumin diethyl disuccinate encapsulated in chitosan/alginate nanoparticles for improvement of its in vitro cytotoxicity against MDA-MB-231 human breast cancer cells. *Pharmazie*, 71, 691-700.
- Buadonpri, W., Wichitnithad, W., Rojsitthisak, P. and Towiwat, P. (2009). Synthetic curcumin inhibits carrageenan-induced paw edema in rats. *Journal of Health Research*, 11-16
- Cabibbo, G. and Craxi, A. (2010). Epidemiology, risk factors and surveillance of hepatocellular carcinoma. *European Review for Medical and Pharmacological Sciences*, 14, 352-55.
- Center, M. M. and Jemal, A. (2011). International trends in liver cancer incidence rates. *Cancer Epidemiology, Biomarkers and Prevention*, 20, 2362-8.
- Chhunchha, B., Fatma, N., Bhargavan, B., Kubo, B., Kuma, A. and Singh, D. P. (2011). Specificity protein, Sp1-mediated increased expression of Prdx6 as a

- curcumin-induced antioxidant defense in lens epithelial cells against oxidative stress. *Cell Death and Disease*, 1-13.
- Chitapanarux, T. and Phornphutkul, K. (2015). Risk factors for the development of hepatocellular carcinoma in Thailand. *Journal of Clinical and Translational Hepatology*, 3, 182-188.
- Constandinou, C., Henderson, N., and Iredale, J. P. (2005). Modeling liver fibrosis in rodents. *Methods in Molecular Medicine*, 117, 237-50.
- Danial, N. N., and Korsmeyer, S. J. (2004). Cell death: Critical control points. *Cell*, 116, 205–219.
- Dasiram J. D., Ganesan, R., Kannan, J., Kotteeswaran, V., & Sivalingam, N. (2017). Curcumin inhibits growth potential by G1 cell cycle arrest and induces apoptosis in p53-mutated COLO 320DM human colon adenocarcinoma cells. *Biomedicine & Pharmacotherapy*, 86, 373-380.
- De Minicis, S., Seki, E., Paik, Y. H. (2010). Role and cellular source of nicotinamide adenine dinucleotide phosphate oxidase in hepatic fibrosis. *Hepatology*, 52, 1420-30.
- Dempe, J. S., Scheerle, R. K., Pfeiffer, E., and Metzler, M. (2013). Metabolism and permeability of curcumin in cultured Caco-2 cells. *Molecular Nutrition*, 57, 1543-1549.
- Dubey, S. K., Sharma, A. K., Narain, U., Misra, K. and Pati, U. (2008). Design, synthesis and characterization of some bioactive conjugates of curcumin with glycine, glutamic acid, valine and demethylenated piperic acid and study of their antimicrobial and antiproliferative properties. *European Journal of Medicinal Chemistry*, 9, 1837-46.
- Elkholi, R., Renault, T. T., Serasinghe, M. N., Chipuk, J. E. (2014). Putting the pieces together: How is the mitochondrial pathway of apoptosis regulated in cancer and chemotherapy? *Cancer Metab*, 2, 16.
- Elmores, S. (2007). Apoptosis: A review of programmed cell death. *Toxicol Pathol*, 35(4), 495–516.

- Epstein, G., Sanderson, I. R., and Macdonald, T. T. (2010). Curcumin as a therapeutic agent: the evidence from in vitro, animal and human studies. *British Journal of Nutrition*, 103, 1545-1557.
- Farazi, P. A. and Depinho, R. A. (2006). Hepatocellular carcinoma pathogenesis: from gene to environment. *Nature*, 6, 674-687.
- Fernández, M., Semela, D., Bruix, J., Colle, I., Pinzani, M., and Bosch, J. (2009). Angiogenesis in liver disease. *Journal of Hepatology*, 50(3), 604-20.
- Fujise, Y., Okano, J. I., Nagahara, T., Abe, R., Imamoto, R. and Murawaki, Y. (2012). Protective effect of caffeine and curcumin on hepato-carcinogenesis in diethylnitrosamine-induced rats. *International Journal of Oncology*, 40, 1779-1788.
- Gallego, J. G., and Tunon, M. J. (2007). Anti-inflammatory properties of dietary flavonoids. *Nutrition Hospitalaria*, 22(3), 287-293.
- Girish, C., Koner, B. C., Jayanthi, S., Rao, K. R., Rajesh, B. and Pradhan, S. C. (2009). Hepatoprotective activity of picroliv, curcumin and ellagic acid compared to silymarin on paracetamol induced liver toxicity in mice. *Fundamental & Clinical Pharmacology*, 23(6), 735-745.
- Goldar, S., Khaniani, M.S., Derakhshan, S.M., and Baradarn, B. (2015). Molecular mechanisms of apoptosis and roles in cancer development and treatment. *Asian Pac. J. Cancer Prev*, 16, 2129–2144.
- Green, D. R., and Llambi, F. (2015). Cell death signaling. *Cold Spring Harb. Perspect. Biol*, 7, a006080.
- Gupta, S. C., Patchva, S., and Aggarwal, B. B. (2012). Therapeutic roles of curcumin: lessons learned from clinical trials. *The Journal of American Association of Pharmaceutical of Scientists*, 15(1), 195-218.
- Harris, R. E. (2009). Cyclooxygenase-2 (cox-2) blockade in the chemoprevention of cancers of the colon, breast, prostate, and lung. *Inflammopharmacology*, 17, 55-67.
- Harish, G., Venkateshappa, C., Mythri, R. B., Dubey, S. K., Mishra, K., Singh, N., Vali, S. and Bharath, M. M. S. (2010). Bioconjugates of curcumin display improved protection against glutathione depletion mediated oxidative stress in a

- dopaminergic neuronal cell line: Implications for Parkinson's disease. *Bioorganic and Medicinal Chemistry*, 18(7), 2631-2638.
- Hassan, M., Watari, H., AbuAlmaaty, A., Ohba, Y., and Sakuragi, N. (2014). Apoptosis and molecular targeting therapy in cancer. *BioMed Res*
- Hooper, L. and Cassidy, A. (2006). A review of the health care potential of bioactive compounds. *Journal of the Science of Food and Agriculture*, 68(12), 1805-1813.
- Hosokawa, M. (2008). Structure and catalytic properties of carboxylesterase isozymes involved in metabolic activation of prodrugs. *Molecules*, 13, 412-431.
- Jurenka, J. S. (2009). Anti-inflammatory properties of curcumin, a major constituent of *Curcuma longa*: A review of preclinical and clinical research. *Alternative Medicine Review*, 14(2), 141-153.
- Kang, N., Wang, M. M., Wang, Y. H., Zhang, Z. N., Cao, H. R., Lv, Y. H., Yang, Y., Fan, P. H., Qiu, F., and Gao, X. M. (2014). Tetrahydrocurcumin induces G2/M cell cycle arrest and apoptosis involving p38 MAPK activation in human breast cancer cells. *Food. Chem. Toxicol.* 67, 193-200.
- Karunagaran, D., Rashmi, R., and Kumar T. R. S. (2005). Induction of Apoptosis by Curcumin and Its Implications for Cancer Therapy. *Current Cancer Drug Targets*, 5, 117-129.
- Kerbel, R. S. (2003). Human tumor xenografts as predictive preclinical models for anticancer drug activity in humans: better than commonly perceived-but they can be improved. *Cancer Biological & Therapy*, 4, 134-9.
- Kisseleva, T., and Brenner, D. A. (2007). Role of hepatic stellate cells in fibrogenesis and the reversal of fibrosis. *Journal of Gastroenterol Hepatology*, 22, S73-8.
- Kim, M. K., Mok, h. and Chong, Y. (2012). Increased water solubility of the curcumin derivatives via substitution with an acetoxo group at the central methylene moiety. *Bulletin of the Korean Chemical Society*, 33(9), 2849-2850.
- Krishnamoorthy, S., and Honn, K. V. (2006). Inflammation and disease progression. *Cancer Metastasis Review*, 25(3), 481-91.

- Kumavat, S. D., Chaudhari, Y. S., Borole, P., Mishra, P., Shenghani, K., and Duvvuri, P. (2013). Degradation studies of curcumin. *International Journal of Pharmacy Review & Research*, 3(2), 50-55.
- Kunnumakkara, A. B., Bordoloi, D., Padmavathi, G., Monisha, J., Roy, N. K., Prasad, S., Aggarwal, B. B. (2017). Curcumin, the golden nutraceutical: multitargeting for multiple chronic diseases. *British Journal of Pharmacology*, 174, 1325-1348.
- Lee, J. C., Kinniry, P. A., Arguiri, E., Serota, M., Kanterakis, S., Chatterjee, S., Solomides, C. C., Javadi, P., Koumenis, C., Cengel, K. A. and Christofidou-Solomidou, M. (2010). Dietary curcumin increase antioxidant defenses in lung, ameliorates, radiation-induced pulmonary fibrosis, and improves survival in mice. *Radiation Research*, 173, 590-601.
- Leo, A., Hansch, C., and Elkins, D. (1971). Partition coefficients and their uses. *Chem. Rev.* 71 (6), 525-616.
- Leonardi, G. C., Candido, S., Cervello, M., Nicolosi, D., Raiti, F., Travali, S., Spandidos, D. A., and Libra, M. (2012). The tumor microenvironment in hepatocellular carcinoma (review). *International Journal of Oncology*, 40(6), 1733-47
- Li, J., Wang, X., Zhang, T., Wang, C., Huang, Z., and Luo, X. (2015). A review on phospholipids and their main applications in drug delivery systems. *Asian Journal of Pharmaceutical Sciences* 10: 81-98.
- Li, W., Zhou, Y., Yang, J., Li, H., Zhang, H. and Zheng, P. (2017). Curcumin induces apoptotic cell death and protective autophagy in human gastric cancer cells. *Oncology Reports*, 37, 3459-3466.
- Liu, D., & Chen, Z. (2013). The Effect of Curcumin on Breast Cancer Cells. *Journal of Breast Cancer*, 16, 133-137.
- Liu, Y., and Zhu, X. (2017). Endoplasmic reticulum-mitochondria tethering in neurodegenerative diseases. *Transl. Neurodegener.* 6, 21.
- Lomonosova, E., and Chinnadurai, G. (2008). BH3-only proteins in apoptosis and beyond: An overview. *Oncogene*, 27, S2-S19.
- Lopez, J., and Tait, S. W. G. (2015). Mitochondrial apoptosis: Killing cancer using the enemy within. *Br. J. Cancer*, 2015,112, 957-962.

- Mann, C. D., Neal, C. P., Garcea, G., Manson, M. M., Dennison, A. R., Berry, D. P. (2007). Prognostic molecular markers in hepatocellular carcinoma: A systematic review. *European Journal of Cancer*, 43(6), 979-992.
- McIlwain, D. R., Berger, T., and Mak, T. W. (2018). Caspase functions in cell death and disease. *Cold Spring Harb Perspect Biol*, 5, 1-28.
- Medzhitov, R. (2008). Origin and physiological roles of inflammation. *Nature*, 454(7203), 428-35.
- Mimeault, M. and Batra, S. K., (2011). Potential applications of curcumin and its novel synthetic analogs and nanotechnology-based formulations in cancer prevention and therapy. *Chinese Medicine*, 6(31), 1-19.
- Mishra, S., Narain, U., Mishra, R. and Misra, K. (2005). Design, development and synthesis of mixed bioconjugates of piperic acid-glycine, curcumin-glycine/alanine and curcumin-glycine-piperic acid and their antibacterial and antifungal properties. *Bioorganic & Medicinal Chemistry*, 5, 1477-1486.
- Mormone, E., George, J., and Nieto, N. (2011). Molecular pathogenesis of hepatic fibrosis and current therapeutic approaches. *Chemico-Biological Interaction*, 193, 225-31.
- Nakagawa, H., Maeda, S., Yoshida, H., Tateishi, R., Masuzaki, R., Ohki, T., Hayakawa, Y., Kinoshita, H., Yamakado, M., Kato, N., Shiina, S., and Omata, M. (2009). Serum IL-6 levels and the risk for the hepatocarcinogenesis in chronic hepatitis C patients: an analysis base on gender differences. *International Journal of Cancer*, 125(10), 2264-2269.
- Newell, P., Villanueva, A., Friedman, S. L., Koike, K., and Llovet, J. M. (2008). Experimental models of hepatocellular carcinoma. *Journal of Hepatology*, 48, 858-79.
- Nonn, L., Duong, D. and Peehl, D. M. (2007). Chemopreventive anti-inflammatory activities of curcumin and other phytochemicals mediated by MAP kinase phosphatase-5 in prostate cells. *Carcinogenesis*, 28(6), 1188-1196.
- Nowak, A. K., Chow Pierce, K. H., and Findlay, M. (2004). Systemic therapy for advanced hepatocellular carcinoma: a review. *European Journal of Cancer*, 40, 1474-1484.

- Organization for Economic Cooperation and Development (OECD), 1995. OECD guideline for the testing of chemicals No. 107, partition coefficient (n-octanol/water): shake flask method.
- Parvathy, K. S., Negi, P. S., & Srinivas, P. (2009). Antioxidant, antimutagenic and antibacterial activities of curcumin- β -diglucoside. *Food Chemistry*, 115, 265-271.
- Parvathy, K. S., Negi, P. S., & Srinivas, P. (2010). Curcumin–amino acid conjugates: Synthesis, antioxidant and antimutagenic attributes. *Food Chemistry*, 120(2), 523-530.
- Pahweenvaj Ratnatilaka Na Bhuket. (2018). A study on the in vitro stability and metabolism of curcumin diethyl disuccinate in plasma. Thesis. Faculty of Pharmaceutical Sciences, Chulalongkorn University.
- Pietras, K. and Ostman, A. (2010). Hallmarks of cancer: interactions with tumor stroma. *Experimental Cell Research*, 316(8), 1324-1331.
- Pinlaor, S., Youngvanit, P., Prakobwong, S., Kaewsamut, B., Khoontawad, J., Pinlaor, P., and Hiraku, Y. (2009). Curcumin reduces oxidative and nitritive DNA damage through balancing of oxidant–antioxidant status in hamsters infected with *Opisthorchis viverrini*. *Molecular Nutrition & Food Research*, 53(10), 1316-1328.
- Porter, A. G. and Janicke. (1999). Emerging roles of caspase-3 in apoptosis. *Cell Death and Differentiation*, 6, 99-104.
- Ratnatilaka Na Bhuket, P., Niwattisaiwong, N., Limpikirati, P., Khemawoot, P., Towiwat, P., Ongpipattanakul, B., et al. (2016). Simultaneous determination of curcumin diethyl disuccinate and its active metabolite curcumin in rat plasma by LC–MS/MS: Application of esterase inhibitors in the stabilization of an ester-containing prodrug. *Journal of Chromatography B* 1033: 301-310.
- Ravindran, J., Prasad, S., and Aggarwal, B. B. (2009). Curcumin and Cancer Cells: How Many Ways Can Curry Kill Tumor Cells Selectively? *The AAPS Journal*, 11, 495-510.
- Reddy, L., Odhav, B., and Bhoola, K. D. (2003). Natural products for cancer prevention: a global perspective. *Pharmacology and Therapeutics*, 99(1), 1-13.

- Reddy, R. C., Vatsala, P. G., Keshamouni, V. G., Padmanaban, G. and Rangarajan, P. N. (2005). Curcumin for malaria therapy. *Biochemical and biophysical research communications*, 2, 472-474.
- Reuter, S., Eifes, S., Dicato, M., Aggarwal, B. B., and Diederich, M. (2008). Modulation of anti-apoptotic and survival pathways by curcumin as a strategy to induce apoptosis in cancer cells. *Biochemical Pharmacology*, 76, 1340-1351.
- Richmond, A. and Su, Y. (2008). Mouse xenograft models vs GEM models for human cancer therapeutics. *Disease Models & Mechanisms*, 1, 78-82.
- Rodríguez, M. L., Estrela, J. M. and Ortega, A. L. (2013). Natural polyphenols and apoptosis induction in cancer therapy. *Carcinogenesis & Mutagenesis*, S6, 1-10.
- Salguero, P. R., Roderfeld, M., Hemmann, S., Rath, T., Atanasova, S., Tschuschner, A. et al. (2008). Activation of hepatic stellate cells is associated with cytokine expression in thioacetamide-induced hepatic fibrosis in mice. *Laboratory Investigation*, 88, 1192–203.
- Saba, A. B., Oyagbemi, A. A., Azeez, O. I. (2010). Amelioration of carbon tetrachloride-induced hepatotoxicity and haemotoxicity by aqueous leaf extract of *Cnidocolus aconitifolius* in rats. *Nigerion Journal of Physiological Sciences*, 25,139–47.
- Sambuy, Y., De Angelis, I., Ranaldi, G., Scarino, M. L., Stamatii, A., and Zucco, F. (2005). The Caco-2 cell line as a model of the intestinal barrier: influence of cell and culture-related factors on Caco-2 cell functional characteristics. *Cell Biology and Toxicology* 21: 1-26.
- Sharma, R. A., Gescher, A. J. and Steward, W. P. (2005). Curcumin: the story so far. *European Journal of Cancer*, 13, 1955-1968.
- Shah, P., Jogani, V., Bagchi, T., and Misra, A. (2006). Role of Caco-2 Cell Monolayers in Prediction of Intestinal Drug Absorption. *Biotechnology Progress*, 22, 186-198.
- Severi, T., van Malenstein, H., Verslype, C., and van Pelt, J. F. (2010). Tumor initiation and progression in hepatocellular carcinoma: risk factors, classification, and therapeutic targets. *Acta Pharmacologica Sinica*, 31(1), 1409-1420.

- Simon-Assmann, P., Turck, N., Sidhoum-Jenny, M., Gradwohl, G., and Kedinger, M. (2007). In vitro models of intestinal epithelial cell differentiation. *Cell Biology and Toxicology*, 23, 241-256.
- Sign, R. K., Rai, D., Yadav, D., Bhargava, A., Balzarini, J., and De, C. E. (2010). Synthesis, antibacterial and antiviral properties of curcumin bioconjugates bearing dipeptide, fatty acids and folic acid. *European Journal of Medicinal Chemistry*, 45(3), 1078-86.
- Srisuttee, R., Koh, S. S., Park, E. H., Cho, I. R., Min, H. J., Jhun, B. H., Yu, D. Y., Park, S., Park, do Y., Lee, M. O., Castrillon, D. H., Johnston, R. N., and Chung, Y. H. (2011). Up-regulation of Foxo4 mediated by hepatitis B virus X protein confers resistance to oxidative stress-induced cell death. *International Journal of Molecular Medicine*, 28(2), 255-60.
- Strimpakos, A. S. and Sharma, R. A. Curcumin: preventive and therapeutic properties in laboratory studies and clinical trials. (2008). *Antioxidants & redox signaling*, 3, 511-545.
- Tanaka, S., Mogushi, K., Yasen, M., Ban, D., Noguchi, N., Irie, T., Kudo, A., Nakamura, N., Tanaka, H, Yamamoto, M., Kokudo, N., Takayama, T., Kawasaki, S., Sakamoto, M., and Arii, S. (2011). Oxidative stress pathways in noncancerous human liver tissue to predict hepatocellular carcinoma recurrence: a prospective, multicenter study. *Hepatology*, 54, 1273-81.
- Thai Ministry of Public Health, Health Information Unit, Bureau of Policy and Strategy, The number of deaths and death rates per 100,000 population by leading causes of death 2003-2007[cited 2013 Sep 11. Available from: <http://bps.ops.moph.go.th/2.3.4-50.pdf>.
- Trivedi, R., and Kompella, U. B. (2010). Nanomicellar formulations for sustained drug delivery: strategies and underlying principles. *Nanomedicine*, 5, 485-505.
- United States Pharmacopoeia 38/National Formulary 33, Test solutions. 2015. United Book Press, Inc., USA.
- van Breemen, R. B., and Li, Y. (2005). Caco-2 cell permeability assays to measure drug absorption. *Expert Opinion on Drug Metabolism & Toxicology*, 1, 175-185.

- Villa-Pulgarín, J. A., Gajate, C., Botet, J., Jimenez, A., Justies, N., Varela-M, R. E., Cuesta-Marbán, A., Müller, I., Modolell, M., and Revuelta, J. L. (2017). Mitochondria and lipid raft-located FoF1-ATP synthase as major therapeutic targets in the antileishmanial and anticancer activities of ether lipid edelfosine. *PLoS Negl. Trop. Di.* 2,11, e0005805.
- Wang, Y. J., Pan, M. H., Cheng, A. L., Lin, L. I., Ho, Y. S., Hsieh, C. Y. and Lin, J. K. (1997). Stability of curcumin in buffer solutions and characterization of its degradation products. *Journal of Pharmaceutical and Biomedical Analysis*, 12, 1867-1876.
- Wang, Q., Qu, C., Xie, F., Chen, L., Liu, L., and Liang, X. (2017). Curcumin suppresses epithelial-to-mesenchymal transition and metastasis of pancreatic cancer cells by inhibiting cancer-associated fibroblasts. *American Journal of Cancer Research*, 7, 125-133.
- Wichitnithad, W., Jongaroonngamsang, N., Pummangura, S. and Rojsitthisak, P. (2009). A simple isocratic HPLC method for the simultaneous determination of curcuminoids in commercial turmeric extracts. *Phytochemical analysis: PCA*, 4, 314-319.
- Wichitnithad, W., Nimmannit, U., Wacharasindhu, S. and Rojsitthisak, P. (2011). Synthesis, characterization and biological evaluation of succinate prodrugs of curcuminoids for colon cancer treatment. *Molecules*, 2, 1888-1900.
- Wongsrisakul, J., Wichitnithad, W., Rojsitthisak, P., and Towiwat, P. (2010). Antinociceptive effects of curcumin diethyl disuccinate in animal models, 24.
- Wu, T. (2006). Cyclooxygenase-2 in hepatocellular carcinoma. *Oncology*, 32(1), 28-44.
- Wu, S. H., Hang, L. W., Yang, J. S., Chen, H. Y., Lin, H. Y., Chiang, J. H., Lu, C. C., Yang, J. L., Lai, T. Y., Ko, Y. C. and Chung, J. G. (2010). Curcumin induces apoptosis in human non-small cell lung cancer NCI-H460 cells through ER stress and caspase cascade- and mitochondria-dependent pathways. *Anticancer Research*, 30, 2125-2134.
- Xin, H., Mitsuru S., Yoh T., and Miyazaki, K. (2004). Absorption of ester prodrugs in Caco-2 and rat intestinal model. *Antimicrobial Agents and Chemotherapy*, 48, 2604-2609.

- Xu, W., Jing, L., Wang, Q., Lin, C.-C., Chen, X., Diao, J., Liu, Y., Sun, X. (2015). Bas-PGAM5L-Drp1 complex is required for intrinsic apoptosis execution. *Oncotarget*, 6, 30017–30034.
- Yang, K. Y., Lin, L. C., Tseng, T. Y., Wang, S. C., and Tsai, T. H. (2007). Oral bioavailability of curcumin in rat and the herbal analysis from *Curcuma longa* by LC–MS/MS. *Journal of Chromatography B*, 853(1-2), 183-189.
- Yip, K. W., and Reed, J. C. (2008). BCL-2 family proteins and cancer. *Oncogene*, 77, 6398–6406.
- Yoysungnoen, B., Wirachwong, P., Bhattarakosol, P., Niimi, H., and Patumraj, S. (2006) Effects of curcumin on tumor angiogenesis and biomarkers, COX-2 and VEGF, in hepatocellular carcinoma cell-implanted nude mice, 34.
- Yoysungnoen, P., Wirachwong, P., Changtam, C., Suksamran, A., and Patumraj, S. (2008) . Anti-cancer and anti-angiogenic effects of curcumin and tetrahydrocurcumin on implanted hepatocellular carcinoma in nude mice. *World Journal of Gastroenterology*, 14, 2003-2009.
- Yu, H., Pardoll, D., and Jove, R. (2009). STATs in cancer inflammation and immunity: a leading role for STAT3. *Nature Reviews Cancer*, 9(11), 798-809.
- Zaman, S., Wang, R., Gandhi, V. (2014). Targeting the apoptosis pathway in hematologic malignancies. *Leuk. Lymphoma*, 2014, 55, 1980–1992.
- Zeng, Z., Shen, Z. L., Zhai, S., Xu, J. L., Liang, H., Shen, Q. (2017). Transport of curcumin derivatives in Caco-2 cell monolayers. *European Journal of Pharmaceutics and Biopharmaceutics*, 117, 123-131.
- Zhang, F., Koh, G. Y., Jeansonne, D. P., Hollingsworth, J., Russo, P. S., Vicente, G., Stout, R. W., & Liu, Z. (2011). A novel solubility-enhanced curcumin formulation showing stability and maintainance of anticancer activity. *Journal of pharmaceutical sciences.*, 100(7), 2778-2789.
- Zhang, Y., Liu, Y., Zou, J., Yan, L., Du, W., Zhang, Y., Sun, H., Lu, P., Geng, S., Gu, R., Zhang, S., and Bi, Z. (2017). Tetrahydrocurcumin induces mesenchymal-epithelial transition and suppresss angiogenesis by targeting HIF-1 α and autophagy in human osteosarcoma. *Oncotarget*. 8(53), 91134-91149.

- Zhi-Dong, L., Xiang-Ping, L., Wei-Jun, Z., Qian, D., Fu-Nian, L., Hai-Bo, W., Bin, K. (2014). Curcumin induces apoptosis in breast cancer cells and inhibits tumor growth in vitro and in vivo. *Int J Clin Exp Pathol*, 7(6), 2818 - 2824.
- Zhu, Y. and Bu, S. (2017). Curcumin induces autophagy, apoptosis, and cell cycle arrest in human pancreatic cancer cells. *Evidence-Based Complementary and Alternative Medicine*, 1-13.
- Zhu, Y., Wang, M., Zhang, J., Peng, W., Firempong, C. K., and Deng, W. (2015). Improved oral bioavailability of capsaicin via liposomal nanoformulation: preparation, in vitro drug release and pharmacokinetics in rats. *Archives of Pharmacal Research*, 38, 512-521.

APPENDIX A

Synthesis and Characterization of Cur and CurDD

1. Synthesis of Cur

Cur was synthesized using a previous published method with some modifications (Wichitnithad *et al*, 2011). The 1.03 mL of acetylacetone (MW 100.12; d 0.972; 10 mmol) and 0.348 g of boron oxide (MW 69.62; 5 mmol) were mixed in the round-bottom flask containing 5 mL of ethyl acetate. This reaction mixture was refluxed until the milky mixture was formed. Simultaneously, the 3.04 g of vanillin (MW 152.15; 20 mmol) and 10.8 mL of tributyl borate (MW 230.15; d 0.853; 40 mmol) were dissolved completely in 20 mL of ethyl acetate in round-bottom flask at the room temperature. Then, the milky mixture was gradually transferred to the clear solution of vanillin and tributyl borate and stirred until obtain a clear solution. Subsequently, 0.1 mL of n-butylamine (MW 73.14; d 0.740; 2 mmol) was added dropwise to the reaction mixture. The mixture would become more yellow. Stirring was continued overnight. The reaction was stopped by adding 50 mL of 0.5 N HCl twice and stirred for 30 minutes to break the product complex. The organic layers were separated and the aqueous fraction was extracted with ethyl acetate. The combined organic layers were washed out with water and saturated NaCl solution, respectively. The organic layer was dried over anhydrous sodium sulfate before being evaporated by rotary evaporator to obtain the crude product. Finally, the crystalline curcumin was obtained by crystallization in methanol.

2. Synthesis of CurDD

CurDD was synthesized using the previously reported method with some modification (Wichitnithad *et al*, 2011). A round-bottomed flask was charged

curcumin (0.54 mmol) and 4-(N, N-dimethylamino) pyridine (DMAP) (1.2 mmol), followed by addition of 15 mL dried ethyl acetate. The mixture was stirred at room temperature until both compounds dissolved completely. Then, 25 mL of dried dichloromethane was added to the mixture. Then, the reaction mixture was slowly added with ethyl-4-chloro-4-oxobutyrate (1.2 mmol) at room temperature. After stirring for 2 h, the solvent was evaporated and the residue was added with 30 mL of deionized water and 20 mL of ethyl acetate. Then, the aqueous phase was removed and the organic layer were washed with 20 mL of 5% sodium bicarbonate for 5 min. The aqueous layer was separated and the organic layer was washed with deionized water. Then, the residual water in the organic phase was removed using saturated saline solution. The organic layer was evaporated by rotary evaporator to obtain the crude product. The crude product was crystallized in methanol to give the CurDD as pale yellowish solids.

3. Characterization of Cur and CurDD

3.1. Mass spectrometry

Cur and CurDD was dissolved with 50% of methanol. The solution at 1 µg/ml was injected in mass spectrometer. Spectrum was recorded by electrospray ionization (ESI) technique and molecular weight was determined.

3.2. Nuclear magnetic resonance (NMR) spectroscopy

Fifteen milligram of Cur and CurDD were dissolved with acetone. The solution was analyzed by nuclear magnetic resonance spectroscopy at 500 MHz. Spectrum of ^1H -NMR was recorded.

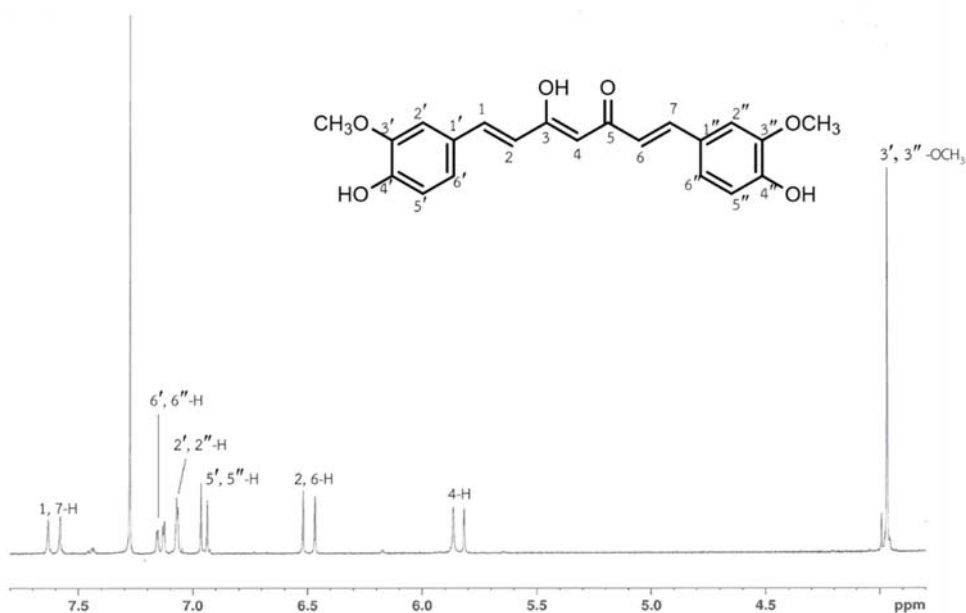


Figure 33 Mass spectrometry of Cur

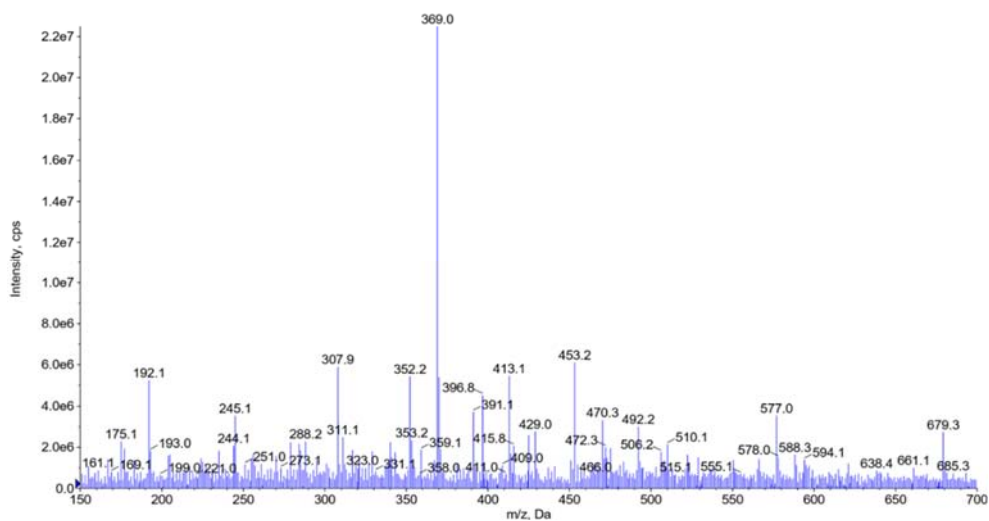


Figure 34 Nuclear magnetic resonance (NMR) spectroscopy of Cur

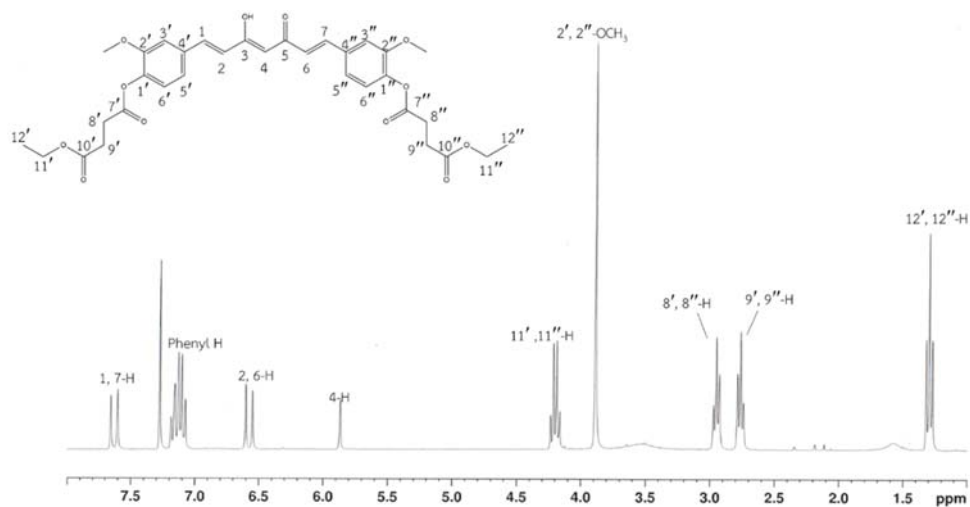


Figure 35 Mass spectrometry of CurDD

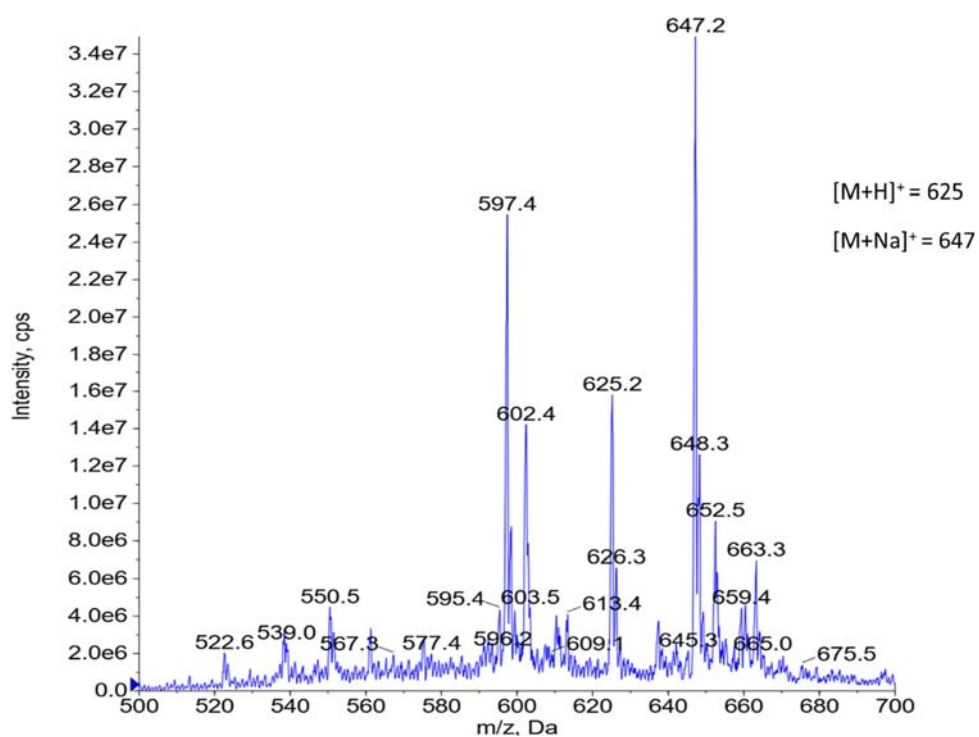


Figure 36 Nuclear magnetic resonance (NMR) spectroscopy of CurDD

CUR showed $^1\text{H-NMR}$ signals (300 MHz, CDCl_3) at δ 7.61 (d, $J = 15.8$ Hz, 1H), 7.19 – 7.04 (m, 2H), 6.95 (d, $J = 8.2$ Hz, 1H), 6.49 (d, $J = 15.8$ Hz, 1H), 5.84 (d, $J = 14.4$ Hz, 1H), 3.99 (s, 3H). The molecular ion of CUR showed a m/z at 369 $[\text{M}+\text{H}]^+$. For CDD, $^1\text{H-NMR}$ (300 MHz, CDCl_3) spectrum shows signals at δ 7.63 (d, $J = 15.8$ Hz, 2H), 7.24 – 7.04 (m, 6H), 6.58 (d, $J = 15.8$ Hz, 2H), 5.87 (s, 1H), 4.20 (q, $J = 7.1$ Hz, 4H), 3.89 (s, 6H), 2.95 (t, $J = 6.9$ Hz, 4H), 2.76 (t, $J = 6.9$ Hz, 4H), 1.29 (t, $J = 7.1$ Hz, 6H). The m/z of the molecular ion of CDD is 625 $[\text{M}+\text{H}]^+$.

APPENDIX B

Chromatogram of Cur, DimethylCur and CurDD from HPLC

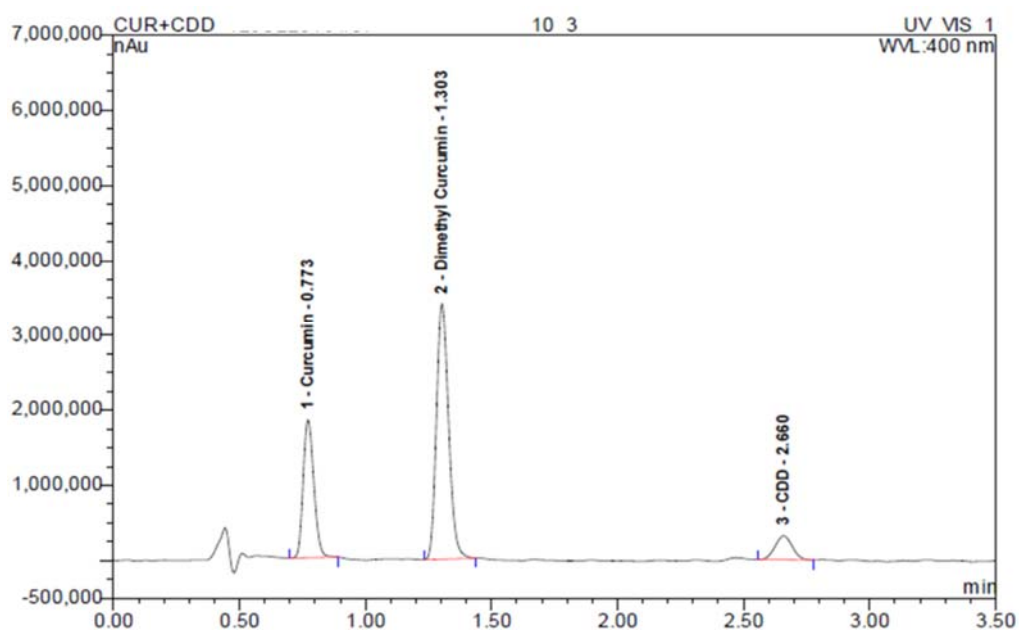


Figure 37 The chromatogram of curcumin, dimethyl curcumin and curcumin diethyl disuccinate from HPLC

APPENDIX C

Culture Media

1. Reagent

- 1.1. Dulbecco's modified Eagle's medium (DMEM) (Gibco 12800, USA)
- 1.2. Fetal bovine serum (FBS) (Gibco, 16000-044)
- 1.3. L-Glutamine 200 mM (100x) (Gibco, 25030-081)
- 1.4. Nonessential amino acids (Gibco, 11140-050)
- 1.5. Penicilin-Streptomycin (Gibco, 15140-122)
- 1.6. Fungizone (Gibco, 15290-081)
- 1.7. Sodium bicarbonate (NaHCO_3) (MW 84.01) (Sigma Co. S5761)

2. Heat-inactivated fetal bovine serum (Δ FBS)

FBS was thawed in water bath at 37°C and then FBS was incubated in water bath at 56.7°C for 30 minute and mix every 10 minute.

3. Basal Dulbecco's Modified Minimum Essential Medium (D7777) (1 L)

(DEMEM or serum free media)

- 3.1. 850 mL DI H₂O
- 3.2. Slowly add contents from 1 pack of powdered DMEM (12800, Gibco) into the beaker with stir bar at moderate speed.
- 3.3. Stir at moderate rate to dissolve for 30 min at room temp.
- 3.4. Add 3.7 g NaHCO_3 /L (44 mM) and stir until solubilized
- 3.5. Adjust pH to 7.2-7.3 with 1M HCl or 1M

- 3.6. Transfer medium to volumetric flask and adjust volume to 1L Filter sterilize, label indicating contents, your initials and date, and store at 4°C

4. Complete media (cDMEM) for Caco-2 cells

4.1. Preparation of cDMEM (complete DMEM) + 15% Δ FBS (100 ml) Sterile

- 4.1.1. Pipette 15 ml of FBS heat inactivate
- 4.1.2. Pipette 1 ml of penicilin-streptomycin
- 4.1.3. Pipette 1 ml of L-glutamine st
- 4.1.4. Pipette 1 ml of nonessential amino acids
- 4.1.5. Pipette 0.2 ml of fungizone
- 4.1.6. Adjust total volume to 100 ml by basal DMEM

4.2. Preparation of cDMEM (complete DMEM) + 7.5% Δ FBS (100 ml)

Sterile

- 4.2.1. Pipette 7.5 ml of FBS heat inactivate
- 4.2.2. Pipette 1 ml of penicilin-streptomycin
- 4.2.3. Pipette 1 ml of L-glutamine
- 4.2.4. Pipette 1 ml of nonessential amino acids
- 4.2.5. Pipette 0.2 ml of fungizone
- 4.2.6. Adjust total volume to 100 ml by basal DMEM

5. Complete media (cDMEM) for HepG2 cells (cDMEM + 10% Δ FBS) 100 ml

- 5.1. Pipette 10 ml of FBS heat inactivate
- 5.2. Pipette 1 ml of penicilin-streptomycin
- 5.3. Adjust total volume to 100 ml by basal DMEM

APPENDIX D

Cell Culture

1. Resuscitation of frozen cells

- 1.1. Warm complete media in a 37°C water bath for 30 min before removing cryogenic tube from liquid nitrogen.
- 1.2. Add 12 ml of cDMEM in 75 cm² flask and incubated in incubator.
- 1.3. Add 4 ml of cDMEM in 15 ml plastic tubes.
- 1.4. Transfer cryogenic tube to a 37°C water bath for 1-2 min until fully thawed. Quickly thawing the cryogenic tube will minimise any damage to the cell membranes. Be careful not to totally immerse the cryogenic tube – this may increase contamination risk.
- 1.5. Wipe cryogenic tube with a tissue soaked in 70% alcohol prior to opening.
- 1.6. Transfer total cell stock solution from cryogenic tube into 15 ml plastic tubes containing 4 ml of cDMEM
- 1.7. Centrifuge at 800 rpm for 5 min
- 1.8. Discard supernate and resuspend with 2-3 ml of cDMEM
- 1.9. Transfer total cell solution into 75 cm² flask containing 13 ml of cDMEM Incubate in CO₂ incubator.

2. Growth and maintenance of live cell cultures

- 2.1. Place media in water bath (37°C) for 15-20 min.
- 2.2. Take dish of cells out of CO₂ incubator.
- 2.3. Examine cells under microscope to determine health/condition.
- 2.4. In hood, label the appropriate number of new dish with the cell line name, the passage number, the date and initial name. Cells will be

subculture or splitted when it showed 70-80% confluence (about 4-5 days after seeding the cells on the flask).

- 2.5. Remove old media from flask by aspiration. Wash cell with 5 ml pre-warmed DMEM.
- 2.6. Add 5 ml 1X trypsin-EDTA and then incubate 37°C for 5-10 min.
- 2.7. Add 5 ml cDMEM + 15% FBS
- 2.8. Transfer total solution to 15 ml tube
- 2.9. Centrifuge at 800 rpm for 5 min
- 2.10. Discard supernate and resuspend with 2-3 ml of cDMEM + 15% FBS for count cell in hemacytometer.
- 2.11. Seed cells on a new 75 cm² flask at 0.4×10^6 /flask with 12 ml cDMEM + 15% FBS /flask and return the plate to the CO₂ incubator.

3. Cell Quantification

- 3.1. Clean the haemocytometer.
- 3.2. Under sterile pipette remove 30 μ l of cell suspension into 30 μ l trypan blue (dilution factor =2) by gentle pipetting.
- 3.3. Fill both sides of the chamber (approx. 10 μ l) with cell suspension and view under a light microscope using x20 magnification.
- 3.4. Count the number of viable (seen as bright cells) and non-viable cells (stained blue).
- 3.5. Calculate the concentration of viable and non-viable cells and the percentage of viable cells

Calculate total cell number as follows:

- a. Mean of 16 square \times 2 (dilution into trypan blue) \times 10⁴ (volume of cell suspension per 16 squares is 0.1 μ L) = number of cells per mL

- b. For example, if 111 and 97 cells in two sets of 16 squares,

$$(111+97)/2 = 104$$

$$10^4 \times 2 \text{ (dilution factor)} \times 10^4 = 2.08 \times 10^6 \text{ cells/mL}$$

Also count cells that accumulate trypan blue (dead cells)

in each set of 16 squares, viable cells/ (viable cells + dead cells) \times 100 = % viability (routinely > 95% viability).

Calculate cell numbers needed for new T-75 flasks and new 6 or 12 well plates

Seeding number at 3.0 – 4.0 \times 10⁵ cells per T75-flask (vol.12 mL/flask)

2.5-3.5 \times 10⁵ cells per well of a 6 well-dish (vol. 2 mL/well)

2.0-2.5 \times 10⁵ cells per well of insert (vol. 1.5 mL/insert)

- c. When preparing cells for seeding new dish or flasks, always make 1.2 flask or for an extra well to account for pipetting errors.

4. Cytotoxicity assay

- 4.1. Cultured cells were transferred in 96-well plates at a density of 5 \times 10³ cells in 200 μ l of complete medium per well and then incubated at 5% CO₂ in 37 °C incubator for 24 h.
- 4.2. The cultured cells were treated with medium containing varies concentration of compounds or DMSO (solvent for solubilized samples) and incubated at 5% CO₂ in 37 °C incubator.
- 4.3. After 24, 48 and 72 h, they were added with 10 μ l of 3-(4,5-dimethylthiazol-2-yl)-2,5-diphenyl tetrazolium bromide (MTT) solution (concentration 5 mg/ml in PBS) into each well and incubated at 5% CO₂ in 37 °C incubator for 4 h.

- 4.4. Removed culture medium and added a mixture of DMSO (150 μ l) and glycine (75 μ l), mixed for cell lysis and dissolving of the formasan crystal. (some studies dissolved formasan crystal by acidic isopropanol)
- 4.5. Measured absorbance at 540 nm

Calculation of % cell viability and IC₅₀

% Cell viability = (OD of sample group x 100)/ OD of control group (DMSO or solvent for solubilized samples)

IC₅₀ derived from standard curve between varies concentration of compounds and % cell viability

APPENDIX E

Characterization of Caco-2 and HepG2 cells

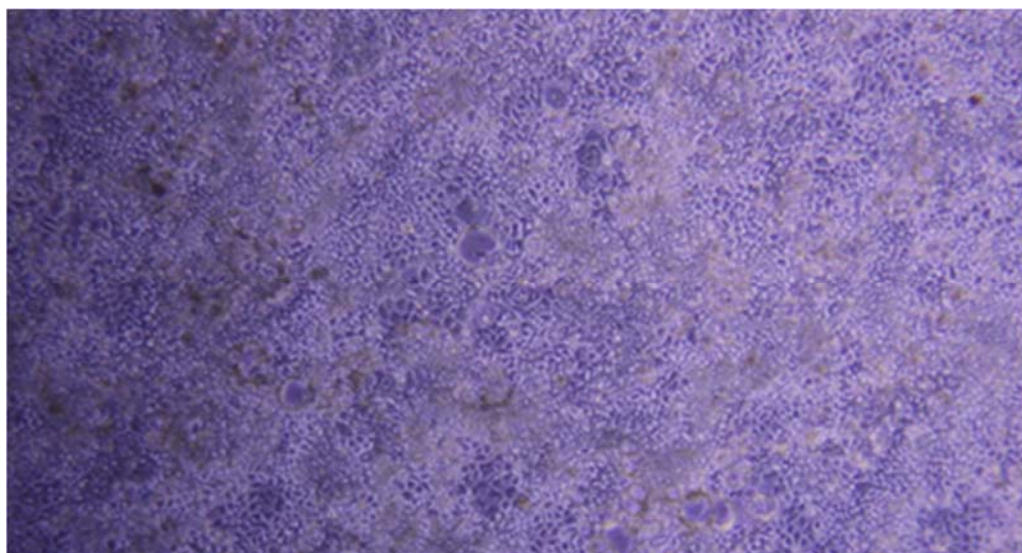


Figure 38 Caco-2 cells at 21 days after confluence

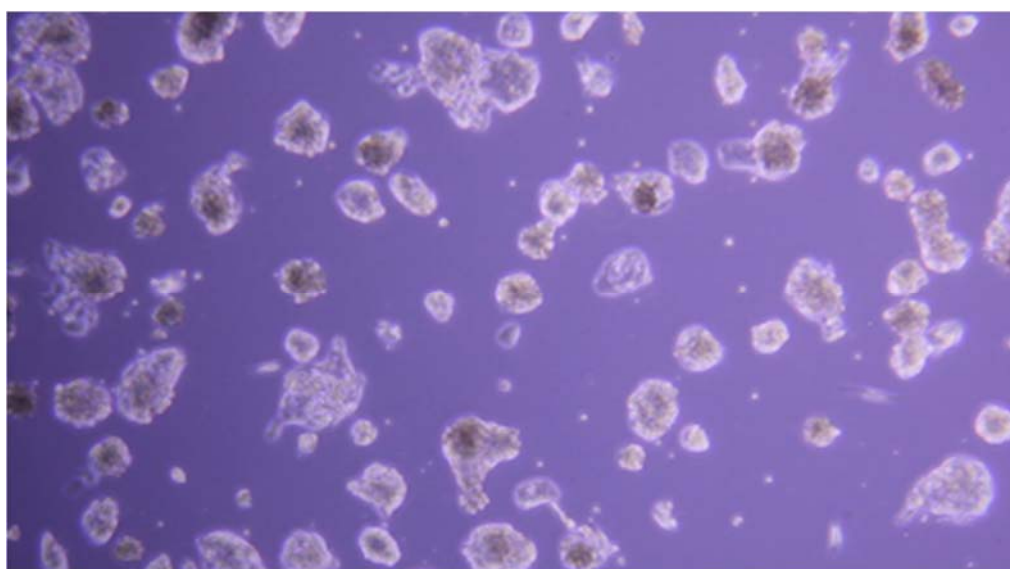


Figure 39 HepG2 cells about 50% confluence

APPENDIX F

Measuring Protein Concentration by BCA Assay

Reagents:

1. BCA™ Protein Assay Reagent A (Thermo Scientific cat.no. 23223)
2. Microreagent A

NaHCO ₃ anhydrous	6.84 g
NaOH	1.6 g
KNa tartrate anhygrous	1.6 g

Add NaHCO₃ to adjust the pH 11.25, make up the volume to 100 ml with dH₂O

3. 4%CuSO₄·5H₂O

CuSO ₄ ·5H ₂ O	4 g
Deionized water	100 ml

Working reagent (freshly prepared)	80 samples	40 samples	20 samples
BCA™ Protein Assay Reagent A	8 ml	4 ml	2 ml
Microreagent B	8 ml	4 ml	2 ml
4%Cu ₂ SO ₄ ·5H ₂ O	320 µl	160 µl	80 µl
Total	16.32 ml	8.16 ml	4.08 ml

Protocol:

1. Dilute protein lysate 1:10 (for RAW 264.7) with deionized water.
2. Prepare serial dilution of standard BSA 0.125, 0.25, 0.5, 1 and 2 mg/ml, used deionized water as blank.
3. Pipette 10 µl of diluted lysate and standard protein to microplate.
4. Add 200µl of working reagent, mix 30s on shaker
5. Incubate 37°C for 30 minute
6. Read absorbance at 562 nm with microplate reader
7. Generate standard curve and quantitate the protein concentration of unknown.

APPENDIX G

Western Blot

1. Lysis buffer for western-blot

Stock	For 2 ml	For 1 ml	Final conc.
1 M Tris-HCl (pH 7.4)	100 ul	50 ul	50 mM
1.5 M NaCl	200 ul	100 ul	150 mM
0.05 M EDTA (pH 8.0)	40 ul	20 ul	1 mM
Triton-x 100	20 ul	10 ul	1%
10%SDS	20 ul	10 ul	0.1%
1 M Sodium fluoride	200 ul	100 ul	50 mM
200 mM Sodium pyrophosphate	200 ul	100 ul	10 mM
Protease inhibitor cocktail	10 ul	5 ul	N/A
Water	1200 ul	600 ul	N/A

2. Loading buffer (Laemmli buffer)

(10x, 62.5mM Tris pH 6.8, 0.625M β -mercaptoethanol, 10% glycerol, 2%SDS, 0.00125% bromophenol blue.)

8ml.

Glycerol 0.8 ml

dH₂O 3.0 ml

0.25M TrisHcl pH 6.8 2.0 ml

10% SDS 1.6 ml

β -mercaptoethanol 0.4 ml

0.05% (w/v) bromophenol blue 0.2ml or a few specs

To sample add ¼ volume of loading buffer before heating (used at 2x) (2x, 31.25mM Tris pH 6.8, 0.125M β -mercaptoethanol, 2%glycerol, 0.4%SDS,0.00025% bromophenol blue.)

3. Resolving gel buffer or Separating gel buffer (Tris-Hcl 3M pH8.85) 100ml

Tris 36.33 g

Add around 80ml dH₂O and pH with Hcl

Make volume up to 100ml.

4. Stacking gel buffer (0.25M Tris-Hcl pH6.8) 100ml

Tris 3.028 g

Add around 80ml dH₂O and pH with Hcl

Make volume up to 100ml.

5. 10% APS (ammonium persulphate)

500ul

0.05g in 500ul dH₂O

6. 10%SDS

50g in 50ml dH₂O

7. 5x running buffer (1L)

(0.125M Tris, 1.25M Glycine, 0.5%SDS)

Tris base 15.1 g

Glycine 94 g

10% SDS 50 ml

Adjust vol to 1L

Use at 1x. (0.025M Tris, 0.25M glycine, 0.1%SDS)

8. Transfer buffer (1L)

5x running buffer 100 ml

100% ethanol 233 ml
make up to 1L with dH₂O

9. 10x TBS (0.2M Tris, pH7.6) 1L

Tris 24.2 g
NaCl 80 g

Adjust pH to 7.6 with HCl and make up to 1L with dH₂O

10. Wash buffer (0.2M Tris M Nacl pH7.6, 0.1% Tween-20) (1L)

10x TBS 100 ml
Tween-20 1 ml

Make volume up to 1000ml with dH₂O

11. Blocking buffer

(0.02M Tris Nacl pH7.6, 0.1% Tween-20 with 5%(w/v) non-fat dry milk) 100ml

powdered milk 5 g
wash buffer 100 ml

APPENDIX H

Chromatogram of Cur and CurDD from cellular uptake

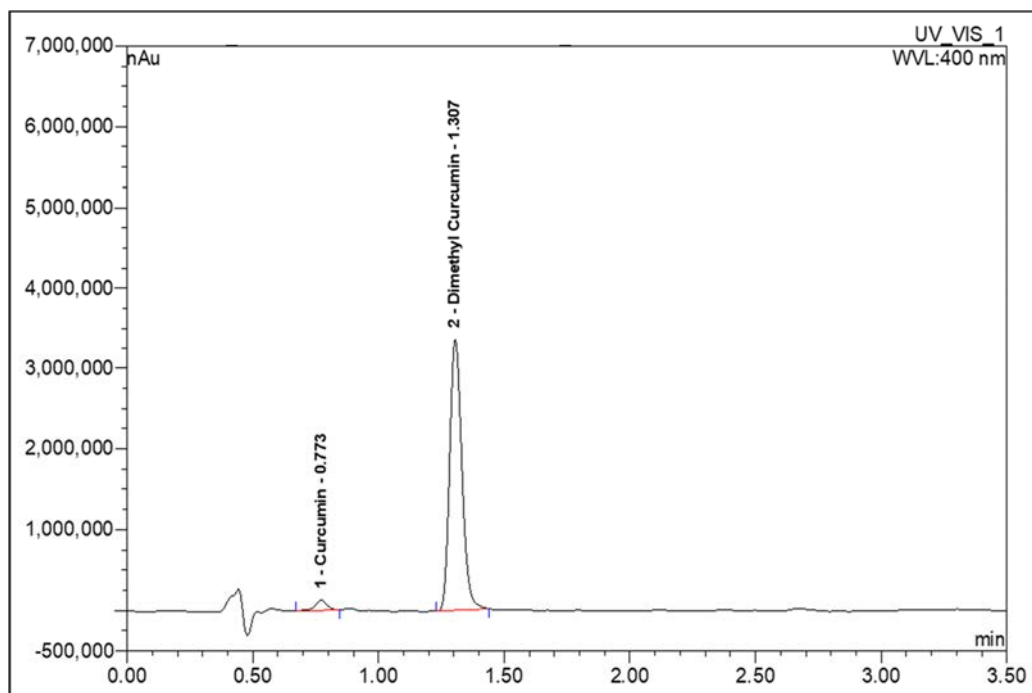


Figure 40 Chromatogram of Cur from cellular uptake of Cur at 4 h

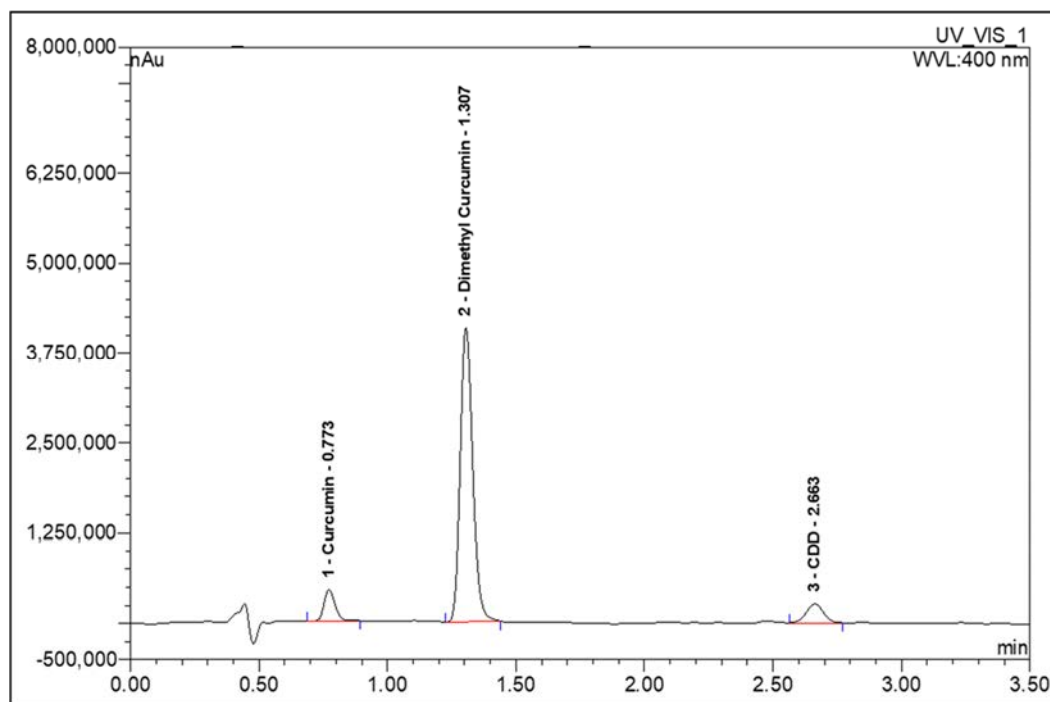


Figure 41 Chromatogram of Cur and CurDD from cellular uptake of CurDD at 4 h

APPENDIX I

Chromatogram of Cur and CurDD from cellular transport

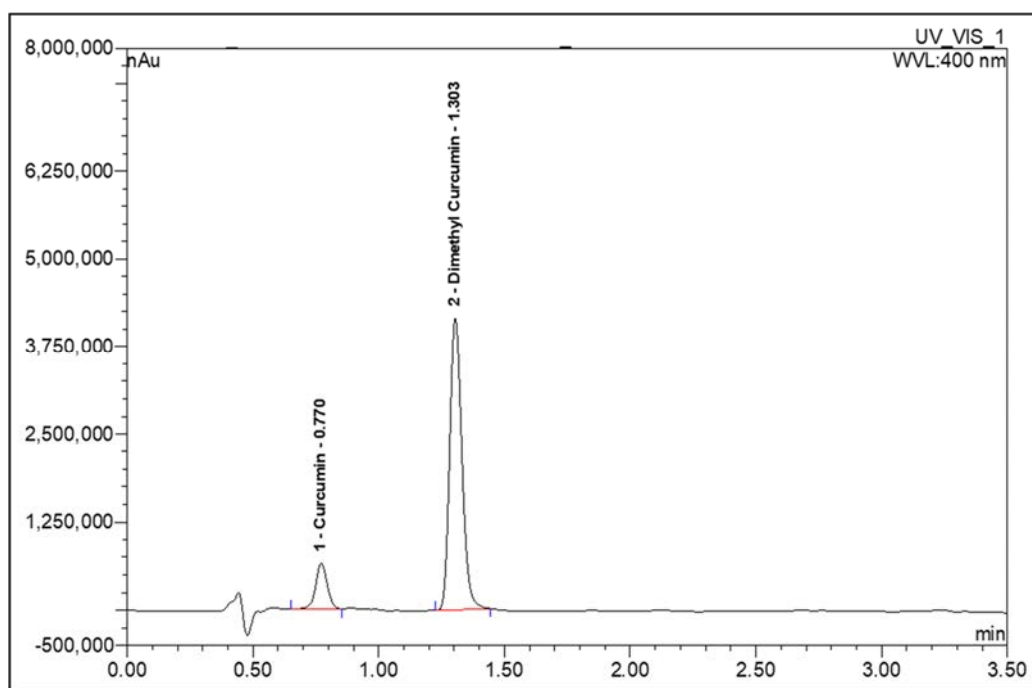


Figure 42 Chromatogram of Cur from cellular transport (bioavailable fraction) of Cur at 4 h

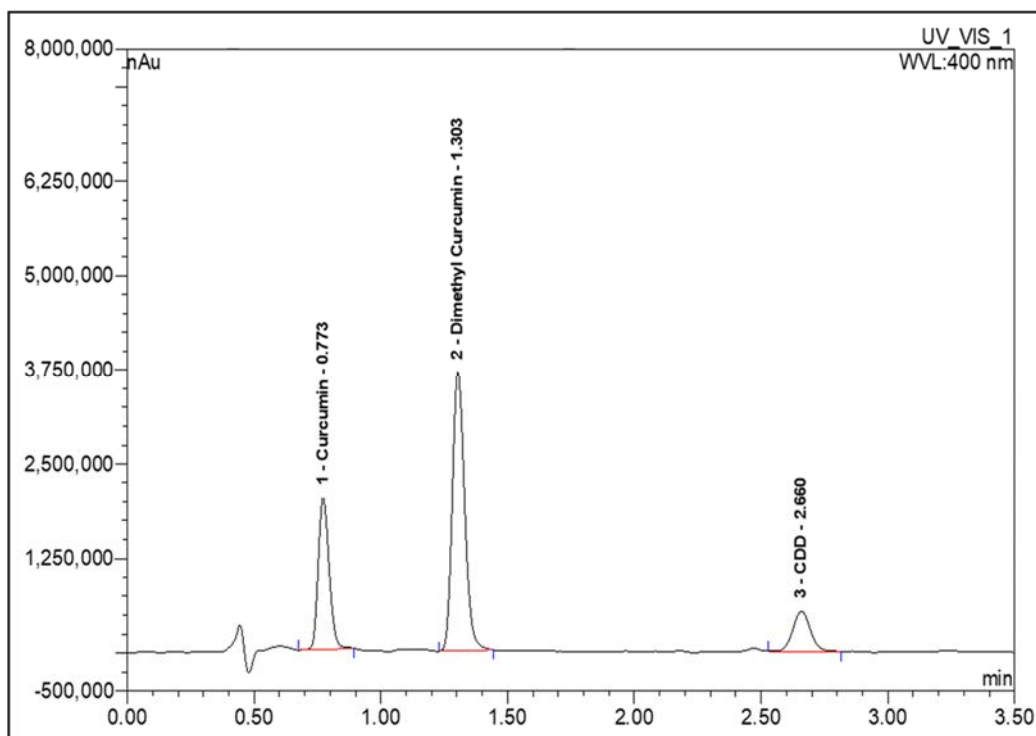



Figure 43 Chromatogram of Cur and CurDD from cellular transport (bioavailable fraction) of CurDD at 4 h

APPENDIX J

Chulalongkorn University Animal Care and Use Protocol
Ethic approval



เลขที่ใบรับรอง 01/2560 เลขที่โครงการวิจัย 019/2559

คณะกรรมการกำกับดูแลการเลี้ยงและใช้สัตว์
คณะแพทยศาสตร์ จุฬาลงกรณ์มหาวิทยาลัย

ใบรับรองการอนุมัติให้ดำเนินการเลี้ยงและใช้สัตว์เพื่องานทางวิทยาศาสตร์
ณ คณะแพทยศาสตร์ จุฬาลงกรณ์มหาวิทยาลัย



(ภาษาไทย) คุณสมบัติทางเคมีกายภาพ ชีวเภสัชกรรม และการต้านมะเร็งระดับของเคอร์คิวมินไดเอทิล ไดซัคซิเนต
โคเคอซิเนต

(ภาษาอังกฤษ) PHYSICOCHEMICAL, BIOPHARMACEUTIC AND ANTI-HEPATOCELLULAR
CARCINOMA PROPERTIES OF CURCUMIN DIETHYL DISUCCINATE

ผู้เสนอโครงการใช้สัตว์ทดลอง ศาสตราจารย์ ดร.สุทธิลักษณ์ ปทุมราช

หน่วยงานที่สังกัด ภาควิชาสรีรวิทยา คณะแพทยศาสตร์ จุฬาลงกรณ์มหาวิทยาลัย

ขอเสนอโครงการใช้สัตว์ทดลองนี้ได้ผ่านการรับรองจากคณะกรรมการกำกับดูแลการเลี้ยงและใช้สัตว์แล้ว เห็นว่า มีความสอดคล้องกับจรรยาบรรณการใช้สัตว์เพื่องานทางวิทยาศาสตร์สภาวิจัยแห่งชาติ จึงเห็นสมควรให้ดำเนินการเลี้ยง และใช้สัตว์ตามที่ขอเสนอโครงการใช้สัตว์ทดลองนี้ได้

ลงนาม  ลงนาม 

(รองศาสตราจารย์ นายแพทย์สมพล สงวนวงศ์ศิริกุล) (ศาสตราจารย์ นายแพทย์สุทธิพงษ์ วีชรินทร์)
ประธานคณะกรรมการกำกับดูแลการเลี้ยงและใช้สัตว์ คณะบดี คณะแพทยศาสตร์ จุฬาลงกรณ์มหาวิทยาลัย

วันที่รับรอง : มีนาคม พ.ศ.2560

วันหมดอายุ : มีนาคม พ.ศ.2561

VITA

NAME	Chawanphat Muangnoi
DATE OF BIRTH	28 Sep 1983
PLACE OF BIRTH	Bangkok
INSTITUTIONS ATTENDED	M.Sc. Nutrition, December 2007 Institute of Nutrition and Faculty of Medicine Ramathibodi, Mahidol University, Thailand
	B.Sc. Medical Science, March 2004 Faculty of Scienced, Burapha University, Chonburi, Thailand
HOME ADDRESS	16/12, Bangkruay-Sainoi Road, Bangkruai, Nonthaburi, 11130
PUBLICATION	<ol style="list-style-type: none"> 1. Feuangthit Niyamissara Sorasitthiyankarn, Chawanphat Muangnoi, Pahweenvaj Ratnatilaka Na Bhuket, Pornchai Rojsitthisak and Pranee Rojsitthisak. Chitosan/alginate nanoparticles as a promising approach for oral delivery of curcumin diglutaric acid for cancer treatment. Mater. Sci. Eng. C, 2018, 93, 178-190 2. Napat Kyokong, Chawanphat Muangnoi, Wuttinont Thaweesest, Virunh Kongkatitham, Kittisak Likhitwitayawuid, Pornchai Rojsitthisak and Boonchoo Sritularak. A New Phenanthrene Dimer from <i>Dendrobium palpebrae</i>. J. Asian Nat. Prod. Res., 2018, DOI: 10.1080/10286020.2018.1429416, p1-7 3. Chawanphat Muangnoi, Ponsiree Jithavech, Pahweenvaj Ratnatilaka Na Bhuket, Wiwat Supasena, Wisut

Wichitnithad, Pasarapa Towiwat, Nuansri Niwattisaiwong, Ian S. Haworth and Pornchai Rojsitthisak. A curcumin-diglutamic acid conjugated prodrug with improved water solubility and antinociceptive properties compared to curcumin. *Biosci. Biotechnol. Biochem.*, 2018, 82(8), 1301–1308

4. Jittima Amie Luckanagul, Chutamart Pitakchatwong, Pahweenvaj Ratnatilaka Na Bhuket, Chawanphat Muangnoi, Pranee Rojsitthisak, Suwabun Chirachanchai, Qian Wang, Pornchai Rojsitthisak. Chitosan-based polymer hybrids for thermo-responsive nanogel delivery of curcumin. *Carbohydr. Polym.*, 2018, 181(1 February 2018), 1119-1127

5. Virunh Kongkatitham, Chawanphat Muangnoi, Napat Kyokong, Wuttinont Thaweesest, Kittisak Likhitwitayawuida, Pornchai Rojsitthisak and Boonchoo Sritularak. Anti-oxidant and Anti-inflammatory Effects of New Bibenzyl Derivatives from *Dendrobium parishii* in Hydrogen Peroxide and Lipopolysaccharide Treated RAW264.7 Cells. *Phytochem Lett.*, 2018, 24, 31-38

6. Napat Kyokong, Chawanphat Muangnoi, Wuttinont Thaweesest, Virunh Kongkatitham, Kittisak Likhitwitayawuid, Pornchai Rojsitthisak and Boonchoo Sritularak. A New Phenanthrene Dimer from *Dendrobium palpebrae*. *J. Asian Nat. Prod. Res.*, 2018, DOI: 10.1080/10286020.2018.1429416, p1-7

7. Praengam K, Muangnoi C, Charoenkiatkul S, Thiyajai P. and Tuntipopipat S. Antioxidant and anti-inflammatory activity of aqueous fraction from *Albizia lebbek* leaves. *Inter Food Res J.* 2017; 24 Issue 3

8. Kunnigar Vongnam, Chawanphat Muangnoi, Pornchai Rojsitthisak, Mongkol Sukwattanasinitt, Paitoon Rashatasakhon. A Highly Selective Turn-on Fluorescent Sensor for Glucosamine from Amidoquinoline-Napthalimide Dyads. *Biosens. Bioelectron.*, 2016, 86(15 Dec), 472-476
9. Settapon Bhunchu, Pornchai Rojsitthisak, Chawanphat Muangnoi and Pranee Rojsitthisak. Curcumin Diethyl Disuccinate Encapsulated in Chitosan/Alginate Nanoparticles for Improvement of Its In Vitro Cytotoxicity Against MDA-MB-231 Human Breast Cancer Cells. *Pharmazie*, 2016, 71(12), 691-700
10. Arparporn Mittraphab, Chawanphat Muangnoi, Kittisak Likhitwitayawuid, Pornchai Rojsitthisak and Boonchoo Sritularak. A New Bibenzyl-phenanthrene Derivative from *Dendrobium signatum* and its Cytotoxic Activity. *Nat. Prod. Comm.*, 2016, 11(5), 657-659.
11. Chingsuwanrote P, Muangnoi C, Parengam K and Tuntipopipat S. Antioxidant and antiinflammatory activities of durian and rambutan pulp extract. *Inter Food Res J.*2016; 23 (3):939- 947.
12. Siriporn Tuntipopipat, Chawanphat Muangnoi, Parunya Thiyajai, Warangkana Srichamnong, Somsri Charoenkiatkul and Kemika Praengam. A bioaccessible fraction of parboiled germinated brown rice exhibits a higher anti-inflammatory activity than that of brown rice. *Food & Function.* 2015; 6(5):1480-8.
13. Kemika Praengam, Chawanphat Muangnoi, Suwittha Dawilaj, Monwirin, Awatchanawong & Siriporn Tuntipopipat. Digested *Moringa oleifera* Boiled Pod Exhibits Anti-Inflammatory Activity in Caco-2 Cells. *J Herbs,*

Spices & Med Plants. 2015; 21:148-160.

14. Sirikanokvilai P, Kriengsinyos W, Nantiruj K, Muangnoi C, Chingsuwanroj P, Praengam K and Tuntipopipat S. Anti-inflammatory activities of digested green curry paste in peripheral blood mononuclear cells from rheumatoid arthritis patients. *Mal J Nutr.* 2014; 20(2): 271-282.
15. Dawilai S, Muangnoi C, Praengamthanachoti P, Tuntipopipat S. Anti-inflammatory activity of bioaccessible fraction from *Eryngium foetidum* leaves. *Biomed Res Int.* 2013; 2013: 958567.
16. Mekhora C, Muangnoi C, Chingsuwanrote P, Dawilai S, Svasti S, Chasri K, Tuntipopipat S. *Eryngium foetidum* suppresses inflammatory mediators produced by macrophages. *Asian Pacific J Cancer Prev.* 2012; 13:723-734.
17. Muangnoi C, Chingsuwanrote P, Praengamthanachoti P, Svasti S, and Tuntipopipat S. *Moringa oleifera* Pod Inhibits Inflammatory Mediator Production by Lipopolysaccharide-Stimulated RAW 264.7 Murine Macrophage Cell Lines. *Inflammation.* 2012; 35(2): 445-455.
18. Charoenkiatkul S, Muangnoi C, Chingsuwanrote P, Praengamthanachoti P, Tuntipopipat S, and Svasti S. Stir-Fry Chicken with Green Curry Suppresses Inflammatory Gene Expression by Lipopolysaccharide-Induced Murine Macrophages. *Food and Nutrition Sciences.* 2011; 2: 770-779.
19. Tuntipopipat S, Muangnoi C, Chingsuwanrote P, Praengam M, Chantravisut P, Charoenkiatkul S and Svasti S. Anti-inflammatory activities of red curry paste extract

on lipopolysaccharide-activated murine macrophage cell line. *Nutrition*. 2011; 2: 479-487.

20. Laohavechvanich P, Muangnoi C, Butryee C and Kriengsinyos W. Protective effect of makrut lime leaf (*Citrus hystrix*) in HepG2 cells: Implications for oxidative Stress. *Science Asia*. 2010; 30: 112-117.

21. Tuntipopipat S, Muangnoi C, and Failla ML. Anti-Inflammatory Activities of Extracts of Thai Spices and Herbs with Lipopolysaccharide-Activated RAW 264.7 Murine Macrophages. *J. Med Food*. 2009; 12(6): 1-8.

AWARD RECEIVED

1. The 90th Anniversary Chulalongkorn University Fund, Ratchadaphiseksomphot Endowment Fund.

2. The Overseas Research Experience Scholarship from the Graduate School and Faculty of Pharmaceutical Sciences, Chulalongkorn University

